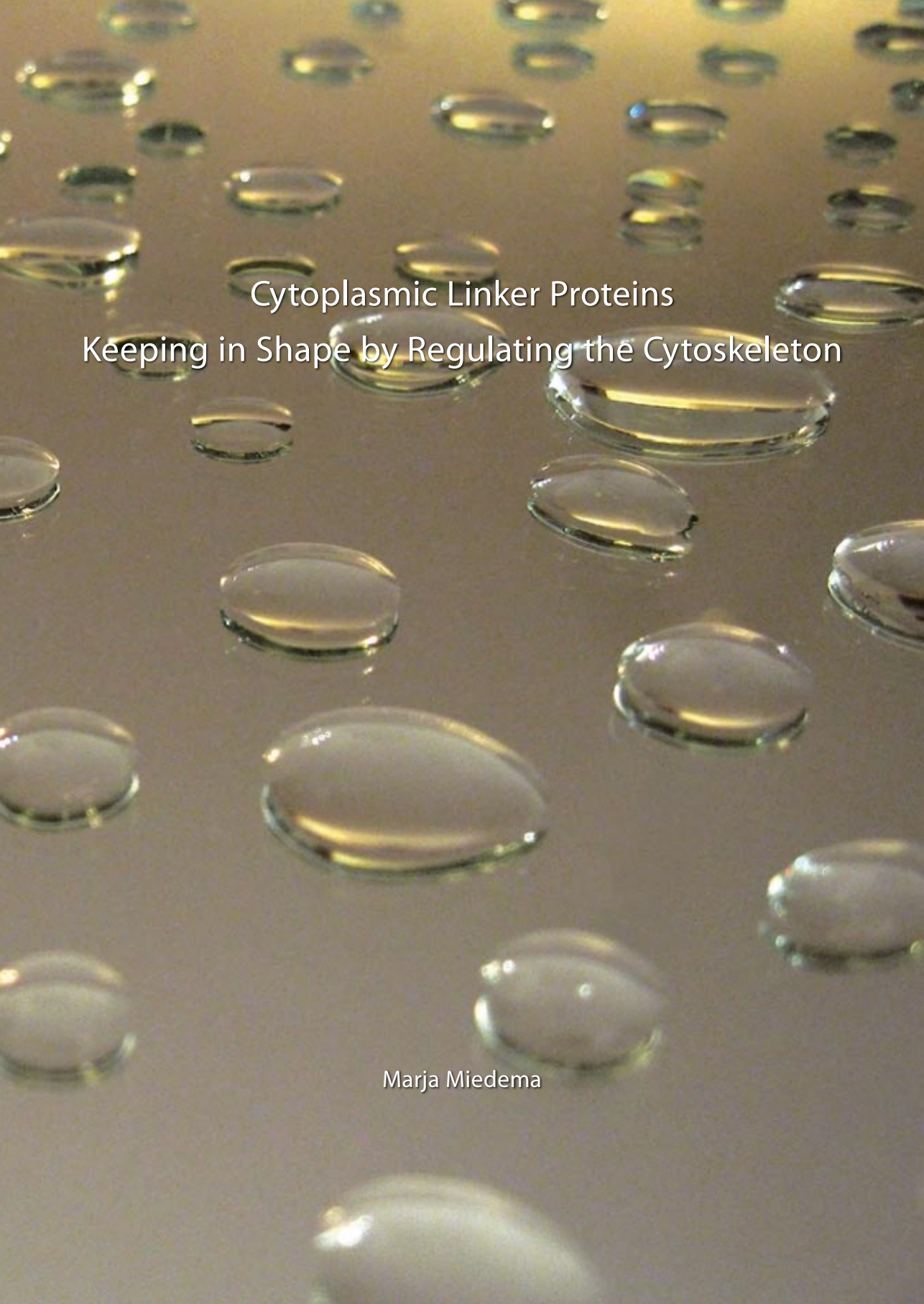

Cytoplasmic Linker Proteins
Keeping in Shape by Regulating the Cytoskeleton

Marja Miedema

Cytoplasmic Linker Proteins
Keeping in Shape by Regulating the Cytoskeleton

Marja Miedema

ISBN/EAN: 978-90-9021698-0

The studies represented in this thesis were performed in the Department of Cell Biology and Genetics of the Erasmus MC in Rotterdam, The Netherlands. Research performed in this thesis was supported by the Netherlands Organization for Scientific Research (NWO).

Layout and graphical assistance: Tom de Vries Lentsch

Printed by: PrintPartners Ipskamp, Enschede

Cytoplasmic Linker Proteins
Keeping in Shape by Regulating the Cytoskeleton

Cytoplasmatische Linker Eiwitten
In vorm blijven door regulatie van het cytoskelet

Proefschrift

ter verkrijging van de graad van doctor aan de
Erasmus Universiteit Rotterdam
op gezag van de
rector magnificus

Prof.dr. S.W.J. Lamberts

en volgens besluit van het College voor Promoties.

De openbare verdediging zal plaatsvinden op
woensdag 4 april 2007 om 15.45 uur

door

Marja Miedema
geboren te Wageningen

ERASMUS UNIVERSITEIT ROTTERDAM

Promotiecommissie

Promotor:	Prof.dr. F.G. Grosveld
Overige leden:	Dr. G.T.J. van der Horst Prof.dr. C.I. de Zeeuw Dr.ir. D.N. Meijer
Copromotor:	Dr.ir. N.J. Galjart

Voor Floris

Contents

Scope of the thesis

Microtubules are an essential component of the eukaryotic cytoskeleton. They are involved in fundamental processes such as cell morphology, cell division and intracellular transport. Microtubules are highly dynamic and their dynamics are regulated by a group of proteins that bind specifically to the growing ends of microtubules, the plus-end-tracking proteins or +TIPs. The concentration of these proteins at the microtubule plus end facilitates an intricate network of interactions. This thesis describes the functional analysis of two of these plus-end binding proteins, the cytoplasmic linker proteins CLIP-115 and CLIP-170.

Chapter 1 gives an introduction to the cytoskeleton with the three components being actin filaments, intermediate filaments and microtubules. The characteristics and functions of several members of the family of +TIPs are highlighted and finally, three disorders that might be caused by alterations in the function of the CLIPs or CLIP-interacting proteins are described.

Chapter 2 describes the generation and characterization of a mouse line deficient for CLIP-115. The gene encoding human CLIP-115 (*CYLN2*) is located in a chromosomal region that is commonly deleted in patients with the neurodevelopmental disorder Williams Syndrome. We provide evidence that haploinsufficiency for *Cyln2* in mice results in mild growth deficiency, brain abnormalities, hippocampal dysfunction and particular deficits in motor coordination. These are all features reminiscent of Williams Syndrome, suggesting involvement of CLIP-115 in the development of this disorder. Cellular analysis shows that the absence of CLIP-115 affects the subcellular distribution of CLIP-170 and the motor protein dynactin, but this does not result in major cellular abnormalities.

Chapter 3 describes the analysis of fibroblasts derived from CLIP-115 and CLIP-170 double knockout mice. These mice were generated to circumvent the redundancy of CLIP-115 and CLIP-170 we suspected after the characterization of the single CLIP-115 and CLIP-170 knockout mice. Indeed, fibroblasts deficient for both CLIP-115 and CLIP-170 show an altered microtubule distribution with microtubule-free areas in which aggregates are found. These aggregates contain the dynactin components $p150^{Glued}$, p50 (dynamitin) and ARP1, but also cytoplasmic dynein and BICD2. The lower frequency of microtubule rescue (transition from a growing phase to a shrinking phase) results in altered microtubule dynamics. In addition, cultured double CLIP deficient fibroblasts show an increased degree of spreading.

Chapter 4 describes the characterization of the CLIP-115 and CLIP-170 double knockout mice. Following the phenotypic features of single CLIP-115 knockout mice, the double knockout mice were subjected to a series of behavioral experiments that challenge their motor coordination skills. Young adult double knockout mice perform significantly poorer in the hanging wire test and on the accelerating rotarod, relative to wild type mice. At later time points, however, their performance improves to wild type level, suggesting that the mice have found a way to circumvent their deficits. Furthermore, a significant number of homozygous double knockout mice developed severe hydrocephalus, which prompted us to analyze the brains of wild type and double knockout mice using high resolution magnetic resonance imaging (MRI). In all homozygous double CLIP-115 and CLIP-170 knockout mice tested the volumes of the lateral and the third brain ventricles were significantly enlarged, suggesting a function of the CLIPs in the maintenance of the ventricular system.

Chapter 5 discusses the results reported in the preceding chapters and speculates on the implications of these results for the function of the CLIPs.

Chapter 1

Introduction

Chapter 1

Introduction

1.1 The cytoskeleton

A network of intracellular filaments in the cytoplasm provides the cell with structural support and is referred to as the cytoskeleton. In addition to its supportive function it is involved in cell motility, muscle contraction, chromosome segregation during cell division, and intracellular transport. The cytoskeleton is composed of three different components, actin filaments (or microfilaments), intermediate filaments and microtubules (Figure 1). These filaments differ from each other in size, the type of subunit they are built up from and the way they are assembled. Each type of filament performs specific functions, but they also show multiple interactions.

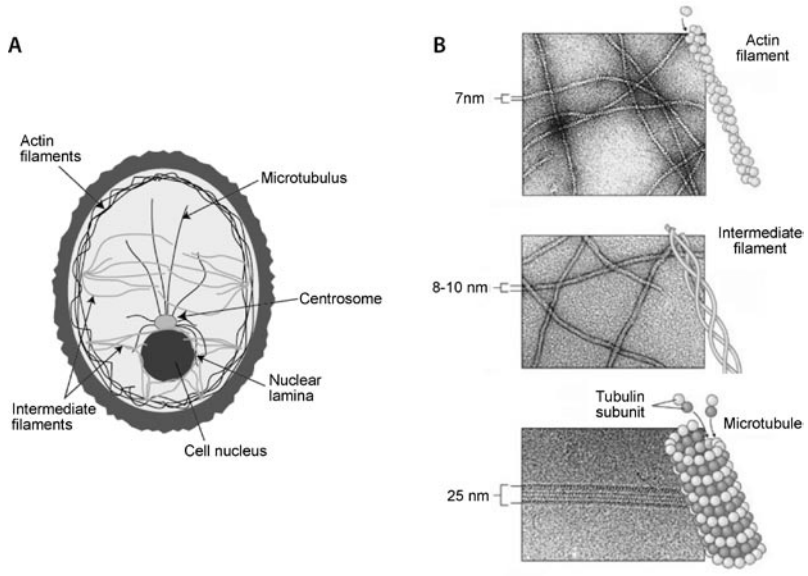

Figure 1. The cytoskeleton
A. Organization of the different cytoskeletal components in the cell. **B.** Electron micrographs and schematic representations of the components of the cytoskeleton. Actin filaments are 7 nm in diameter, intermediate filaments 8-10 nm and microtubules 25 nm. *(http://img.sparknotes.com/figures/D/d479f5da672c08a54f986ae699069d7a/cytoskeleton.gif; Adapted from Asking About Life, A.J. Tobin & J. Dusheck, 2nd edition; http://campus.queens.edu/faculty/jannr/cells/ cell%20pics/cytoskeleton.jpg)*

1.1.1 Actin filaments

The actin cytoskeleton is a dynamic network of polarized filaments of 5-7 nm in diameter. It is crucial for maintaining cell morphology and polarity, for endocytosis and intracellular trafficking, for motility and for cell division (Furukawa and Fechheimer, 1997). Apart from the organization in a finely meshed network, actin filaments can also form bundles, either in response to mechanic stress (stress fibers) or in filopodia. In muscle cells actin interacts with type II myosin to create muscle fibers, which are responsible for contraction.

Actin is the most abundant cytoskeletal protein in the cell. The total pool of actin consists of polymerized, filamentous (F) actin and unpolymerized, globular (G) actin. Only a small

portion of the globular actin is truly 'free actin', i.e. not in a complex with other proteins. A large pool of unpolymerized actin is essential for rapid reorganization of the network when motility is needed. Since monomeric actin has a strong tendency to polymerize, actin-binding proteins are present to ensure the existence of a pool of actin monomers. These proteins prevent polymerization either by sequestering ATP-actin or by capping the barbed ends of existing filaments (Pollard et al., 2000).

ATP-bound actin monomers polymerize head-to-tail to form two-stranded rod-like helical filaments. These filaments have an intrinsic polarity, both in their structure and in their way of assembly. The two ends of the filament polymerize at different rates resulting in a fast growing and a slower growing end (Wegner, 1976). Because of the 'arrow-head' appearance in electron microscopic analyses the rapid growing end is called the barbed end and the slower growing end is called the pointed end (Huxley, 1963).

Polymerization starts with the formation of a nucleation site. These can be formed *de novo*, from the sides of existing filaments or by severing of an existing filament. *In vivo*, actin binding proteins such as the Arp2/3 complex, are essential to promote initiation of new actin filaments (Mullins et al., 1998). Once nucleated, rapid polymerization occurs as ATP-bound monomers are added to the exposed ends of the growing polymer. As the filament matures, the ATP is hydrolyzed and ADP-actin is released from the pointed end, where nucleotide exchange regenerates ATP-actin monomers that can again be added to the growing end of the filament. After the initial fast polymerization an equilibrium phase is reached when the growth of polymer due to monomer addition is precisely balanced by the shrinkage due to monomer loss. At this point, the net length of the filament remains constant, even though polymer addition and loss continues. This process is called 'treadmilling' (Margolis and Wilson, 1978).

1.1.2 Intermediate filaments

Intermediate filaments are found in most, but not all eukaryotic cells. They are tough filaments that are particularly prominent in cells that are subject to mechanical stress. They are called 'intermediate' because their diameter of 8-10 nm is in between that of actin filaments and myosin filaments in muscle cells, where they were first described. Their size is also in between actin filaments and microtubules.

Intermediate filaments are composed of a large family of cytoskeletal proteins that are expressed in a cell- and tissue-specific manner. The assembly starts with two chains interacting in parallel to form a coiled-coil dimer. Two of these dimers associate in an anti-parallel manner into a tetrameric subunit that subsequently adds to elongating intermediate filaments by aligning along the axis of the filament and packing together in a helical pattern. In contrast to actin filaments and microtubules, intermediate filaments are non-polarized structures because of the anti-parallel arrangement of the dimers. Another major distinction is that intermediate filaments, because they are non-polar filaments, do not support motor protein-mediated transport. However, recent research indicates that intermediate filaments interact in complex manners with the actin and microtubule network and may therefore indirectly influence transport processes (Chang and Goldman, 2004; Esue et al., 2006; Woll et al., 2005).

Intermediate filaments have long been thought to be static cytoskeletal structures. However, this is not in accordance with their plasticity during many physiological activities such as cell division and axon outgrowth in neurons. Indeed, it has been shown that continuous assembly of intermediate filament protein subunits into existing networks takes place, although the pool of unpolymerized proteins is small (Eriksson et al., 1992). During different phases of the cell

cycle or during differentiation, intermediate filaments undergo drastic structural modifications, that have been shown to be predominantly regulated by phosphorylation (Eriksson et al., 2004; Shea et al., 2004).

1.1.3 Microtubules

Microtubules are the third major type of cytoskeletal element in cells. They are involved in multiple essential cellular processes such as cell morphogenesis and organization, cell division, motility and intracellular transport. The dynamic properties of the microtubule network are crucial for many of these functions and they vary considerably between different areas of the cell and during the different stages of the cell cycle. For instance, migration of cells depends on a 'search-and-capture' mechanism in which searching microtubules interact with specific sites near the cell cortex, mainly at the 'leading edge' of a cell (Figure 3). Subsequent stabilization of the interacting microtubules gradually leads to a reorientation of the microtubule arrays, leaving the cell polarized in the direction of migration (Kirschner and Mitchison, 1986).

The basic subunits of microtubules are the closely related proteins α- and β-tubulin. With the help of several tubulin folding cofactors, α- and β-tubulin monomers form heterodimers (Gao et al., 1993; Tian et al., 1997). The heterodimers interact in a head-to-tail arrangement to form linear protofilaments. Subsequently, thirteen protofilaments associate laterally to form a 25 nm-wide hollow cylindrical tube. The organization of αβ-heterodimers in the microtubule lattice is polarized with the β-tubulin subunit exposed at the faster growing end (the plus-end) and the α-tubulin subunit exposed at the slower growing end (the minus-end) (Wade and Hyman, 1997). *In vivo*, microtubules are generally organized into radial arrays with the plus-ends exploring the cell periphery and the minus-ends anchored near the center of the cell in the centrosome or microtubule organizing center (MTOC). The centrosome is a ring-like structure that consists of two centrioles linked by centriole-interacting proteins and matrix proteins such as tektins and γ-tubulin (Bornens, 2002). Because of the accumulation of so-called γ-tubulin ring complexes, which greatly facilitate the nucleation and assembly of microtubules by serving as a template, the MTOC is the major, but not the only, site of microtubule assembly.

Both α- and β-tubulin monomers bind a GTP molecule, but because GTP bound to alpha-tubulin is 'sandwiched' between the two subunits of the dimer, only GTP bound to β-tubulin can be hydrolyzed. During microtubule polymerization GTP-bound tubulin heterodimers are added to the exposed ends. The GTP bound to the tubulin heterodimers is not hydrolyzed because β-tubulin is a weak GTPase when it is not inside the microtubule lattice. In the GTP-bound form the tubulin dimer is straight and supports both longitudinal and lateral interactions, thereby promoting microtubule assembly. As the polymer continues assembly, the GTP of β-tubulin inside the microtubule lattice is hydrolyzed to GDP, because the GTPase activity of β-tubulin is activated during its incorporation in the microtubule. In the GDP-bound state the tubulin dimer would favor a more curved conformation, but because it is 'captured' inside the lattice, this cannot happen. Thus, the energy accompanying tubulin curving is 'stored' inside the lattice. However, if GTP hydrolysis is faster than microtubule assembly, GDP-tubulin subunits will appear at the microtubule tip. These can assume a curved conformation and break up lateral interactions. This will start microtubule disassembly at the plus-end. Depolymerization is a rapid process because all of the tubulin inside the microtubule lattice is in the GDP conformation and 'ready' for disassembly (Figure 2).

When assembly remains faster than GTP hydrolysis, the microtubule is presumed to have a stabilizing 'cap' of GTP bound tubulin subunits, which prevents it from shrinking. Consequently,

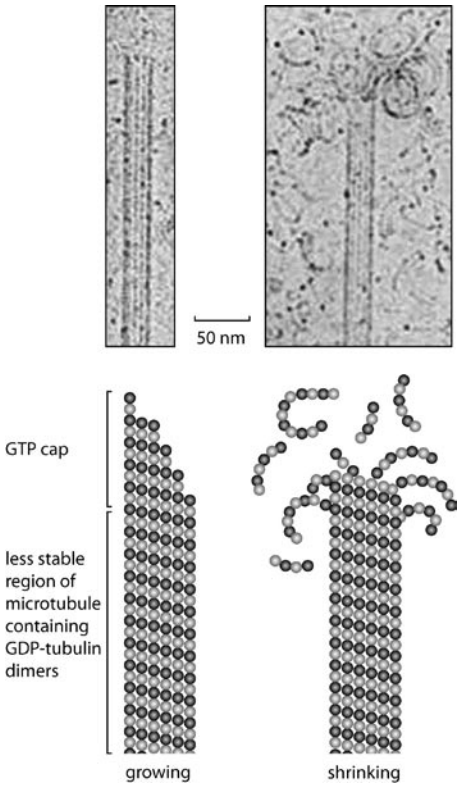

Figure 2. Dynamic microtubules
Electron micrograph and schematic representation of a growing and a shrinking microtubule. During growth, the microtubule is prevented from depolymerization through a stabilizing 'cap' of GTP bound tubulin subunits. When this cap is lost microtubules undergo catastrophe, i.e. transition from growth to shrinkage. Notice the change in microtubule structure, with straight protofilaments in the growing microtubule and outwardly curved protofilaments in the shrinking microtubule.
(*Molecular Biology Of The Cell, B. Alberts & others, 4th edition*)

the microtubule will continue to grow until a steady state is reached, that is, a state where the exchange of soluble tubulin with microtubule-associated molecules is constant. The energy required for this exchange is provided by the continuous hydrolysis of the GTP molecule bound to β-tubulin. Tubulin exchanges are thought to be caused by two mechanisms: treadmilling and dynamic instability.

The treadmilling-model, which is comparable to the one described for actin, is based on the differential behavior of the two microtubule ends. The plus-end continuously incorporates new tubulin heterodimers, while at the same time the minus-end loses them, leaving the length of the microtubule unchanged. This process causes the microtubule to move within cells. For treadmilling to occur the minus-end can obviously not be solidly anchored to the MTOC, otherwise no disassembly could occur there. The observed flux of tubulin molecules from kinetochores to centrosomes in spindle microtubules during mitosis (Margolis et al., 1978), can only be explained if the minus-ends are not solidly anchored.

When the microtubule minus-end is anchored and cannot contribute the free tubulin subunits necessary to sustain microtubule growth at the plus-ends dynamic instability is observed (Desai and Mitchison, 1997). Dynamic instability is explained by assuming a reduction in microtubule growth rate, which, as explained above, is associated with an increased chance of a switch from microtubule growth to depolymerization (i.e. catastrophe). As microtubules disassemble the higher concentration of tubulin subunits increases the chance of reverting microtubule shrinkage to growth (i.e. rescue). Both in vitro and in vivo microtubules undergo these frequent transitions from prolonged episodes of assembly to rapid disassembly (catastrophe) and vice

versa (rescue). Moreover, a microtubule can be pausing, during which its net length does not change. This dynamic behavior allows the microtubules to constantly explore the cytoplasm at the cell periphery.

Dynamic instability explains the observed behavior of individual microtubules at the cell periphery, where microtubules encounter the cell membrane, which acts as a barrier (Janson et al., 2003) and causes a drastic reduction in microtubule growth rates, resulting in catastrophe. The fact that microtubules oscillate between phases of growth and shrinkage at the cell periphery has lead to the suggestion that there must be microtubule rescue factors at work in the cytoplasm of cells (Komarova et al., 2002a).

The most drastic rearrangement of the microtubule network is observed when the mitotic

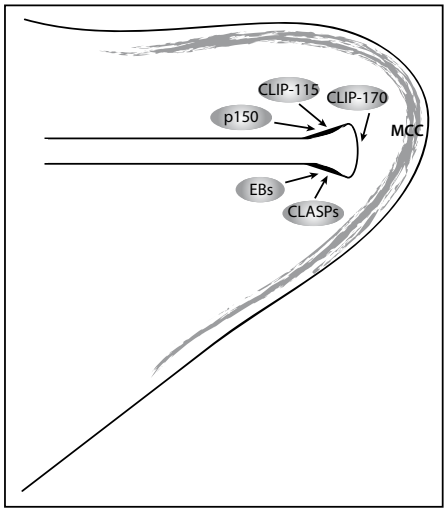

Figure 3. Microtubule binding proteins and the cell cortex
Simplified schematic representation of the proteins associating with the microtubule plus-end at the cell cortex based on what was known in 2001, when the project described in this thesis was started. At that time, the depicted proteins had been shown to interact with the microtubule plus-end, but the relationship between the proteins was largely unknown. It had also already been suggested that microtubules could be stabilized by a microtubule-capture-complex (MCC) at the cellular cortex. Although the composition of this complex remained to be elucidated, plus-end-binding proteins had already been implicated.

spindle is formed during mitosis and meiosis. This spindle contains three sets of microtubules. First, the chromosome-bound microtubules, with their plus-ends growing away from the poles and binding to the kinetochores of the chromosomes in a 'search-and-capture' manner. Secondly, the interpolar microtubules that do not bind the chromosomes. These serve to stabilize the spindle and enable spindle pole separation. A third set, the astral microtubules, projects out from the centrosomes toward the cell periphery and is important for the positioning of the spindle (Kline-Smith and Walczak, 2004; McIntosh and McDonald, 1989). The segregation of the chromosomes relies on the dynamic behavior of the mitotic microtubules and the function of microtubule based motor proteins (Sharp et al., 2000).

1.2 Microtubule plus-end-tracking proteins (+TIPs)

The structure of the microtubule network and its dynamic properties are greatly influenced by proteins that attach to microtubules, the microtubule-associated proteins (MAPs). Several of these proteins localize specifically to the microtubule plus-end and have, in living cultured mammalian cells, been shown to mark the plus-ends of growing microtubules, giving the appearance of 'tracking'. These proteins have therefore been termed plus-end-tracking proteins (+TIPs) (Schuyler and Pellman, 2001). At the time the project described in this thesis was started, only a few +TIPs had been identified and little was known about the interactions between the proteins (Figure 3).

During the recent years, the family of +TIPs has extended steadily (Akhmanova and Hoogenraad, 2005) and has been shown to contain the cytoplasmic linker proteins (CLIPs), the CLIP-associated proteins (CLASPs), the end-binding proteins (EB1-like family), the dynactin complex, and a number of other proteins such as the adenomatous polyposis coli (APC) tumor suppressor protein, the dynein regulatory factor LIS1, which is also a subunit of the platelet activating factor acetyl hydrolase enzyme complex, the spektraplakin ACF7, a RhoGEF, and even kinesin-13 family members, which are thought to catalyze microtubule catastrophe. In some organisms the microtubule-based, minus-end directed motor dynein has also been observed at microtubule plus-ends. Most of these proteins are highly conserved during evolution, which emphasizes the importance of a proper functioning microtubule cytoskeleton and the localization of +TIPs.

Although most +TIPs associate with microtubules directly, the distribution of the individual proteins might be influenced by interactions with different +TIPs. For example, APC is transported by kinesin II towards microtubule ends, but it can also associate directly with microtubules in vitro together with EB1 (Su et al., 1995), and in cultured cells APC localizes at microtubule ends by associating with EB1 (Mimori-Kiyosue et al., 2000b). On the other hand CLIP-170 and CLIP-115, which have very similar binding sites, are thought to compete for binding sites on the microtubule ends, since removal of CLIP-115 enhances the binding of CLIP-170 (Hoogenraad et al., 2002).

1.2.1 Cytoplasmic linker proteins (CLIPs)

Human CLIP-170 was the first protein shown to behave as a +TIP in living cells. A GFP-CLIP-170 fusion protein moved in comet-like dashes from the centrosome toward the cell periphery, highlighting the plus-ends of microtubules (Figure 4A) (Perez et al., 1999). Comparison of microtubule growth with GFP-CLIP-170 behavior showed that CLIP-170 specifically binds to the ends of growing microtubules and is displaced upon catastrophe (Komarova et al., 2002b; Perez et al., 1999). The tracking behavior of CLIP-170 is thought to be mediated by a treadmilling mechanism, in which the protein is added to the growing plus-end of the microtubule, remains stationary for a short period of time and dissociates shortly thereafter. This process creates the optical illusion of CLIP-170 molecules moving with the growing plus-end. Actually, individual molecules remain stationary, but because of the constant addition of new protein and the dissociation of previously bound protein, it looks as if the population of CLIP-170 molecules is surfing on the microtubule plus-end. Other proteins that are thought to treadmill are EB1 and dynactin (Carvalho et al., 2003).

Apart from treadmilling, two other mechanisms have been described to explain the specific association of protein with microtubule plus-ends. Some proteins track the plus-end by association with other +TIPs. This is called ‘hitchhiking’ on microtubules. For example, the budding yeast homologue of APC (Kar9p) is recruited to microtubules by the homologue of EB1 (Miller et al., 2000), as is the *Drosophila* homologue of CLIP-170 (D-CLIP-190) (Dzhindzhev et al., 2005). The third mechanism is motor-dependent transport towards the plus-ends, which requires the action of anterograde motor proteins, i.e. kinesins. This has been described for cytoplasmic dynein and dynactin in the filamentous fungus *Aspergillus nidulans* (Zhang et al., 2003) and for the yeast CLIP-170 homologues Tip1p (*S. pombe*) and Bik1p (*S. cervisiae*) (Busch et al., 2004; Carvalho et al., 2004). The three mechanisms described are not mutually exclusive. For example, APC is shown to interact with microtubule plus-ends in three ways: its microtubule binding domain allows direct binding, interaction with EB1 might result in hitchhiking and it is also actively transported (Askham et al., 2000; Jimbo et al., 2002; Mimori-Kiyosue et al., 2000).

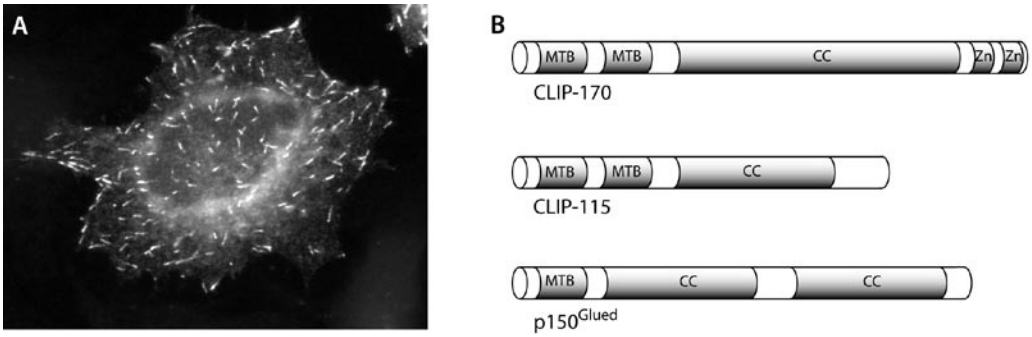

Figure 4. Cytoplasmic Linker Proteins
A. Visualization of CLIP-170 in a living cell. CLIP-170 fused to green fluorescent protein (GFP) appears as comet-like dashes at the tips of growing microtubules. **B.** Schematic representations of CLIP-170, CLIP-115 and the structurally similar dynactin component $p150^{Glued}$. MTB, microtubule-binding domain; CC, coiled coil; Zn, zinc knuckle (putative metal binding domain).
(Picture courtesy of A.J. van Haren)

After first having been identified as a nucleotide-sensitive microtubule binding protein (Rickard and Kreis, 1990), CLIP-170 was subsequently shown to be essential for the binding of endocytic vesicles to microtubules (Pierre et al., 1992). Later studies showed that CLIP-170 influences microtubule dynamics, serving as an anti-catastrophe factor in fission yeast (Brunner and Nurse, 2000), or as a rescue factor in mammalian cells (Bershadsky et al., ; Komarova et al., 2002a). CLIP-170 was also proposed to be involved in the capture of microtubules at the cell cortex via IQGAP1 and Cdc42 (Fukata et al., 2002) and in the formation of kinetochore-microtubule interactions (Tanenbaum et al., 2006). The localization of CLIP-170 at the kinetochores depends on the dynein-dynactin complexes (see section 1.2.4) (Dujardin et al., 1998). The link between CLIP-170 and the dynein-dynactin complexes is further established by the fact that overexpression of CLIP-170 enhances the accumulation of dynactin at the plus-end (Goodson et al., 2003; Valetti et al., 1999), while downregulation of CLIP-170 reduces dynactin accumulation (Lansbergen et al., 2004). The association between CLIP-170 and dynactin was proven to be direct (Lansbergen et al., 2004). In addition to its binding to dynactin, CLIP-170 has been shown to interact with other +TIPs. It directly binds to LIS1 (Coquelle et al., 2002), to CLASP1 and CLASP2 (Akhmanova et al., 2001), to IQGAP1 (Fukata et al., 2002) and to EB1, EB2 and EB3 (Komarova et al., 2005). Finally, CLIP-170 was shown to fold back upon itself through an interaction between its N- and C-termini, perhaps to prevent unwanted interactions with other proteins (Lansbergen et al., 2004).

The closest homologue of CLIP-170 in vertebrates, CLIP-115, is highly similar in structure (Figure 4B). They share two microtubule-binding (MTB) domains at their NH_2-terminus, that consist of two CAP_GLY motifs, surrounded by basic, serine-rich stretches. These CAP_GLY regions bind to microtubules by recognizing the COOH-terminal EEY/F motif of alpha-tubulin, which is also present in EB1-like proteins and in CLIP-170 itself (Honnappa et al., 2006). Accumulation of CLIPs at the microtubule end actually depends on the C-terminal tyrosine of alpha-tubulin (Peris et al., 2006). In both proteins, the microtubule binding domains are followed by long coiled-coil regions, which are involved in homo-dimerization. However, CLIP-115 lacks the C-terminal metal binding domain present in CLIP-170 (Figure 4B; De Zeeuw et al., 1997). Like CLIP-170, CLIP-115 interacts with the CLASPs and with EB1-like proteins, but not with LIS1, since this interaction depends on the CLIP-170-specific C-terminus. CLIP-115 has been implicated in the neurodevelopmental disorder Williams Syndrome (see also chapter 2) (Hoogenraad et al., 2002).

A third CLIP, CLIPR-59, does not localize to microtubules but is associated with the *trans*-Golgi network and the plasma membrane, in particular with lipid rafts. It was suggested to inhibit microtubule polymerization hence preventing the linkage between microtubules and the lipid rafts (Lallemand-Breitenbach et al., 2004). Thus, although CLIPR-59 carries similar microtubule binding domains as CLIP-115 and -170, it differs completely in function.

1.2.2 CLIP-associating proteins (CLASPs)

The search for common protein partners for CLIP-170 and CLIP-115 led to the identification of CLASP1 and CLASP2 (Akhmanova et al., 2001). Several isoforms of these proteins have been found, each containing a C-terminal CLIP-interaction region, but differing in their N-terminal domains. Apart from binding to CLIPs the CLASPs also associate with microtubules (Akhmanova et al., 2001), with EB1 and EB3 (Mimori-Kiyosue et al., 2005), with dynein (Grallert et al., 2006) and with CENPE (Hannak and Heald, 2006).

In interphase cells, CLASPs localize to the plus-ends of microtubules and to the Golgi apparatus, but their affinity for microtubules is spatially regulated in migrating cells (Akhmanova et al., 2001; Wittmann and Waterman-Storer, 2005). The local stabilization of microtubules at the leading edge by CLASP2 has been shown to polarize cells, which is necessary for efficient migration (Drabek et al., 2006). CLASPs exert their stabilizing function through repeated rescues of dynamic microtubule plus-ends at specific cortical regions (Mimori-Kiyosue et al., 2005) and through interaction with membrane-bound protein clusters. These clusters contain, among others, LL5β, ELKS and phosphatidylinositol-3,4,5-triposphate (PIP3) (Lansbergen et al., 2006). The function of CLASPs in polarization is also apparent during oogenesis in *Drosophila* (Mathe et al., 2003).

In addition to their function in migrating cells, CLASPs play an essential role in mitosis and meiosis. The *Drosophila* homologue Orbit/Mast and the *Xenopus* homologue Xorbit are involved in chromosome alignment, attachment of microtubules to kinetochores and maintenance of spindle bipolarity (Hannak and Heald, 2006; Inoue et al., 2000; Maiato et al., 2002). Human CLASPs are a component of the outer kinetochore region and are required for normal dynamics of kinetochore-associated microtubules and proper chromosome alignment and segregation (Maiato et al., 2003; Pereira et al., 2006).

1.2.3 End binding proteins (EBs)

The family of end binding proteins (EBs) represents a group of highly conserved proteins that have been found in every organism and nearly every cell type examined. While budding and fission yeast possess a single EB1 homologue (Beinhauer et al., 1997; Schwartz et al., 1997), higher organisms like *Drosophila melanogaster* and humans have at least three EB1 related genes (Tirnauer and Bierer, 2000). EB1 was first described as a protein interacting with APC (Su et al., 1995). A complex of EB1 and APC, together with the Rho-effector mDia, has been suggested to be involved in the local stabilization of microtubules at the leading edge of migrating cells (Wen et al., 2004). However, a recent report on the role of CLASP2 in microtubule stabilization contradicts an essential role of an APC-EB1 interaction in this process (Drabek et al., 2006). This does not rule out the possibility of EB1 involvement in microtubule stabilization via its interaction with the CLASPs (Mimori-Kiyosue et al., 2005).

Until now, several interaction partners have been established in addition to APC and the CLASPs, e.g. the CLIPs (Komarova et al., 2005), cytoplasmic dynein and components of the dynactin complex (Berrueta et al., 1999). The fact that EB1 has been shown to interact

with virtually all other +TIPs, and that these interactions have been demonstrated in different species, suggests a central and evolutionary conserved role for EB1 in several microtubule-based processes, such as the regulation of microtubule dynamics and microtubule-cortex interactions (Lansbergen and Akhmanova, 2006).

EB1 is considered to be a classical +TIP, localizing mainly to the growing tips of microtubules both during interphase and during mitosis (Berrueta et al., 1998; Busch and Brunner, 2004; Morrison et al., 1998). In fission yeast, however, it also binds the microtubule lattice with a low affinity (Busch and Brunner, 2004; Sandblad et al., 2006). With regard to the function of EB1, contradictory results have been reported. Although EB1 homologues in budding yeast and in *Drosophila melanogaster* seem to enhance microtubule dynamics by increasing the frequencies of catastrophe and rescue and inhibiting pausing (Rogers et al., 2002; Tirnauer et al., 1999), EB1 family proteins in fission yeast and *Xenopus* appear to function in microtubule stabilization by promoting microtubule growth and inhibiting catastrophes (Busch and Brunner, 2004; Tirnauer et al., 2002). Recently, the *Schizosaccharomyces pombe* homologue of EB1, Mal3p, was shown to bind specifically to the microtubule lattice seam which has a stabilizing effect (Sandblad et al., 2006).

In addition to their functions in interphase cells, EB1 homologues are important during cell division. EB1 was shown to be essential during all phases of the cell cycle. For example, the budding yeast homologue Bim1p is involved in spindle positioning. It forms the physical link between the microtubule end and the bud in the first step (Korinek et al., 2000; Lee et al., 2000) and was suggested to be required in a cytokinesis checkpoint (Muhua et al., 1998). In *Drosophila*, EB1 is also required for spindle positioning and for chromosomal segregation and spindle elongation (Rogers et al., 2002).

1.2.4 Microtubule-based motors

Among the proteins that localize to the microtubule plus-ends a number of motor proteins can be found. These include the kinesins, most of which are plus-end-directed, and the minus-end-directed dyneins. Together with the actin-based myosins these proteins are responsible for most intracellular movement.

The most extensively studied kinesin is kinesin-1, a dimeric protein that consists of two head-domains each containing a single ATP-binding site, a coiled-coil stalk domain and two tail domains. Hydrolysis of the ATP bound to the head-domains induces a conformational change. This conformational change is amplified through structural changes in the neck linker, a flexible region connecting the heads to the stalk domain (Mallik and Gross, 2004; Schliwa and Woehlke, 2003). These changes are used for movement of the motor protein. The head domains bind directly to the microtubule, while the tail domains associate with the cargo. Kinesin is an example of a processive motor, which means it can move along the microtubule for long distances without detaching. It is thought to move with a 'hand-over-hand' mechanism, in which one head domain at the time is attached to the microtubule and the free head moves towards a new binding site past the bound head (Asbury et al., 2003; Yildiz et al., 2004).

The accumulation of kinesins at the microtubule plus-ends allows them to exert functions in addition to intracellular transport. In budding yeast, kinesin Kip2p stabilizes microtubules by recruiting the CLIP-170 homologue Bik1p to the plus-end. It was also suggested to contribute to the cell cycle-specific changes in cytoplasmic microtubule dynamics by increasing the dynein accumulation at the plus-ends (Carvalho et al., 2004). The fission yeast kinesin Tea2 also regulates microtubule dynamics by recruiting a CLIP-170 homologue to the plus-ends (Busch

et al., 2004). Finally, MCAK is a very specialized kinesin. It slides along microtubules and localizes to the plus-end to then use its ATP-derived energy to depolymerize the microtubule (Helenius et al., 2006).

Another molecular motor accumulating at the microtubule plus-end is cytoplasmic dynein 1, hereafter referred to as dynein (cytoplasmic dynein 2 has not been identified as a +TIP and is mainly involved in slow transport within the flagellum (Pazour et al., 1999; Porter et al., 1999)). Dynein structure is fundamentally different from that of kinesins and myosins. A ring of seven globular domains of which six are ATPase domains forms the dynein head. Two projections extend from the head, the stalk and the stem. The stalk contains a microtubule-binding site and, hence is responsible for the contact with the microtubule. The stem, which is the N-terminal region of the heavy chain, mediates interactions of the head with other parts of the dynein complex and is responsible for cargo binding (Mallik and Gross, 2004; Vallee et al., 2004). Hydrolysis of ATP and subsequent release of ADP and phosphate is associated with the power stroke. Microtubule movement starts with binding of the stalk to the microtubule, causing a conformational change in the ATPases. This activates the release of ADP and phosphate. The rigid coupling between the head and the stem causes the rotation of the head around the motor-stem junction, leading to a translocation of the microtubule (Burgess et al., 2003).

Dynein is involved in a broad range of functions, including transport of membranous organelles, different aspects of chromosome behavior, mitotic spindle orientation, nuclear migration and cell migration (Schroer, 2004). Its localization to the microtubule plus-end, where it influences microtubule dynamics, is important in several of these functions. Dynein function in vesicle transport was shown to require the multisubunit protein complex dynactin (Gill et al., 1991). Each dynactin molecule contains 11 different polypeptide subunits, combined into an asymmetric molecule with two distinct structural domains, a rod domain and a projecting arm. The rod consists of the actin-related protein Arp1 and several other proteins and is thought to be responsible for cargo binding. The projecting arm contains the subunits p150^{Glued}, dynamitin and p24/22 (Schroer, 2004).

The largest subunit of dynactin, p150^{Glued}, is structurally highly similar to the CLIPs, with a microtubule-binding domain at the N-terminus and coiled-coil domains for dimerization. Hence, within the dynactin complex, p150^{Glued} is responsible for binding to microtubules. Here it transiently tethers cargo, which transforms dynein into a processive motor (King and Schroer, 2000). The second subunit, dynamitin, links the projecting arm of dynactin to the rod domain (Eckley et al., 1999; Schafer et al., 1994). Both p150^{Glued} and dynamitin are involved in motor binding and associate with cargo, e.g. via the Golgi-associated protein BICD (Hoogenraad et al., 2001; Hoogenraad et al., 2003). The p24/22 subunit of the projecting arm is suggested to interact with both p150^{Glued} and dynamitin (Eckley et al., 1999).

The opposing motors kinesin and dynein have been shown to function in the bi-directional transport of cargo, which has been shown for mitochondria, endosomes, secretory vesicles and others. Three mechanisms are possible in which opposing motor proteins might interact to establish bi-directional motion. First, they might bind the cargo alternately, with one motor dissociating and being replaced by a motor with opposite polarity (Figure 5A). Second, they might be involved in a tug of war, in which motor proteins bind the cargo and are active at the same moment and transport in a certain direction results when one of the motors successfully competes against the opposing motor (Figure 5B). Third, opposing motors bind simultaneously, but competition is avoided because the motor proteins coordinate their activity in such a way that the plus-end directed motor is turned off when the minus-end directed motor is active and vice versa (Figure 5C). Several results have been reported favoring the model of motor coordination,

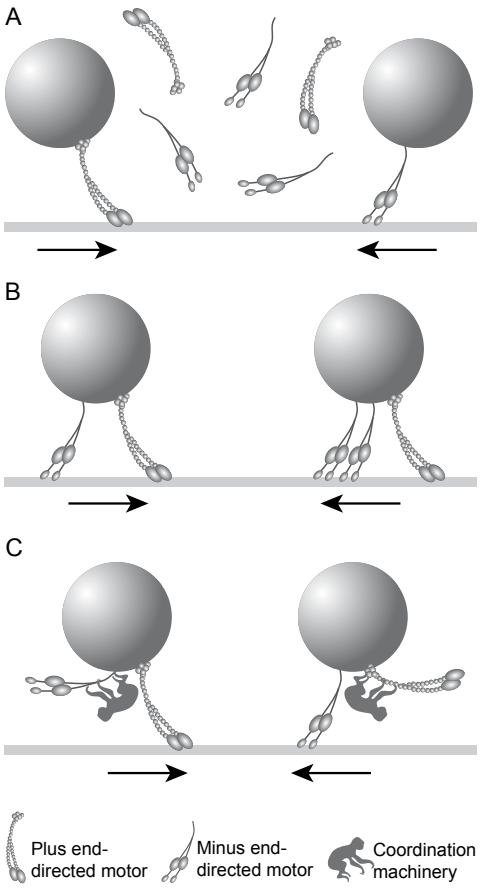

Figure 5. Possible mechanisms for bi-directional transport
A. Alternate binding. One type of motor replaces the other type of motor upon binding, thereby reversing the direction of transport. **B.** Tug-of-war. Opposite motors are bound simultaneously and compete against each other. The direction of transport depends on the relative strength of the competing motors. **C.** Coordinated activity. Opposite motors bind simultaneously and coordinate their activity in such a way that one type of motor is turned of when the opposite type of motor is active and vice versa. *(Adapted from Welte, M.A. 2004. Current Biology 14:R525-37)*

although no direct evidence has been provided (Welte, 2004). The tight coordination of the opposing motors is suggested to involve dynactin, since this complex has been shown to be required for the transport activity of both cytoplasmic dynein and kinesin II (Deacon et al., 2003).

1.2.5 Other +TIPs

As mentioned above, the group of +TIPs has expanded rapidly over the past few years (Akhmanova and Hoogenraad, 2005). Here a short description is given of a number of proteins that might interact with the CLIPs, either directly or via other +TIPs.

The protein LIS1 is involved in neuronal migration, hence it plays an essential role during brain development. Mutations in the *LIS1* gene result in severe brain malformation known as lissencephaly or smooth brain (Reiner et al., 1993). LIS1 localizes to the plus-ends of microtubules in interphase cells where it is shown to interact with CLIP-170, dynein and dynactin (Faulkner et al., 2000; Morris et al., 1998; Smith et al., 2000; Xiang et al., 1995). It was shown to affect microtubule dynamics, as it influences the frequencies of catastrophe and rescue (Han et al., 2001; Sapir et al., 1997). In addition it was found at the cortical sites contacting astral microtubules in mitotic cells, the cortex of dividing epithelial cells and the kinetochores where

it was shown to play a role at several points during cell division (Coquelle et al., 2002; Faulkner et al., 2000; Smith et al., 2000).

The adenomatous polyposis coli (APC) protein localizes to multiple parts of the cell and its distribution has been shown to be influenced by cell density and phosphorylation (Zhang et al., 2001). With regard to its microtubule-dependent localization, the subcellular distribution of APC is peculiar. It only localizes to the plus-ends of microtubules that protrude into actively migrating membrane structures, indicating a role in microtubule-dependent cell migration (Nathke, 1999). It was also observed to move along microtubules toward the plus-ends in the periphery of cell extensions, where it accumulates in nonmembrane-bounded clusters on the growing microtubule ends (Mimori-Kiyosue et al., 2000). The association of APC with the microtubules can be direct or via its interaction with EB1 (Su et al., 1995). APC was shown to stabilize microtubules and promote net growth in cellular extensions independent of EB1 (Kita et al., 2006). During mitosis APC localizes to the attachment sites between microtubules and kinetochores (Fodde et al., 2001; Kaplan et al., 2001). Together with EB1 it is involved in chromosome alignment, preventing chromosome missegregation (Draviam et al., 2006; Green et al., 2005).

Actin-crosslinking factor 7 (ACF7; also called MACF1) belongs to the plakin family of cytoskeletal linker proteins (Ruhrberg and Watt, 1997). It binds microtubules and actin, although its subcellular organization depends on the microtubule network rather than the actin cytoskeleton (Karakesisoglou et al., 2000). ACF7 decorates microtubules along their length but concentrates at the plus-ends in polarized cells. It was shown to transiently tether microtubules to the cortical actin cytoskeleton, a feature important for cell polarization (Kodama et al., 2003; Leung et al., 1999). Hence, ACF7 appears to function as a link between the actin and microtubule cytoskeleton. The localization of ACF7 at the cell cortex was shown to overlap with that of CLASP2, suggesting a regulatory function in the cortical localization of CLASP2 (Drabek et al., 2006). This resembles the relationship between CLASP2 and its interaction partners LL5β en ELKS (Lansbergen et al., 2006). It is yet unknown whether ACF7 and LL5β/ELKS function independently or in conjunction.

Finally, the neuron navigator proteins NAV1, NAV2 and NAV3 are the mammalian homologues of the *C. elegans* protein UNC-53, a protein controlling the directional guidance of a subset of migratory cells (Hedgecock et al., 1987; Maes et al., 2002). Only NAV1 has been shown to associate with microtubules, concentrating at the plus-ends. Protein expression is largely restricted to the nervous system, localizing mainly in neuritic distal ends, growth cones and branching points. Like Unc-53, NAV1 was proposed to function in the directional migration of neurons (Martinez-Lopez et al., 2005).

1.3 Microtubules and disease

Since an intact and functional cytoskeleton is essential for the maintenance of cells, it is not surprising that its malfunctioning has been implicated in numerous diseases. For example, cytoskeletal protein aberrations have been associated with several cardiovascular syndromes, neurodegenerative disorders, skin- and liver diseases and cancer (Ramaekers and Bosman, 2004). Although defects in all components of the cytoskeleton can lead to disease, the following section focuses on three disorders that have been linked to microtubules, namely Williams Syndrome (WS), Amyotrophic Lateral Sclerosis (ALS) and hydrocephalus caused by ciliary defects. These disorders might be linked to alterations in the function of the CLIPs or CLIP-interacting proteins such as dynein and dynactin.

1.3.1 Williams Syndrome

Williams Syndrome (or Williams-Beuren Syndrome) is a neurodevelopmental disorder for which prevalence estimates range from 1 in 20,000 to 1 in 7,500 live births (Morris and Mervis, 2000; Stromme et al., 2002). It is caused by a hemizygous deletion of the Williams Syndrome Critical Region (WSCR), a ~1,6 Mb region on chromosome 7q11.23 that contains ~28 genes. Patients are characterized by a typical 'elfin-like' facial appearance, combined with cardiovascular and neurological abnormalities. The cardiovascular problems, which include supravalvular aortic stenosis (SVAS), are caused by haploinsufficiency for elastin (*ELN*). This gene is deleted in 99% of the WS patients and is also implicated in some of the facial characteristics (Morris et al., 2003).

Not in all patients the complete WSCR is deleted. Analysis of the symptoms of individuals with smaller deletions has narrowed down the number of genes that could be responsible for the neurological and cognitive features of WS. At present, the candidate genes are *WBSCR11*, *CYLN2*, *GTF2I*, *NCF1* and *LIMK1*. To date, there are no reports linking *WBSCR11* or *NCF1* to any of the neurological symptoms of WS, but loss of *NCF1* is thought to protect a proportion of patients against hypertension caused by deletion of *ELN* (Del Campo et al., 2006). *GTF2I* is proposed to be associated with the mental retardation found in the majority of the individuals with WS (Morris et al., 2003). The other two genes (*LIMK1* and *CYLN2*) encode proteins involved in the regulation of actin and microtubule dynamics, respectively. LIM-kinase 1 phosphorylates the actin depolymerisation factor cofilin, preventing its binding to F-actin. It has recently been shown to control growth cone motility and morphology by regulating the activity of cofilin (Endo et al., 2003). As discussed above, CLIP-115 (encoded by *CYLN2*) regulates microtubule dynamics.

Analyses of mice deficient for either *Limk1* or *Cyln2* suggest the possible responsibility of these genes for some of the neurological abnormalities of WS patients (Hoogenraad et al., 2004). Both mouse strains show neurodevelopmental abnormalities that might mimic those found in WS. The *Limk1* deficient mouse suffers from increased locomotor activity and impaired spatial learning, combined with enhanced hippocampal long-term potentiation (LTP) (Meng et al., 2002). Studies of brain sections revealed changes in the morphology of dendritic spines of pyramidal neurons of cortex and hippocampus, probably caused by disruption of the actin cytoskeleton. Structural modifications of dendritic spines have recently been associated with learning and memory (Fukazawa et al., 2003; Pak et al., 2001), suggesting a direct link between *Limk1* deficiency and learning deficits. The *Cyln2* knockout mouse shows growth retardation, specific motor coordination defects, lower fear response and decreased hippocampal LTP (Hoogenraad et al., 2002). Morphological analysis of the brain showed enlargement of the ventricles and a smaller corpus callosum. Taken together, the absence of the genes *LIMK1* and *CYLN2* is likely to underlie at least part of the neurological features in WS, but further investigation into the functions of the other genes located in the WS region remains highly important.

1.3.2 Amyotrophic Lateral Sclerosis

Amyotrophic lateral sclerosis (ALS), also known as motor neuron disease (MND), is one of the most common adult onset neurodegenerative diseases. It has an incidence of 1-2 per 100,000 with a average age of onset between 50 and 60 years. The vast majority of the cases of ALS is sporadic, but 5-10% is familial. The disease is characterized by progressive muscle weakness and wasting because of progressive injury and cell death of motor neurons in the spinal cord, the brain stem and the motor cortex. Most patients die from neuromuscular respiratory failure.

The current understanding of the factors causing the neurodegeneration in ALS suggests the involvement of multiple mechanisms, including genetic factors, oxidative stress, protein aggregation and damaged cellular processes such as axonal transport (Shaw, 2005). One of the major causes of ALS is a mutated gene encoding the free radical scavenging enzyme superoxide dismutase 1 (SOD1) (Rosen et al., 1993). To date, more than 100 different mutations have been reported throughout the gene. The function of SOD1 is to convert the toxic waste product of mitochondrial oxidative phosphorylation, the superoxide free radicals, to hydrogen peroxide. Although not much is known about the pathways via which mutant SOD1 leads to the death of motor neurons, the evidence suggests that the mutant protein works through a toxic gain of function rather than a loss of function. The gain of function might influence different, possibly reinforcing, mechanisms such as oxidative stress, malfunction of mitochondria and protein aggregation (Bruijn et al., 2004).

One of the mechanisms proposed to cause ALS is the disruption of retrograde axonal transport, initiating the degeneration of motor neurons. Retrograde transport is driven by the motor protein cytoplasmic dynein and its essential cofactor dynactin. A point mutation in the gene encoding the p150 subunit of dynactin (*DCTN1*) was found in a family of ALS patients (Puls et al., 2003). In addition, overexpression of the dynamitin (p50) subunit of dynactin has been shown to disassemble dynactin (Echeverri et al., 1996). A similar disassembly of the dynactin complex was shown by overexpression of p50 in transgenic mice, resulting in the inhibition of retrograde axonal transport (LaMonte et al., 2002).

Studies of a SOD1 transgenic mouse model demonstrates that expression of the mutant SOD1 protein affects the accumulation of a neurotracer in motor neurons and alters the cellular distribution of dynein in primary motor neurons (Ligon et al., 2005). The decreased accumulation of neurotracer can either be caused by slowing of the dynein/dynactin mediated axonal transport along microtubules or by slowing of the uptake at neuromuscular junctions. The latter might also be an effect of impaired dynein/dynactin function, since these proteins also mediate synaptic stabilization (Eaton et al., 2002). Hence, multiple results suggest an important role for microtubule mediated retrograde transport in ALS.

1.3.3 Hydrocephalus

Hydrocephalus is a net accumulation of cerebrospinal fluid (CSF) resulting in dilatation of the inner brain ventricles (Figure 5A). If the hydrocephalus develops before the cranial sutures have closed the typical feature is a rounded and enlarged skull (Figure 5B). Hydrocephalus can be caused by overproduction of CSF, but more commonly it is a consequence of impairment of the CSF flow within the ventricular system (non-communicating hydrocephalus) or in the subarchnoid space (communicating hydrocephalus). Non-communicating hydrocephalus is typically accompanied with obstructions in the ventricular system, especially the narrowed segments such as the aqueduct of Sylvius. It is not yet clear whether the observed obstructions are causing the hydrocephalus or if they are the result of the compression exerted by the expanding hydrocephalic ventricles (Perez-Figares et al., 2001).

Non-communicating hydrocephalus is seen in a series of different transgenic mouse models e.g. mice lacking axonemal dynein heavy chain 5 (*MDNAH5*), neural adhesion molecule L1, sperm-associated antigen 6 (*Spag6*), DNA polymerase λ, and in mice expressing mutated Polaris (Ibanez-Tallon et al., 2002; Kobayashi et al., 2002; Rolf et al., 2001; Sapiro et al., 2002; Taulman et al., 2001). The hydrocephalus in these mice is often, but not always, accompanied by randomization of left-right asymmetry, recurrent respiratory infections and infertility.

In the mouse models mentioned above, the hydrocephalus has been ascribed to lost motility of the cilia of the ependymal cells lining the ventricular system. These motile cilia have a highly organized structure with a core (the axoneme) consisting of nine peripheral microtubule doublets surrounding two central microtubules (9+2 axoneme), in contrast to the generally immotile sensory cilia that lack the central microtubules (9+0 axoneme). Two dynein motors, the outer

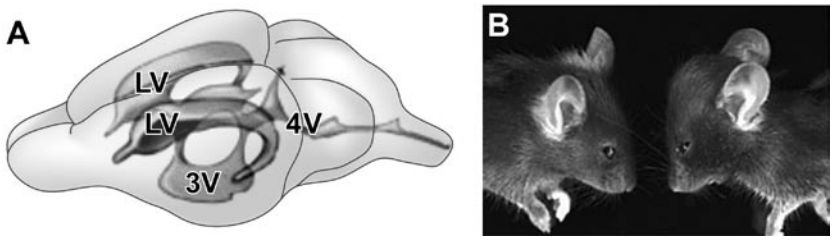

Figure 6. Hydrocephalus in mice
A. Schematic representation of the brain ventricles of normal mice. LV: lateral ventricle, 3V: 3rd ventricle, 4V: 4th ventricle. **B.** Example of a normal mouse (left) and a mouse suffering from hydrocephalus (right). The rounded and enlarged cranium of the mouse with hydrocephalus is typical, i.e. when the hydrocephalus develops before the cranial sutures have closed.
(http://jaxmice.jax.org/library/notes/490f.html)

and the inner dynein arms, are attached to the microtubule doublets. The ATPase activity of these dynein arms causes the microtubules to slide resulting in the beating of the cilia (Ibanez-Tallon et al., 2003). Although the bulk transport of CSF is achieved by changing blood pressures during systole and diastole (Bradley et al., 1986), the ciliary movement appears to be essential to maintain the flow of CSF through the ventricular system.

In conclusion, microtubules are involved in several highly important cellular processes like cell division, migration and intracellular transport. In particular the specialized microtubule plus-ends have an unique role in recruiting and concentrating proteins allowing them to interact and cooperate in a very intricate manner. Disturbance of the microtubule network and the protein interactions at the plus-ends can lead to a great variety of diseases, emphasizing the importance of this cellular component.

References

Akhmanova, A., and C.C. Hoogenraad. 2005. Microtubule plus-end-tracking proteins: mechanisms and functions. *Curr Opin Cell Biol*. 17:47-54.

Akhmanova, A., C.C. Hoogenraad, K. Drabek, T. Stepanova, B. Dortland, T. Verkerk, W. Vermeulen, B.M. Burgering, C.I. De Zeeuw, F. Grosveld, and N. Galjart. 2001. Clasps are CLIP-115 and -170 associating proteins involved in the regional regulation of microtubule dynamics in motile fibroblasts. *Cell*. 104:923-35.

Asbury, C.L., A.N. Fehr, and S.M. Block. 2003. Kinesin moves by an asymmetric hand-over-hand mechanism. *Science*. 302:2130-4.

Askham, J.M., P. Moncur, A.F. Markham, and E.E. Morrison. 2000. Regulation and function of the interaction between the APC tumour suppressor protein and EB1. *Oncogene*. 19:1950-8.

Beinhauer, J.D., I.M. Hagan, J.H. Hegemann, and U. Fleig. 1997. Mal3, the fission yeast homologue of the human APC-interacting protein EB-1 is required for microtubule integrity and the maintenance of cell form. *J Cell Biol*. 139:717-28.

Berrueta, L., S.K. Kraeft, J.S. Tirnauer, S.C. Schuyler, L.B. Chen, D.E. Hill, D. Pellman, and B.E. Bierer. 1998. The adenomatous polyposis coli-binding protein EB1 is associated with cytoplasmic and spindle microtubules. *Proc Natl Acad Sci U S A*. 95:10596-601.

Berrueta, L., J.S. Tirnauer, S.C. Schuyler, D. Pellman, and B.E. Bierer. 1999. The APC-associated protein EB1 associates with components of the dynactin complex and cytoplasmic dynein intermediate chain. *Curr Biol*. 9:425-8.

Bershadsky, A., A. Chausovsky, E. Becker, A. Lyubimova, and B. Geiger. 1996. Involvement of microtubules in the control of adhesion-dependent signal transduction. *Curr Biol*. 6:1279-89.

Bornens, M. 2002. Centrosome composition and microtubule anchoring mechanisms. *Curr Opin Cell Biol*. 14:25-34.

Bradley, W.G., Jr., K.E. Kortman, and B. Burgoyne. 1986. Flowing cerebrospinal fluid in normal and hydrocephalic states: appearance on MR images. *Radiology*. 159:611-6.

Bruijn, L.I., T.M. Miller, and D.W. Cleveland. 2004. Unraveling the mechanisms involved in motor neuron degeneration in ALS. *Annu Rev Neurosci*. 27:723-49.

Brunner, D., and P. Nurse. 2000. CLIP170-like tip1p spatially organizes microtubular dynamics in fission yeast. *Cell*. 102:695-704.

Burgess, S.A., M.L. Walker, H. Sakakibara, P.J. Knight, and K. Oiwa. 2003. Dynein structure and power stroke. *Nature*. 421:715-8.

Busch, K.E., and D. Brunner. 2004. The microtubule plus end-tracking proteins mal3p and tip1p cooperate for cell-end targeting of interphase microtubules. *Curr Biol*. 14:548-59.

Busch, K.E., J. Hayles, P. Nurse, and D. Brunner. 2004. Tea2p kinesin is involved in spatial microtubule organization by transporting tip1p on microtubules. *Dev Cell*. 6:831-43.

Carvalho, P., M.L. Gupta, Jr., M.A. Hoyt, and D. Pellman. 2004. Cell cycle control of kinesin-mediated transport of Bik1 (CLIP-170) regulates microtubule stability and dynein activation. *Dev Cell*. 6:815-29.

Carvalho, P., J.S. Tirnauer, and D. Pellman. 2003. Surfing on microtubule ends. *Trends Cell Biol*. 13:229-37.

Chang, L., and R.D. Goldman. 2004. Intermediate filaments mediate cytoskeletal crosstalk. *Nat Rev Mol Cell Biol*. 5:601-13.

Coquelle, F.M., M. Caspi, F.P. Cordelieres, J.P. Dompierre, D.L. Dujardin, C. Koifman, P. Martin, C.C. Hoogenraad, A. Akhmanova, N. Galjart, J.R. De Mey, and O. Reiner. 2002. LIS1, CLIP-170's key to the dynein/dynactin pathway. *Mol Cell Biol*. 22:3089-102.

De Zeeuw, C.I., C.C. Hoogenraad, E. Goedknegt, E. Hertzberg, A. Neubauer, F. Grosveld, and N. Galjart. 1997. CLIP-115, a novel brain-specific cytoplasmic linker protein, mediates the localization of dendritic lamellar bodies. *Neuron*. 19:1187-99.

Deacon, S.W., A.S. Serpinskaya, P.S. Vaughan, M. Lopez Fanarraga, I. Vernos, K.T. Vaughan, and V.I. Gelfand. 2003. Dynactin is required for bidirectional organelle transport. *J Cell Biol*. 160:297-301.

Del Campo, M., A. Antonell, L.F. Magano, F.J. Munoz, R. Flores, M. Bayes, and L.A. Perez Jurado. 2006. Hemizygosity at the NCF1 gene in patients with Williams-Beuren syndrome decreases their risk of hypertension. *Am J Hum Genet*. 78:533-42.

Desai, A., and T.J. Mitchison. 1997. Microtubule polymerization dynamics. *Annu Rev Cell Dev Biol*. 13:83-117.

Drabek, K., M. van Ham, T. Stepanova, K. Draegestein, R. van Horssen, C.L. Sayas, A. Akhmanova, T. Ten Hagen, R. Smits, R. Fodde, F. Grosveld, and N. Galjart. 2006. Role of CLASP2 in Microtubule Stabilization and the Regulation of Persistent Motility. *Curr Biol*. 16:2259-64.

Draviam, V.M., I. Shapiro, B. Aldridge, and P.K. Sorger. 2006. Misorientation and reduced stretching of aligned sister kinetochores promote chromosome missegregation in EB1- or APC-depleted cells. *Embo J*. 25:2814-27.

Dujardin, D., U.I. Wacker, A. Moreau, T.A. Schroer, J.E. Rickard, and J.R. De Mey. 1998. Evidence for a role of CLIP-170 in the establishment of metaphase chromosome alignment. *J Cell Biol*. 141:849-62.

Dzhindzhev, N.S., S.L. Rogers, R.D. Vale, and H. Ohkura. 2005. Distinct mechanisms govern the localisation of Drosophila CLIP-190 to unattached kinetochores and microtubule plus-ends. *J Cell Sci*. 118:3781-90.

Eaton, B.A., R.D. Fetter, and G.W. Davis. 2002. Dynactin is necessary for synapse stabilization. *Neuron*. 34:729-41.

Echeverri, C.J., B.M. Paschal, K.T. Vaughan, and R.B. Vallee. 1996. Molecular characterization of the 50-kD subunit of dynactin reveals function for the complex in chromosome alignment and spindle organization during mitosis. *J Cell Biol*. 132:617-33.

Eckley, D.M., S.R. Gill, K.A. Melkonian, J.B. Bingham, H.V. Goodson, J.E. Heuser, and T.A. Schroer. 1999. Analysis of dynactin subcomplexes reveals a novel actin-related protein associated with the arp1 minifilament pointed end. *J Cell Biol*. 147:307-20.

Endo, M., K. Ohashi, Y. Sasaki, Y. Goshima, R. Niwa, T. Uemura, and K. Mizuno. 2003. Control of growth cone motility and morphology by LIM kinase and Slingshot via phosphorylation and dephosphorylation of cofilin. *J Neurosci*. 23:2527-37.

Eriksson, J.E., T. He, A.V. Trejo-Skalli, A.S. Harmala-Brasken, J. Hellman, Y.H. Chou, and R.D. Goldman. 2004. Specific in vivo phosphorylation sites determine the assembly dynamics of vimentin intermediate filaments. *J Cell Sci*. 117:919-32.

Eriksson, J.E., P. Opal, and R.D. Goldman. 1992. Intermediate filament dynamics. *Curr Opin Cell Biol*. 4:99-104.

Esue, O., A.A. Carson, Y. Tseng, and D. Wirtz. 2006. A direct interaction between actin and vimentin filaments mediated by the tail domain of vimentin. *J Biol Chem*. 281:30393-9.

Faulkner, N.E., D.L. Dujardin, C.Y. Tai, K.T. Vaughan, C.B. O'Connell, Y. Wang, and R.B. Vallee. 2000. A role for the lissencephaly gene LIS1 in mitosis and cytoplasmic dynein function. *Nat Cell Biol*. 2:784-91.

Fodde, R., J. Kuipers, C. Rosenberg, R. Smits, M. Kielman, C. Gaspar, J.H. van Es, C. Breukel, J. Wiegant, R.H. Giles, and H. Clevers. 2001. Mutations in the APC tumour suppressor gene cause chromosomal instability. *Nat Cell Biol*. 3:433-8.

Fukata, M., T. Watanabe, J. Noritake, M. Nakagawa, M. Yamaga, S. Kuroda, Y. Matsuura, A. Iwamatsu, F. Perez, and K. Kaibuchi. 2002. Rac1 and Cdc42 capture microtubules through IQGAP1 and CLIP-170. *Cell*. 109:873-85.

Fukazawa, Y., Y. Saitoh, F. Ozawa, Y. Ohta, K. Mizuno, and K. Inokuchi. 2003. Hippocampal LTP is accompanied by enhanced F-actin content within the dendritic spine that is essential for late LTP maintenance in vivo. *Neuron*. 38:447-60.

Furukawa, R., and M. Fechheimer. 1997. The structure, function, and assembly of actin filament bundles. *Int Rev Cytol*. 175:29-90.

Gao, Y., I.E. Vainberg, R.L. Chow, and N.J. Cowan. 1993. Two cofactors and cytoplasmic chaperonin are required for the folding of alpha- and beta-tubulin. *Mol Cell Biol*. 13:2478-85.

Gill, S.R., T.A. Schroer, I. Szilak, E.R. Steuer, M.P. Sheetz, and D.W. Cleveland. 1991. Dynactin, a conserved, ubiquitously expressed component of an activator of vesicle motility mediated by cytoplasmic dynein. *J Cell Biol*. 115:1639-50.

Goodson, H.V., S.B. Skube, R. Stalder, C. Valetti, T.E. Kreis, E.E. Morrison, and T.A. Schroer. 2003. CLIP-170 interacts with dynactin complex and the APC-binding protein EB1 by different mechanisms. *Cell Motil Cytoskeleton*. 55:156-73.

Grallert, A., C. Beuter, R.A. Craven, S. Bagley, D. Wilks, U. Fleig, and I.M. Hagan. 2006. S. pombe CLASP needs dynein, not EB1 or CLIP170, to induce microtubule instability and slows polymerization rates at cell tips in a dynein-dependent manner. *Genes Dev*. 20:2421-36.

Green, R.A., R. Wollman, and K.B. Kaplan. 2005. APC and EB1 function together in mitosis to regulate spindle dynamics and chromosome alignment. *Mol Biol Cell*. 16:4609-22.

Han, G., B. Liu, J. Zhang, W. Zuo, N.R. Morris, and X. Xiang. 2001. The Aspergillus cytoplasmic dynein heavy chain and NUDF localize to microtubule ends and affect microtubule dynamics. *Curr Biol*. 11:719-24.

Hannak, E., and R. Heald. 2006. Xorbit/CLASP links dynamic microtubules to chromosomes in the Xenopus meiotic spindle. *J Cell Biol*. 172:19-25.

Hedgecock, E.M., J.G. Culotti, D.H. Hall, and B.D. Stern. 1987. Genetics of cell and axon migrations in Caenorhabditis elegans. *Development*. 100:365-82.

Helenius, J., G. Brouhard, Y. Kalaidzidis, S. Diez, and J. Howard. 2006. The depolymerizing kinesin MCAK uses lattice diffusion to rapidly target microtubule ends. *Nature*. 441:115-9.

Honnappa, S., O. Okhrimenko, R. Jaussi, H. Jawhari, I. Jelesarov, F.K. Winkler, and M.O. Steinmetz. 2006. Key interaction modes of dynamic +TIP networks. *Mol Cell*. 23:663-71.

Hoogenraad, C.C., A. Akhmanova, N. Galjart, and C.I. De Zeeuw. 2004. LIMK1 and CLIP-115: linking cytoskeletal defects to Williams syndrome. *Bioessays*. 26:141-50.

Hoogenraad, C.C., A. Akhmanova, S.A. Howell, B.R. Dortland, C.I. De Zeeuw, R. Willemsen, P. Visser, F. Grosveld, and N. Galjart. 2001. Mammalian Golgi-associated Bicaudal-D2 functions in the dynein-dynactin pathway by interacting with these complexes. *Embo J*. 20:4041-54.

Hoogenraad, C.C., B. Koekkoek, A. Akhmanova, H. Krugers, B. Dortland, M. Miedema, A. van Alphen, W.M. Kistler, M. Jaegle, M. Koutsourakis, N. Van Camp, M. Verhoye, A. van der Linden, I. Kaverina, F. Grosveld, C.I. De Zeeuw, and N. Galjart. 2002. Targeted mutation of Cyln2 in the Williams syndrome critical region links CLIP-115 haploinsufficiency to neurodevelopmental abnormalities in mice. *Nat Genet*. 32:116-27.

Hoogenraad, C.C., P. Wulf, N. Schiefermeier, T. Stepanova, N. Galjart, J.V. Small, F. Grosveld, C.I. de Zeeuw, and A. Akhmanova. 2003. Bicaudal D induces selective dynein-mediated microtubule minus end-directed transport. *Embo J*. 22:6004-15.

Huxley, H.E. 1963. Electron Microscope Studies on the Structure of Natural and Synthetic Protein Filaments from Striated Muscle. *J Mol Biol*. 16:281-308.

Ibanez-Tallon, I., S. Gorokhova, and N. Heintz. 2002. Loss of function of axonemal dynein Mdnah5 causes primary ciliary dyskinesia and hydrocephalus. *Hum Mol Genet*. 11:715-21.

Ibanez-Tallon, I., N. Heintz, and H. Omran. 2003. To beat or not to beat: roles of cilia in development and disease. *Hum Mol Genet*. 12 Spec No 1:R27-35.

Inoue, Y.H., M. do Carmo Avides, M. Shiraki, P. Deak, M. Yamaguchi, Y. Nishimoto, A. Matsukage, and D.M. Glover. 2000. Orbit, a novel microtubule-associated protein essential for mitosis in Drosophila melanogaster. *J Cell Biol*. 149:153-66.

Janson, M.E., M.E. de Dood, and M. Dogterom. 2003. Dynamic instability of microtubules is regulated by force. *J Cell Biol*. 161:1029-34.

Jimbo, T., Y. Kawasaki, R. Koyama, R. Sato, S. Takada, K. Haraguchi, and T. Akiyama. 2002. Identification of a link between the tumour suppressor APC and the kinesin superfamily. *Nat Cell Biol*. 4:323-7.

Kaplan, K.B., A.A. Burds, J.R. Swedlow, S.S. Bekir, P.K. Sorger, and I.S. Nathke. 2001. A role for the Adenomatous Polyposis Coli protein in chromosome segregation. *Nat Cell Biol*. 3:429-32.

Karakesisoglou, I., Y. Yang, and E. Fuchs. 2000. An epidermal plakin that integrates actin and microtubule networks at cellular junctions. *J Cell Biol*. 149:195-208.

King, S.J., and T.A. Schroer. 2000. Dynactin increases the processivity of the cytoplasmic dynein motor. *Nat Cell Biol*. 2:20-4.

Kirschner, M., and T. Mitchison. 1986. Beyond self-assembly: from microtubules to morphogenesis. *Cell*. 45:329-42.

Kita, K., T. Wittmann, I.S. Nathke, and C.M. Waterman-Storer. 2006. Adenomatous polyposis coli on microtubule plus ends in cell extensions can promote microtubule net growth with or without EB1. *Mol Biol Cell*. 17:2331-45.

Kline-Smith, S.L., and C.E. Walczak. 2004. Mitotic spindle assembly and chromosome segregation: refocusing on microtubule dynamics. *Mol Cell*. 15:317-27.

Kobayashi, Y., M. Watanabe, Y. Okada, H. Sawa, H. Takai, M. Nakanishi, Y. Kawase, H. Suzuki, K. Nagashima, K. Ikeda, and N. Motoyama. 2002. Hydrocephalus, situs inversus, chronic sinusitis, and male infertility in DNA polymerase lambda-deficient mice: possible implication for the pathogenesis of immotile cilia syndrome. *Mol Cell Biol*. 22:2769-76.

Kodama, A., I. Karakesisoglou, E. Wong, A. Vaezi, and E. Fuchs. 2003. ACF7: an essential integrator of microtubule dynamics. *Cell*. 115:343-54.

Komarova, Y., G. Lansbergen, N. Galjart, F. Grosveld, G.G. Borisy, and A. Akhmanova. 2005. EB1 and EB3 control CLIP dissociation from the ends of growing microtubules. *Mol Biol Cell*. 16:5334-45.

Komarova, Y.A., A.S. Akhmanova, S. Kojima, N. Galjart, and G.G. Borisy. 2002a. Cytoplasmic linker proteins promote microtubule rescue in vivo. *J Cell Biol*. 159:589-99.

Komarova, Y.A., I.A. Vorobjev, and G.G. Borisy. 2002b. Life cycle of MTs: persistent growth in the cell interior, asymmetric transition frequencies and effects of the cell boundary. *J Cell Sci*. 115:3527-39.

Korinek, W.S., M.J. Copeland, A. Chaudhuri, and J. Chant. 2000. Molecular linkage underlying microtubule orientation toward cortical sites in yeast. *Science*. 287:2257-9.

Lallemand-Breitenbach, V., M. Quesnoit, V. Braun, A. El Marjou, C. Pous, B. Goud, and F. Perez. 2004. CLIPR-59 is a lipid raft-associated protein containing a cytoskeleton-associated protein glycine-rich domain (CAP-Gly) that perturbs microtubule dynamics. *J Biol Chem*. 279:41168-78.

LaMonte, B.H., K.E. Wallace, B.A. Holloway, S.S. Shelly, J. Ascano, M. Tokito, T. Van Winkle, D.S. Howland, and E.L. Holzbaur. 2002. Disruption of dynein/dynactin inhibits axonal transport in motor neurons causing late-onset progressive degeneration. *Neuron*. 34:715-27.

Lansbergen, G., and A. Akhmanova. 2006. Microtubule plus end: a hub of cellular activities. *Traffic*. 7:499-507.

Lansbergen, G., I. Grigoriev, Y. Mimori-Kiyosue, T. Ohtsuka, S. Higa, I. Kitajima, J. Demmers, N. Galjart, A.B. Houtsmuller, F. Grosveld, and A. Akhmanova. 2006. CLASPs attach microtubule plus ends to the cell cortex through a complex with LL5beta. *Dev Cell*. 11:21-32.

Lansbergen, G., Y. Komarova, M. Modesti, C. Wyman, C.C. Hoogenraad, H.V. Goodson, R.P. Lemaitre, D.N. Drechsel, E. van Munster, T.W. Gadella, Jr., F. Grosveld, N. Galjart, G.G. Borisy, and A. Akhmanova. 2004. Conformational changes in CLIP-170 regulate its binding to microtubules and dynactin localization. *J Cell Biol*. 166:1003-14.

Lee, L., J.S. Tirnauer, J. Li, S.C. Schuyler, J.Y. Liu, and D. Pellman. 2000. Positioning of the mitotic spindle by a cortical-microtubule capture mechanism. *Science*. 287:2260-2.

Leung, C.L., D. Sun, M. Zheng, D.R. Knowles, and R.K. Liem. 1999. Microtubule actin cross-linking factor (MACF): a hybrid of dystonin and dystrophin that can interact with the actin and microtubule cytoskeletons. *J Cell Biol*. 147:1275-86.

Ligon, L.A., B.H. LaMonte, K.E. Wallace, N. Weber, R.G. Kalb, and E.L. Holzbaur. 2005. Mutant superoxide dismutase disrupts cytoplasmic dynein in motor neurons. *Neuroreport*. 16:533-6.

Maes, T., A. Barcelo, and C. Buesa. 2002. Neuron navigator: a human gene family with homology to unc-53, a cell guidance gene from Caenorhabditis elegans. *Genomics*. 80:21-30.

Maiato, H., E.A. Fairley, C.L. Rieder, J.R. Swedlow, C.E. Sunkel, and W.C. Earnshaw. 2003. Human CLASP1 is an outer kinetochore component that regulates spindle microtubule dynamics. *Cell*. 113:891-904.

Maiato, H., P. Sampaio, C.L. Lemos, J. Findlay, M. Carmena, W.C. Earnshaw, and C.E. Sunkel. 2002. MAST/Orbit has a role in microtubule-kinetochore attachment and is essential for chromosome alignment and maintenance of spindle bipolarity. *J Cell Biol*. 157:749-60.

Mallik, R., and S.P. Gross. 2004. Molecular motors: strategies to get along. *Curr Biol*. 14:R971-82.

Margolis, R.L., and L. Wilson. 1978. Opposite end assembly and disassembly of microtubules at steady state in vitro. *Cell*. 13:1-8.

Margolis, R.L., L. Wilson, and B.I. Keifer. 1978. Mitotic mechanism based on intrinsic microtubule behaviour. *Nature*. 272:450-2.

Martinez-Lopez, M.J., S. Alcantara, C. Mascaro, F. Perez-Branguli, P. Ruiz-Lozano, T. Maes, E. Soriano, and C. Buesa. 2005. Mouse neuron navigator 1, a novel microtubule-associated protein involved in neuronal migration. *Mol Cell Neurosci*. 28:599-612.

Mathe, E., Y.H. Inoue, W. Palframan, G. Brown, and D.M. Glover. 2003. Orbit/Mast, the CLASP orthologue of Drosophila, is required for asymmetric stem cell and cystocyte divisions and development of the polarised microtubule network that interconnects oocyte and nurse cells during oogenesis. *Development*. 130:901-15.

McIntosh, J.R., and K.L. McDonald. 1989. The mitotic spindle. *Sci Am*. 261:48-56.

Meng, Y., Y. Zhang, V. Tregoubov, C. Janus, L. Cruz, M. Jackson, W.Y. Lu, J.F. MacDonald, J.Y. Wang, D.L. Falls, and Z. Jia. 2002. Abnormal spine morphology and enhanced LTP in LIMK-1 knockout mice. *Neuron*. 35:121-33.

Miller, R.K., S.C. Cheng, and M.D. Rose. 2000. Bim1p/Yeb1p mediates the Kar9p-dependent cortical attachment of cytoplasmic microtubules. *Mol Biol Cell*. 11:2949-59.

Mimori-Kiyosue, Y., I. Grigoriev, G. Lansbergen, H. Sasaki, C. Matsui, F. Severin, N. Galjart, F. Grosveld, I. Vorobjev, S. Tsukita, and A. Akhmanova. 2005. CLASP1 and CLASP2 bind to EB1 and regulate microtubule plus-end dynamics at the cell cortex. *J Cell Biol*. 168:141-53.

Mimori-Kiyosue, Y., N. Shiina, and S. Tsukita. 2000. Adenomatous polyposis coli (APC) protein moves along microtubules and concentrates at their growing ends in epithelial cells. *J Cell Biol*. 148:505-18.

Mimori-Kiyosue, Y., N. Shiina, and S. Tsukita. 2000b. The dynamic behavior of the APC-binding protein EB1 on the distal ends of microtubules. *Curr Biol*. 10:865-8.

Morris, C.A., and C.B. Mervis. 2000. Williams syndrome and related disorders. *Annu Rev Genomics Hum Genet*. 1:461-84.

Morris, C.A., C.B. Mervis, H.H. Hobart, R.G. Gregg, J. Bertrand, G.J. Ensing, A. Sommer, C.A. Moore, R.J. Hopkin, P.A. Spallone, M.T. Keating, L. Osborne, K.W. Kimberley, and A.D. Stock. 2003. GTF2I hemizygosity implicated in mental retardation in Williams syndrome: genotype-phenotype analysis of five families with deletions in the Williams syndrome region. *Am J Med Genet A*. 123:45-59.

Morris, N.R., V.P. Efimov, and X. Xiang. 1998. Nuclear migration, nucleokinesis and lissencephaly. *Trends Cell Biol*. 8:467-70.

Morrison, E.E., B.N. Wardleworth, J.M. Askham, A.F. Markham, and D.M. Meredith. 1998. EB1, a protein which interacts with the APC tumour suppressor, is associated with the microtubule cytoskeleton throughout the cell cycle. *Oncogene*. 17:3471-7.

Muhua, L., N.R. Adames, M.D. Murphy, C.R. Shields, and J.A. Cooper. 1998. A cytokinesis checkpoint requiring the yeast homologue of an APC-binding protein. *Nature*. 393:487-91.

Mullins, R.D., J.A. Heuser, and T.D. Pollard. 1998. The interaction of Arp2/3 complex with actin: nucleation, high affinity pointed end capping, and formation of branching networks of filaments. *Proc Natl Acad Sci U S A*. 95:6181-6.

Nathke, I.S. 1999. The adenomatous polyposis coli protein. *Mol Pathol*. 52:169-73.

Pak, D.T., S. Yang, S. Rudolph-Correia, E. Kim, and M. Sheng. 2001. Regulation of dendritic spine morphology by SPAR, a PSD-95-associated RapGAP. *Neuron*. 31:289-303.

Pazour, G.J., B.L. Dickert, and G.B. Witman. 1999. The DHC1b (DHC2) isoform of cytoplasmic dynein is required for flagellar assembly. *J Cell Biol*. 144:473-81.

Pereira, A.L., A.J. Pereira, A.R. Maia, K. Drabek, C.L. Sayas, P.J. Hergert, M. Lince-Faria, I. Matos, C. Duque, T. Stepanova, C.L. Rieder, W.C. Earnshaw, N. Galjart, and H. Maiato. 2006. Mammalian CLASP1 and CLASP2 Cooperate to Ensure Mitotic Fidelity by Regulating Spindle and Kinetochore Function. *Mol Biol Cell*. 17:4526-4542.

Perez-Figares, J.M., A.J. Jimenez, and E.M. Rodriguez. 2001. Subcommissural organ, cerebrospinal fluid circulation, and hydrocephalus. *Microsc Res Tech*. 52:591-607.

Perez, F., G.S. Diamantopoulos, R. Stalder, and T.E. Kreis. 1999. CLIP-170 highlights growing microtubule ends in vivo. *Cell*. 96:517-27.

Peris, L., M. Thery, J. Faure, Y. Saoudi, L. Lafanechere, J.K. Chilton, P. Gordon-Weeks, N. Galjart, M. Bornens, L. Wordeman, J. Wehland, A. Andrieux, and D. Job. 2006. Tubulin tyrosination is a major factor affecting the recruitment of CAP-Gly proteins at microtubule plus ends. *J Cell Biol*. 174:839-49.

Pierre, P., J. Scheel, J.E. Rickard, and T.E. Kreis. 1992. CLIP-170 links endocytic vesicles to microtubules. *Cell*. 70:887-900.

Pollard, T.D., L. Blanchoin, and R.D. Mullins. 2000. Molecular mechanisms controlling actin filament dynamics in nonmuscle cells. *Annu Rev Biophys Biomol Struct*. 29:545-76.

Porter, M.E., R. Bower, J.A. Knott, P. Byrd, and W. Dentler. 1999. Cytoplasmic dynein heavy chain 1b is required for flagellar assembly in Chlamydomonas. *Mol Biol Cell*. 10:693-712.

Puls, I., C. Jonnakuty, B.H. LaMonte, E.L. Holzbaur, M. Tokito, E. Mann, M.K. Floeter, K. Bidus, D. Drayna, S.J. Oh, R.H. Brown, Jr., C.L. Ludlow, and K.H. Fischbeck. 2003. Mutant dynactin in motor neuron disease. *Nat Genet*. 33:455-6.

Ramaekers, F.C., and F.T. Bosman. 2004. The cytoskeleton and disease. *J Pathol*. 204:351-4.

Reiner, O., R. Carrozzo, Y. Shen, M. Wehnert, F. Faustinella, W.B. Dobyns, C.T. Caskey, and D.H. Ledbetter. 1993. Isolation of a Miller-Dieker lissencephaly gene containing G protein beta-subunit-like repeats. *Nature*. 364:717-21.

Rickard, J.E., and T.E. Kreis. 1990. Identification of a novel nucleotide-sensitive microtubule-binding protein in HeLa cells. *J Cell Biol*. 110:1623-33.

Rogers, S.L., G.C. Rogers, D.J. Sharp, and R.D. Vale. 2002. Drosophila EB1 is important for proper assembly, dynamics, and positioning of the mitotic spindle. *J Cell Biol*. 158:873-84.

Rolf, B., M. Kutsche, and U. Bartsch. 2001. Severe hydrocephalus in L1-deficient mice. *Brain Res*. 891:247-52.

Rosen, D.R., T. Siddique, D. Patterson, D.A. Figlewicz, P. Sapp, A. Hentati, D. Donaldson, J. Goto, J.P. O'Regan, H.X. Deng, and et al. 1993. Mutations in Cu/Zn superoxide dismutase gene are associated with familial amyotrophic lateral sclerosis. *Nature*. 362:59-62.

Ruhrberg, C., and F.M. Watt. 1997. The plakin family: versatile organizers of cytoskeletal architecture. *Curr Opin Genet Dev*. 7:392-7.

Sandblad, L., K.E. Busch, P. Tittmann, H. Gross, D. Brunner, and A. Hoenger. 2006. The Schizosaccharomyces pombe EB1 Homolog Mal3p Binds and Stabilizes the Microtubule Lattice Seam. *Cell*. 127:1415-24.

Sapir, T., M. Elbaum, and O. Reiner. 1997. Reduction of microtubule catastrophe events by LIS1, platelet-activating factor acetylhydrolase subunit. *Embo J*. 16:6977-84.

Sapiro, R., I. Kostetskii, P. Olds-Clarke, G.L. Gerton, G.L. Radice, and I.J. Strauss. 2002. Male infertility, impaired sperm motility, and hydrocephalus in mice deficient in sperm-associated antigen 6. *Mol Cell Biol*. 22:6298-305.

Schafer, D.A., S.R. Gill, J.A. Cooper, J.E. Heuser, and T.A. Schroer. 1994. Ultrastructural analysis of the dynactin complex: an actin-related protein is a component of a filament that resembles F-actin. *J Cell Biol*. 126:403-12.

Schliwa, M., and G. Woehlke. 2003. Molecular motors. *Nature*. 422:759-65.

Schroer, T.A. 2004. Dynactin. *Annu Rev Cell Dev Biol*. 20:759-79.

Schuyler, S.C., and D. Pellman. 2001. Microtubule "plus-end-tracking proteins": The end is just the beginning. *Cell*. 105:421-4.

Schwartz, K., K. Richards, and D. Botstein. 1997. BIM1 encodes a microtubule-binding protein in yeast. *Mol Biol Cell*. 8:2677-91.

Sharp, D.J., G.C. Rogers, and J.M. Scholey. 2000. Microtubule motors in mitosis. *Nature*. 407:41-7.

Shaw, P.J. 2005. Molecular and cellular pathways of neurodegeneration in motor neurone disease. *J Neurol Neurosurg Psychiatry*. 76:1046-57.

Shea, T.B., J.T. Yabe, D. Ortiz, A. Pimenta, P. Loomis, R.D. Goldman, N. Amin, and H.C. Pant. 2004. Cdk5 regulates axonal transport and phosphorylation of neurofilaments in cultured neurons. *J Cell Sci*. 117:933-41.

Smith, D.S., M. Niethammer, R. Ayala, Y. Zhou, M.J. Gambello, A. Wynshaw-Boris, and L.H. Tsai. 2000. Regulation of cytoplasmic dynein behaviour and microtubule organization by mammalian Lis1. *Nat Cell Biol*. 2:767-75.

Stromme, P., P.G. Bjornstad, and K. Ramstad. 2002. Prevalence estimation of Williams syndrome. *J Child Neurol*. 17:269-71.

Su, L.K., M. Burrell, D.E. Hill, J. Gyuris, R. Brent, R. Wiltshire, J. Trent, B. Vogelstein, and K.W. Kinzler. 1995. APC binds to the novel protein EB1. *Cancer Res*. 55:2972-7.

Tanenbaum, M.E., N. Galjart, M.A. van Vugt, and R.H. Medema. 2006. CLIP-170 facilitates the formation of kinetochore-microtubule attachments. *Embo J*. 25:45-57.

Taulman, P.D., C.J. Haycraft, D.F. Balkovetz, and B.K. Yoder. 2001. Polaris, a protein involved in left-right axis patterning, localizes to basal bodies and cilia. *Mol Biol Cell*. 12:589-99.

Tian, G., S.A. Lewis, B. Feierbach, T. Stearns, H. Rommelaere, C. Ampe, and N.J. Cowan. 1997. Tubulin subunits exist in an activated conformational state generated and maintained by protein cofactors. *J Cell Biol*. 138:821-32.

Tirnauer, J.S., and B.E. Bierer. 2000. EB1 proteins regulate microtubule dynamics, cell polarity, and chromosome stability. *J Cell Biol*. 149:761-6.

Tirnauer, J.S., S. Grego, E.D. Salmon, and T.J. Mitchison. 2002. EB1-microtubule interactions in Xenopus egg extracts: role of EB1 in microtubule stabilization and mechanisms of targeting to microtubules. *Mol Biol Cell*. 13:3614-26.

Tirnauer, J.S., E. O'Toole, L. Berrueta, B.E. Bierer, and D. Pellman. 1999. Yeast Bim1p promotes the G1-specific dynamics of microtubules. *J Cell Biol*. 145:993-1007.

Valetti, C., D.M. Wetzel, M. Schrader, M.J. Hasbani, S.R. Gill, T.E. Kreis, and T.A. Schroer. 1999. Role of dynactin in endocytic traffic: effects of dynamitin overexpression and colocalization with CLIP-170. *Mol Biol Cell*. 10:4107-20.

Vallee, R.B., J.C. Williams, D. Varma, and L.E. Barnhart. 2004. Dynein: An ancient motor protein involved in multiple modes of transport. *J Neurobiol*. 58:189-200.

Wade, R.H., and A.A. Hyman. 1997. Microtubule structure and dynamics. *Curr Opin Cell Biol*. 9:12-7.

Wegner, A. 1976. Head to tail polymerization of actin. *J Mol Biol*. 108:139-50.

Welte, M.A. 2004. Bidirectional transport along microtubules. *Curr Biol*. 14:R525-37.

Wen, Y., C.H. Eng, J. Schmoranzer, N. Cabrera-Poch, E.J. Morris, M. Chen, B.J. Wallar, A.S. Alberts, and G.G. Gundersen. 2004. EB1 and APC bind to mDia to stabilize microtubules downstream of Rho and promote cell migration. *Nat Cell Biol*. 6:820-30.

Wittmann, T., and C.M. Waterman-Storer. 2005. Spatial regulation of CLASP affinity for microtubules by Rac1 and GSK3beta in migrating epithelial cells. *J Cell Biol*. 169:929-39.

Woll, S., R. Windoffer, and R.E. Leube. 2005. Dissection of keratin dynamics: different contributions of the actin and microtubule systems. *Eur J Cell Biol*. 84:311-28.

Xiang, X., A.H. Osmani, S.A. Osmani, M. Xin, and N.R. Morris. 1995. NudF, a nuclear migration gene in Aspergillus nidulans, is similar to the human LIS-1 gene required for neuronal migration. *Mol Biol Cell*. 6:297-310.

Yildiz, A., M. Tomishige, R.D. Vale, and P.R. Selvin. 2004. Kinesin walks hand-over-hand. *Science*. 303:676-8.

Zhang, F., R.L. White, and K.L. Neufeld. 2001. Cell density and phosphorylation control the subcellular localization of adenomatous polyposis coli protein. *Mol Cell Biol*. 21:8143-56.

Zhang, J., S. Li, R. Fischer, and X. Xiang. 2003. Accumulation of cytoplasmic dynein and dynactin at microtubule plus ends in Aspergillus nidulans is kinesin dependent. *Mol Biol Cell*. 14:1479-88.

Chapter 2

Targeted mutation of *Cyln2* in the Williams syndrome critical region links CLIP-115 haploinsufficiency to neurodevelopmental abnormalities in mice

Nat. Genet. (2002) 32: 116-127

Chapter 2

Targeted mutation of *Cyln2* in the Williams syndrome critical region links CLIP-115 haploinsufficiency to neurodevelopmental abnormalities in mice

Casper C. Hoogenraad[1,2], Bas Koekkoek[2], Anna Akhmanova[1], Harm Krugers[3], Bjorn Dortland[1], **Marja Miedema**[1], Arjan van Alphen[2], Werner M. Kistler[2], Martine Jaegle[1], Manoussos Koutsourakis[1], Nadja Van Camp[4], Marleen Verhoye[4], Annemie van der Linden[4], Irina Kaverina[5], Frank Grosveld[1], Chris. I De Zeeuw[2] and Niels Galjart[1]

[1] MGC Department of Cell Biology and Genetics, Erasmus University, P.O. Box 1738, 3000 DR Rotterdam, The Netherlands. [2] MGC Department of Neuroscience, Erasmus University, P.O. Box 1738, 3000 DR Rotterdam, The Netherlands. [3] Swammerdam Institute for Life Sciences, University of Amsterdam, The Netherlands. [4] Bio-Imaging Lab, University of Antwerp (RUCA), Belgium. [5] Institute of Molecular Biology, Austrian Academy of Sciences, Salzburg, Austria.

Abstract

Williams Syndrome is a neurodevelopmental disorder caused by the hemizygous deletion of 1.6 Mb on human chromosome 7q11.23. This region comprises the *CYLN2* gene, encoding CLIP-115, a microtubule binding protein of 115 kD. Using a gene-targeting approach, we provide evidence that mice with haploinsufficiency for *Cyln2* have features reminiscent of Williams syndrome, including mild growth deficiency, brain abnormalities, hippocampal dysfunction and particular deficits in motor coordination. Absence of CLIP-115 also leads to increased levels of CLIP-170 (a closely related cytoplasmic linker protein) and dynactin at the tips of growing microtubules. This protein redistribution may affect dynein motor regulation and, together with the loss of CLIP-115-specific functions, underlie neurological alterations in Williams syndrome.

Introduction

Williams (or Williams-Beuren) Syndrome (OMIM 194050) is a rare neurodevelopmental disorder, with an incidence of 1 in 20,000. It is characterized by cardiovascular abnormalities (particularly supravalvular aortic stenosis, SVAS), transient juvenile hypercalcemia, abnormal weight gain and growth, and unusual facial features (Morris et al., 1988). In addition, individuals with Williams syndrome generally have a unique neurological and behavioral profile (Bellugi et al., 1999). Affected individuals have poor spatial cognition, but have notably intact language and musical abilities and relatively strong face-processing ability. Although they are not ataxic, individuals with Williams syndrome have coordination problems that are particularly obvious in walking up or down a staircase. Affected individuals are highly sensitive to certain classes of sounds, and have IQs in the mild to moderate range of mental retardation. Other characteristic behaviors include a friendly, outgoing personality and an apparent lack of fear.

Williams syndrome is caused by the hemizygous deletion of a region of approximately 1.6 Mb (the WS critical region, or WSCR) of chromosome band 7q11.23 (Francke, 1999). The WSCR contains at least 17 genes, including those encoding syntaxin 1A (*STX1A*), elastin (*ELN*), LIM kinase 1 (*LIMK1*) and CLIP-115 (*CYLN2*). The region is bordered by repeats, leading to the hypothesis that Williams syndrome is caused by illegitimate homologous recombination at the repeats during meiosis. Affected individuals carrying minor deletions that span only part of the WSCR (Osborne, 1999) have been identified, however. Study of these individuals and of affected individuals with point mutations has established that haploinsufficiency for *ELN* is linked to cardiovascular abnormalities in Williams syndrome, particularly SVAS (Olson et al., 1995; Tassabehji et al., 1997). It has also been suggested that insufficiency of LIM kinase 1 results in visuo-spatial cognition problems (Frangiskakis et al., 1996), although more recent studies have not verified this hypothesis (Tassabehji et al., 1999). Therefore, although deficiency of the *LIMK1* gene may contribute to part of the cognitive problems in Williams syndrome, it is now thought that other genes are responsible for most of the behavioral abnormalities associated with Williams syndrome. Deletion mapping in individuals with partial phenotypes and atypical deletions indicates that these genes are probably located in a region telomeric to *RFC2* that contains the *CYLN2*, *GTF2IRD1* and *GTF2I* loci (Francke, 1999; Osborne, 1999; Tassabehji et al., 1999).

We have cloned the cDNA encoding the CLIP-115, which is most abundantly expressed in dendrites and cell bodies of many neurons in the brain (De Zeeuw et al., 1997). Both CLIP-115 and CLIP-170 belong to a group of proteins that specifically associate with the ends of growing microtubules (Perez et al., 1999; Schuyler and Pellman, 2001). These proteins are believed to have distinct roles in regulating MT dynamics and in establishing interactions between microtubule tips and various cellular structures, including cargoes destined for microtubule-based, minus-end directed transport by dynein. In line with this view, both CLIPs interact with CLASPs, which are proteins involved in the regional stabilization of microtubules at the leading edge of motile fibroblasts (Akhmanova et al., 2001). Moreover, the ortholog of CLIP170 in fission yeast has been shown to spatially organize microtubular dynamics (Brunner and Nurse, 2000). In turn, CLIP-170 functions in the recruitment of dynactin, a protein complex that regulates dynein processivity, to the distal ends of microtubules (Valetti et al., 1999; Vaughan et al., 1999). CLIP-170 also regulates localization of LIS1, a protein implicated in brain development (Coquelle et al., 2002) and in several processes mediated by the dynein-dynactin pathway, to microtubule tips (Reiner et al., 1993). These data indicate that CLIP-170 has a role related to dynein and that this is mediated by the carboxy-terminal metal-binding motif of CLIP-170 that is not conserved in CLIP-115.

The gene *CYLN2*, encoding CLIP-115, is located in the WSCR (Hoogenraad et al., 1998; Osborne et al., 1996). In mice, *Cyln2* is located at the telomeric end of chromosome 5 (Hoogenraad et al., 1998), in an area orthologous to human chromosome 7q11.23 (Valero et al. 2000). In both organisms, the gene is positioned between the *LIMK1* and *GTF2I* loci (Peoples et al., 2000; Valero et al., 2000). Here we describe the generation of an inducible *Cyln2*-knockout allele. Mice carrying a deletion of *Cyln2* show mild growth deficiency and brain abnormalities, altered hippocampal functioning and specific deficits in motor coordination. These features partially mimic those of Williams syndrome and were observed in heterozygous *Cyln2*-knockout mice, indicating that haploinsufficiency for *CYLN2* is linked to neurodevelopmental features of Williams syndrome. Cell biological analysis revealed that absence of CLIP-115 did not significantly alter MT dynamics, but did enhance accumulation of CLIP-170 and dynactin at microtubule tips. This might affect the proper regulation of dynein motor activity. Together with the loss of functions specific to CLIP-115, the perturbation of CLIP-like protein distributions at microtubule tips might underlie neurodevelopmental problems in *Cyln2*-knockout mice and individuals with Williams syndrome.

Results

An inducible Cyln2 knock out allele

To inactivate *Cyln2*, we introduced a neomycin-resistance gene surrounded by *lox*P sequences into intron 2, and a puromycin-selection marker, surrounded by *lox*P sequences and followed by a modified β-galactosidase (*lacZ*) reporter gene, downstream of *Cyln2* (Fig. 1*a*). We introduced the resistance markers by two sequential rounds of homologous recombination (first round, puromycin cassette, 12 % of picked clones targeted; second round, neomycin cassette, 15 % targeted). Their integration was confirmed by a combination of Southern-blot, PCR and FISH analysis (Fig. 1*b*, *c* and data not shown). We named the doubly targeted *Cyln2* allele CLIP-T (Fig. 1*a*). Subsequent Cre-mediated excision of the region between the outermost *lox*P sites in the CLIP-T allele generated a knocked-out *Cyln2* allele that we named CLIP-L (Fig. 1*a*). In the CLIP-L allele, the *lacZ* reporter gene is located close to exon 2 of *Cyln2*. We engineered a splice acceptor site at the 5' end of the reporter cassette, which spliced onto *Cyln2* exon 2 sequences, generating a hybrid *Cyln2-lacZ* transcript.

We obtained germ line transmission with both the CLIP-T and CLIP-L alleles and crossed mice back to the C57Bl6 background. Northern-blot experiments on total RNA derived from the brains of these mice demonstrated that *Cyln2* mRNA was expressed from the CLIP-T allele but not from the CLIP-L allele, which expressed *lacZ* instead (Fig. 2*a*). Genes surrounding the *Cyln2* locus (*Wbscr1, Rfc2* and *Gtf2ird1*) were not affected by the targeting (data not shown). By western-blot analysis, we demonstrated that CLIP-115 was not produced in homozygous *Cyln2*-knockout mice ($Cyln2^{-/-}$), but was produced in reduced amounts in heterozygous mice ($Cyln2^{+/-}$) and in normal amounts in wild type and CLIP-T mice (Fig. 2*b*). Reduction in the amount of CLIP-115 produced by CLIP-L mice does not lead to a significant upregulation of CLIP-170 (Fig. 2*b*), indicating that there was no compensation by CLIP-170 for the absence of CLIP-115.
We used the *lacZ* marker in CLIP-L mice as an indicator of *Cyln2* gene activity, either on whole-brain mounts or on 40 μm sections of the brain, to identify regional variations in expression levels of CLIP-115. The *LacZ* gene was expressed abundantly in the CA areas of the hippocampus and more moderately in a number of other brain regions, including the amygdala, cerebral cortex

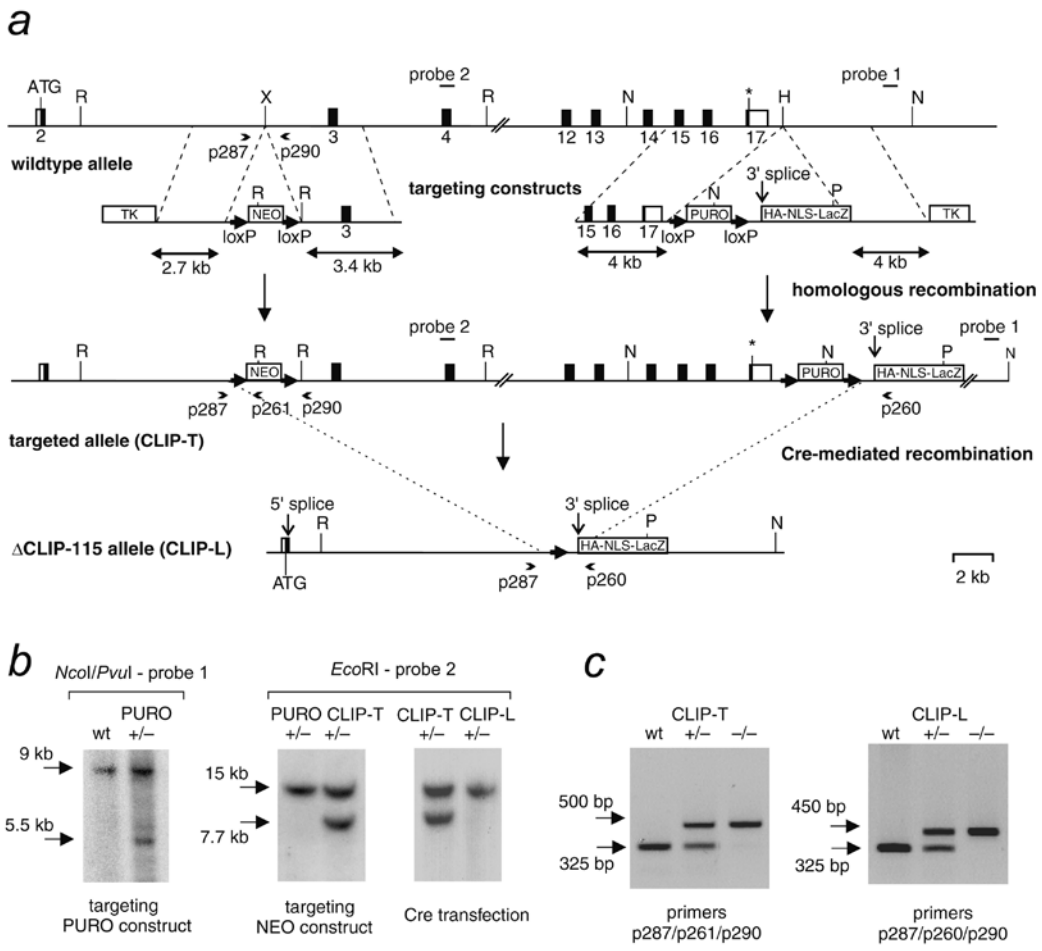

Figure 1. Inducible targeting of the Cyln2 gene

a, The *Cyln2* locus and gene-targeting constructs. The top line represents *Cyln2*, with exons indicated by solid boxes (white boxes, 5′ and 3′ UTRs; black boxes, coding regions). Exon 2 contains the start codon (ATG) and exon 17 contains the stop codon (asterisk). The positions of Southern-blot probes 1 and 2 (horizontal lines) and PCR primers p287, p260, p261 and p290 (arrowheads) are indicated. Selected restriction enzyme sites are shown (R, *Eco*RI; H, *Hin*dIII; X, *Xba*I; N, *Nco*I; P, *Pvu*I). The targeting constructs are shown below *Cyln2*. Homology with the *Cyln2* gene is indicated, as are the lengths of the homologous regions. The *lox*P sites are represented by arrows (not to scale). NEO, neomycin-resistance cassette; PURO, puromycin-resistance cassette, TK, thymidine kinase gene; HA-NLS-LacZ, HA- and NLS-tagged *lac*Z cassette, containing an engineered splice acceptor site (3′ splice) and polyadenylation signal (not indicated). The doubly targeted *Cyln2* allele, CLIP-T(argeted), is shown below the targeting constructs. Cre-mediated recombination at the outermost *lox*P sites of the CLIP-T allele removes most of the *Cyln2* sequences and generates the CLIP-L(oxed) allele, which is represented by the bottom line. The splice acceptor site at the 5′end of the reporter *lac*Z cassette can be spliced onto *Cyln2* exon 2 sequences, generating a hybrid *Cyln2-lacZ* transcript. ***b,*** Southern-blot analysis of gene targeting and Cre-mediated recombination events. Left, Southern blot of DNA derived from wild type (wt) and 3′ PURO-targeted ES cells (PURO) and digested with *Nco*I and *Pvu*I. The blot was hybridized with (external) probe 1, which detects fragments of 9 kb (wild type allele) and 5.5 kb (PURO-targeted allele). One PURO- targeted clone with the correct karyotype was electroporated with the NEO targeting construct. Middle, blot with *Eco*RI-digested DNA from the original PURO-targeted ES cell clone and from a doubly targeted line (CLIP-T) probed with external probe 2, which detects fragments of 15 kb (PURO allele) and 7.7 kb (CLIP-T allele). One of the CLIP-T ES cell lines was electroporated with a Cre-recombinase construct to obtain the knocked-out *Cyln2* locus (CLIP-L). Cre-mediated recombination is identified (right) by the elimination of the 7.7-kb fragment. ***c,*** PCR analysis of wild type, CLIP-T and CLIP-L alleles. Genomic tail DNA of wild type, heterozygous and homozygous CLIP-T and CLIP-L mice was subjected to PCR with the indicated cocktails of primers, which yielded the expected fragments in the different genotypes (wild type, p287-p290: 325 bp; CLIP-L, p287-p260: 450 bp and CLIP-T, p287-p261: 500 bp).

and cerebellum (Fig. 2*c-f*). In the hippocampus, the pyramidal cells of the CA1 and CA3 areas were densely labeled, whereas the dentate gyrus was virtually devoid of labeling (Fig. 2*d, e*). In the cerebellum, *lacZ* was expressed in bands, resembling the topographical organization of the olivocerebellar system (Voogd and Glickstein, 1998) (Fig. 2*c, f*). Within the cerebellar cortex, *lacZ* was expressed most prominently in the hemispheres and paravermis and relatively weakly in the vestibulocerebellum (data not shown).

With longer periods of *lacZ* staining, many other areas of the brain expressed the marker (albeit with comparatively less intensity), and the sagittal pattern of expression in the cerebellum, though still present, became less obvious (data not shown). The *lacZ* staining patterns were consistent with those seen on immunocytochemical analysis in which sections were incubated with antibodies against CLIP-115 (antiserum no. 2238; Hoogenraad et al. 2000; Fig. 2*g-j*). Electron microscopic analysis of the inferior olive in the *Cyln2*$^{-/-}$ mice revealed that the absence of CLIP-115 did not affect the ultrastructure, distribution or density of dendritic lamellar bodies. These data indicate that CLIP-115 is not involved in the transport of dendritic lamellar bodies (De Zeeuw et al., 1997), as we had originally suggested.

Growth deficits and brain abnormalities in Cyln2-knockout mice

Both the CLIP-L and CLIP-T strains of mice were viable and fertile, and offspring derived from heterozygous crosses were born in a normal Mendelian ratio (data not shown). Newborn (P1) and adult *Cyln2*-knockot mice had blood calcium levels and total brain weights (including cerebrospinal fluid) comparable to those of wild type littermates and control CLIP-T mice (Table 1). Calcium levels in postnatal day 14 (P14) wild type, *Cyln2*$^{+/-}$ and *Cyln2*$^{-/-}$ mice were also comparable (data not shown). Body weights of adult female *Cyln2*-knockout mice were significantly lower than those of control mice, and those of adult male *Cyln2*-knockout mice were also lower, although this difference was not statistically significant (Table 1, Fig. 3*a*). The lower body weight in female *Cyln2*-knockout mice was paralleled by shorter body and bone length (Fig. 3*b*), suggesting that these mice experienced a general growth deficit. Because growth deficiency in infancy is characteristic of Williams syndrome (Morris et al., 1988; Pankau et al., 1992), we examined the growth curves of CLIP-L and CLIP-T mice from two to ten weeks of age (Fig. 3*c, d*). A significant growth retardation was apparent in male and female *Cyln2* mice as compared to wild type littermates and CLIP-T mice. Weights of *Cyln2*$^{+/-}$ mice were intermediate between those of wild type mice and *Cyln2*$^{-/-}$ homozygotes. Taken together, these data indicate that haploinsufficiency of *Cyln2* gene causes a mild growth retardation during the first weeks of postnatal development, an effect that persists in adult female mice.

X-ray analysis revealed no obvious craniofacial irregularities in *Cyln2*-knockout mice, and investigation of brain sections stained with hematoxylin and eosin did not show gross abnormalities in brain morphology (data not shown). To investigate whether the mice had subtle macroscopic abnormalities, we carried out high-resolution magnetic resonance imaging (MRI) analysis, which allows accurate surface and volume calculations of brain structures. Volumes of the cerebellum, cerebrum, hippocampus and amygdala do not differ significantly between *Cyln2*-knockout and wild type mice (data not shown). Notably, the average brain-ventricle volume of *Cyln2*-knockout mice was significantly larger than that of wild type littermates, and the average corpus callosum volume was significantly smaller (Fig. 3*e-g*). Thus, a reduction in CLIP-115 levels in mice caused mild brain abnormalities.

Behavioral and physiological analyses of CLIP-L and CLIP-T mouse strains

The prominent distribution of CLIP-115 in the hippocampus, amygdala and cerebellum of mice raises the possibility that behavioral functions controlled by these brain regions may be disturbed in *Cyln2*-knockout mice. We assessed this by subjecting the mice to a number of behavioral tests. We investigated the functioning of hippocampus and amygdala with the elevated zero-maze assay and contextual and cued fear-conditioning paradigms. The elevated zero-maze test revealed no differences among *Cyln2*-knockout, CLIP-T and wild type mice (data not shown),

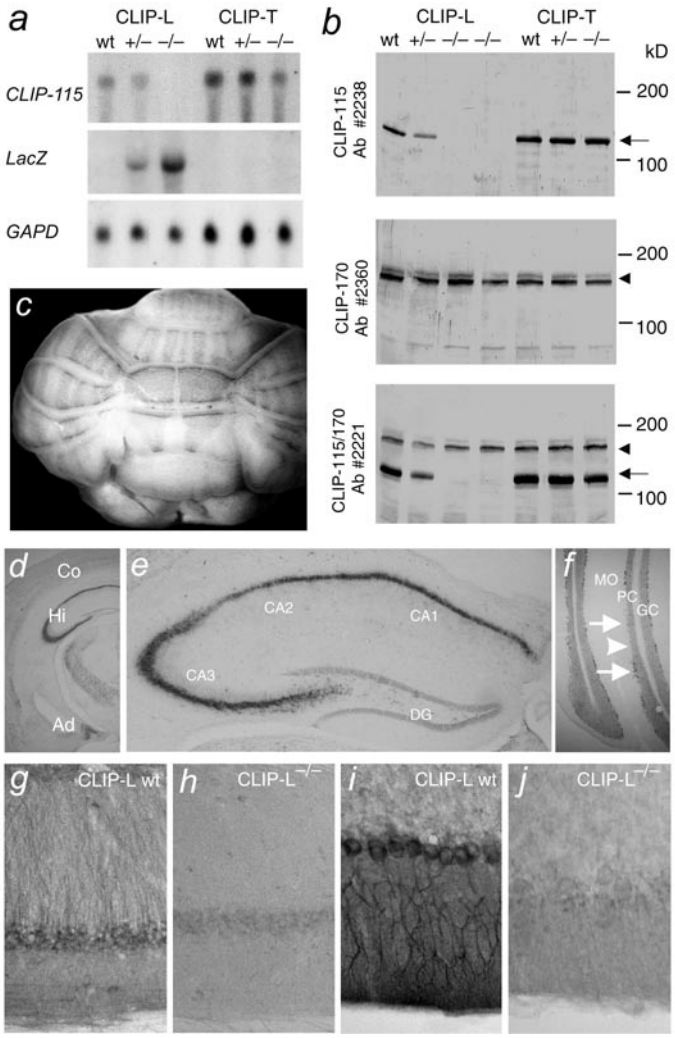

Figure 2. Expression of CLIP-115 in CLIP-L and CLIP–T mice

a, Northern blot analysis of total brain RNA from wild type (wt), CLIP-T$^{+/-}$, CLIP-T$^{-/-}$, CLIP-L$^{+/-}$ and CLIP-L$^{-/-}$ mice. The blot was sequentially hybridized with *Cyln2* (top), *LacZ* (middle) and *Gapd* (bottom) probes. ***b,*** Western-blot analysis of brain proteins of wild type (wt), CLIP-T$^{+/-}$, CLIP-T$^{-/-}$, CLIP-L$^{+/-}$ and CLIP-L$^{-/-}$ mice, separated by SDS-PAGE on 6% gels. Blots were incubated with antibodies against CLIP-115 (no. 2238), antibodies against CLIP-170 (no. 2360) and antibodies that recognize both CLIP-115 and CLIP-170 (no. 2221). Arrows indicate the position of CLIP-115 and arrowheads the position of CLIP-170. ***c,*** Whole-mount CLIP-L$^{-/-}$ mouse cerebellum expressing *lacZ*. The *lacZ* expression (corresponding to CLIP-115 expression) is distributed in sagittal bands. ***d-f,*** Brain sections of CLIP-L$^{-/-}$ mice expressing *lacZ*. Labeling in the hippocampus (Hi) is much more intense than in other areas, such as the cerebral cortex (Co) and amygdala (Ad). A high magnification view of the hippocampus **(*e*)** shows intense labeling of the pyramidal cells of the CA1 and CA3 areas and virtually no staining in the dentate gyrus (DG). The cerebellum **(*f*)** shows variable *lacZ* expression in the Purkinje cells (PC), consistent with the sagittal pattern in whole mounts. Arrows, Purkinje cells expressing *lacZ*; arrowhead, Purkinje cells not expressing *lacZ*. MO, molecular layer; GC, granular cell layer. ***g-j)*** Immunocytochemical staining of brain sections from wild type (wt; *g, i*) and knockout (CLIP-L$^{-/-}$; *h, j*) littermates with antibodies against CLIP-115 (antiserum no. 2238). The sagittal banding pattern of CLIP-115 in the cerebellum cannot be seen in the section in **(*i*)**, which was chosen to demonstrate the abundant dendritic staining of Purkinje cells.

indicating that amygdala functioning was not measurably affected by the deletion of *Cyln2*. In the contextual fear-conditioning experiment, mice were placed in a test cage, subjected to a foot shock and then removed and placed back in the test cage 24 hours later. The amount of time spent 'freezing' while in the test cage on each occasion was measured.

Wild type and CLIP-T mice showed a significant increase in the average amount of time spent freezing when they were placed back in the test cage 24 hours after foot shock (Fig. 4*a*). Both the *Cyln2*$^{+/-}$ and *Cyln2*$^{-/-}$ mutants also showed an increase in average freezing time, but this increase was significantly smaller than that observed in control mice (Fig. 4*a*). In the cued fear-conditioning test, mice were placed in a conditioning chamber, where they received a cue followed by a foot shock. They were then removed, and after 24 hours were placed in a different

Table 1. Body weights, brain weights and calcium levels in *Cyln2*-knockout mice

Sex/age	Genotype	Sample size (n)	Body weight (g)	Brain weight [a] (mg)	Calcium level (mg/dl serum)
Male					
P1	CLIP-T	11	1.37 ± 0.02	79.0 ± 1.8	9.4 ± 0.7
	wt	11	1.39 ± 0.03	83.7 ± 2.7	9.0 ± 0.5
	CLIP-L$^{+/-}$	19	1.42 ± 0.04	83.2 ± 2.3	9.1 ± 0.4
	CLIP-L$^{-/-}$	4	1.48 ± 0.11	90.1 ± 9.5	9.0 ± 1.6
Adult	CLIP-T	7 (7)[b]	33.7 ± 2.14	ND[c]	ND
	wt	13 (7)[b]	33.3 ± 0.63	ND[c]	9.9 ± 0.2
	CLIP-L$^{+/-}$	11 (7)[b]	32.6 ± 0.65	ND[c]	9.6 ± 0.2
	CLIP-L$^{-/-}$	10 (7)[b]	32.0 ± 0.81	ND[c]	9.5 ± 0.2
Female					
P1	CLIP-T	15	1.33 ± 0.02	75.9 ± 1.4	9.8 ± 0.4
	wt	7	1.38 ± 0.07	81.0 ± 2.8	9.5 ± 1.2
	CLIP-L$^{+/-}$	14	1.34 ± 0.04	76.8 ± 2.3	9.5 ± 0.7
	CLIP-L$^{-/-}$	12	1.44 ± 0.05	85.6 ± 3.2	9.2 ± 0.5
Adult	CLIP-T	19 (11)[b]	27.40 ± 0.84	476.0 ± 5.9	ND
	wt	8 (7)[b]	27.07 ± 0.94	476.3 ± 8.7	10.2 ± 0.2
	CLIP-L$^{+/-}$	13 (34)[b]	24.61 ± 0.30[d]	ND	10.0 ± 0.2
	CLIP-L$^{-/-}$	14 (5)[b]	23.20 ± 0.95[d]	481.1 ± 6.8	10.1 ± 0.2

Data are expressed as mean ± s.e.m. ND, not determined. [a]Includes cerebrum, cerebellum and brain stem. [b]The number of adult mice used for body weight determination differs from that used for other analyses and is indicated between brackets. [c]Mice were reserved for MRI analysis. [d]Values are significantly different from wild type ($P < 0.05$), as determined by one-way ANOVA.

chamber where they received the same cue but no foot shock. The amount of time the mice spent freezing was measured on each occasion. Mutant and control mice behaved similarly in this test, showing increased freezing time in response to the cue when placed in a different environment (Fig. 4*b*). Because lesions in the hippocampus affect contextual fear conditioning, whereas lesions in the amygdala affect both contextual and cued fear conditioning (Bourtchuladze et al., 1994; Kim and Fanselow, 1992; Phillips and LeDoux, 1992), the data from the zero-maze and fear-conditioning tests suggest that absence of CLIP-115 affects hippocampal-dependent memory processes.

We therefore examined hippocampal synaptic plasticity in *Cyln2*$^{+/-}$ and *Cyln2*$^{-/-}$ mice by studying long-term potentiation, a prominent cellular model of learning and memory formation. In support of our behavioral data, we found that synaptic plasticity in the hippocampal CA1 area

was significantly lower in both *Cyln2*$^{+/-}$ and *Cyln2*$^{-/-}$ mice than in wild type and CLIP-T mice (Fig. 4*c*). Taken together, these behavioral and electrophysiological data strongly suggest that hippocampal synaptic function is affected in *Cyln2*-knockout mice.

In a second series of behavioral tests, we examined motor behavior in control and mutant mice. In the open-field activity test, the *Cyln2*-knockout mice performed similarly to control mice (Fig. 5*a*), indicating that spontaneous locomotor activity was not affected by reduced CLIP-115 levels. Because the expression of CLIP-115 in the cerebellum was variable, we subjected *Cyln2*-knockout mice to more subtle test of motor coordination, each addressing a specific cerebellar function controlled by a particular cerebellar area. These investigations included recordings of compensatory eye movements to investigate the vestibulocerebellum, the hanging wire and beam-walk tests to investigate the cerebellar vermis, and coordination tests on the accelerating rotarod to investigate the cerebellar hemispheres and paravermis (Armstrong, 1986; Bloedel and Courville, 1981; De Zeeuw et al., 1998a; De Zeeuw et al., 1998b). The cerebellar vermis, which controls proximal musculature involved in balance, was functionally intact, as the *Cyln2*-knockout mice demonstrated normal performance on the hanging wire test (Fig. 5*b*) and the horizontal and vertical beam-walk tests (Fig. 5*c* and data not shown). The vestibulocerebellum was also not impaired in *Cyln2*-knockout mice, because the gain and phase values of both the optokinetic and vestibulo-ocular reflex were normal, and the adaptation of the vestibulo-ocular reflex was also adequate (Fig. 5*d, e* and data not shown). Both *Cyln2*$^{+/-}$ and *Cyln2*$^{-/-}$ mice remained on the accelerating rotarod for significantly shorter periods than did control mice (Fig. 5*f*). Consistent with this, *Cyln2*-knockout mice showed poor initial coordination on a running wheel, resulting in highly erratic motions and occasional ejection from the wheel (see Web Movies online). Taken together, these results suggest that the CLIP-L mutant mice were not ataxic, but that their motor coordination was impaired when the function of the cerebellar hemispheres and paravermis was challenged.

Cell biological analysis of CLIP-115 deficiency

To analyze the effect of CLIP-115 deficiency on microtubule dynamics and protein distribution at microtubule tips, we derived embryonic and adult primary cultured fibroblasts from *Cyln2*-knockout mice and wild type littermates and from the CLIP-T strain. We chose fibroblasts instead of cultured hippocampal neurons for our analysis because it is difficult to analyze individual microtubules in the narrow dendritic and axonal compartments, and we have shown that both CLIP-170 and CLIP-115 are expressed in cultured fibroblasts (Akhmanova et al., 2001). Injection of Cy3-labeled tubulin into fibroblasts and measurement of microtubule dynamic events by fluorescence microscopy in living cells showed no significant differences between knockout cells and wild type fibroblasts in the rates of microtubule growth and shrinkage or in the frequencies of catastrophe (transition from a growing microtubule to a shrinking one) and rescue (transition from a shrinking microtubule to a growing one; data not shown). Transfection of adult and embryonic fibroblasts with green fluorescent protein-tagged EB3-GFP, a marker that specifically associates with the ends of growing microtubules in living cells (T. Stepanova, A.A., C.C.H., F.G. and N.G., unpublished data), revealed similar microtubule growth rates in knockout cells (0.51 ± 0.10 μm s^{-1}, 159 microtubule plus-ends measured, derived from 17 cells in 3 independent experiments) and wild type fibroblasts (0.47 ± 0.10 μm s^{-1}, 133 microtubule plus-ends measured, derived from 14 cells in 3 independent experiments). Thus, absence of CLIP-115 did not significantly affect microtubule growth rates, as measured by two independent methods, or overall microtubule dynamic events, as measured by Cy3-tubulin injection in living cells.

Furthermore, stabilized microtubule arrays formed normally in cells at the edge of a wounded monolayer in *Cyln2*-knockout fibroblasts, suggesting that CLASP function was not measurably compromised in these cells.

We have previously shown that CLIP-115 tagged with green fluorescent protein (GFP-CLIP-115) and CLIP-170 tagged with hemagglutinin (HA-CLIP-170) are detected at the same microtubule distal ends (Hoogenraad et al., 2000). Because these proteins have highly similar microtubule-binding domains, we tested the possibility that CLIPs actually compete for binding sites at growing microtubule distal ends. Expression of GFP-CLIP-115 in COS-1 cells displaced endogenous CLIP-170 from microtubule tips (Fig. 6*a, b*), supporting the hypothesis

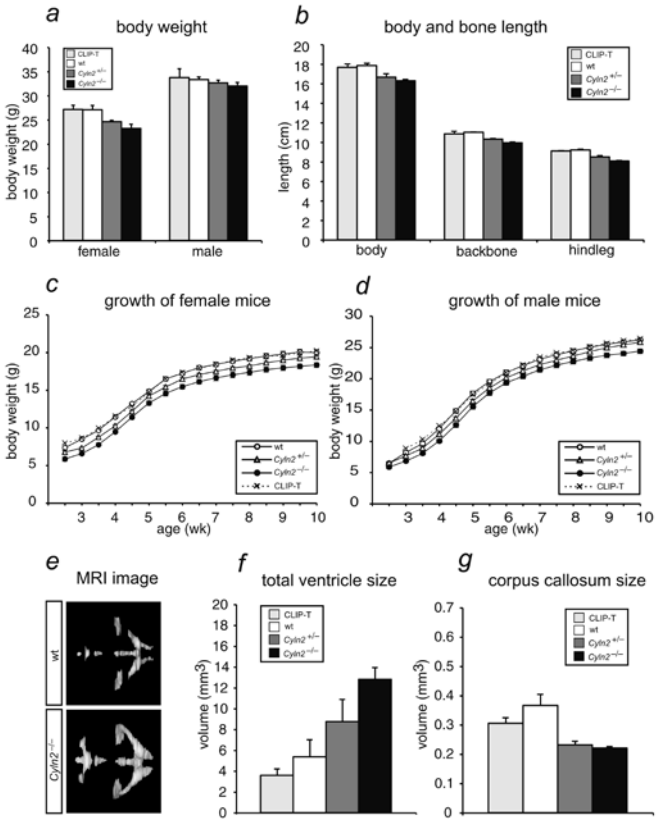

Figure 3. Growth deficiency and brain abnormalities in Cyln2-knockout mice

a, Body weights of adult mice (mean ± s.e.m.). Wild type littermates from the CLIP-L strain (wt; 7 female, 7 male), CLIP-T (11 female, 7 male), CLIP-L$^{+/-}$ (*Cyln2*$^{+/-}$; 34 female, 17 male) and CLIP-L$^{-/-}$ (*Cyln2*$^{-/-}$: 5 female, 7 male) mice 6.5 months of age were weighed. Heterozygous and homozygous female CLIP-L mice have a lower body weight (9% and 15%, respectively) than their wild type littermates ($P < 0.05$). CLIP-T mice do not differ significantly from wild type CLIP-L mice. The body weights of heterozygous and homozygous male CLIP-L mice are not significantly different from those of wild type littermates, although a trend towards reduced body weight is detected. ***b,*** Body and bone length of female wild type (wt; $n = 5$), CLIP-L$^{+/-}$ (*Cyln2*$^{+/-}$; $n = 5$), CLIP-L$^{-/-}$ (*Cyln2*$^{-/-}$; $n = 5$) and CLIP-T ($n=5$) mice. The body and bone length of 6-month female mice was determined by X-ray analysis. Lengths of total body, backbone and bones in left hind leg were statistically shorter ($P < 0.05$) by 11% in homozygous CLIP-L mice and 7% in heterozygous CLIP-L mice relative to wild type mice. CLIP-T mice did not differ significantly from wild type mice of the CLIP-L strain. ***c,*** Growth curves of wild type (wt; $n = 15$), CLIP-T ($n = 24$), CLIP-L$^{+/-}$ (*Cyln2*$^{+/-}$; $n = 40$) and CLIP-L$^{-/-}$ (*Cyln2*$^{-/-}$; $n = 12$) female mice. Body weights of the mice were measured twice per week starting at two weeks. Depending on their age, heterozygous and homozygous CLIP-L female mice are 5-14% and 10-22%, respectively, lighter than their wild type littermates and the CLIP-T mice. Pairwise comparisons show that the differences in body weight between the genotypes were statistically significant ($P < 0.005$), except between wild type mice of the CLIP-L strain and mice of the CLIP-T strain. ***d,*** Growth curves of wild type (wt; $n = 20$), CLIP-T ($n = 17$), CLIP-L$^{+/-}$ (*Cyln2*$^{+/-}$; $n = 31$) and CLIP-L$^{-/-}$ (*Cyln2*$^{-/-}$; $n = 23$) male mice. Body weights were measured as described above. Depending on their age, heterozygous and homozygous CLIP-L male mice are 2-8% and 7-17%, respectively, lighter than their wild type littermates and the CLIP-T mice. Pairwise comparisons demonstrated that differences in body weight among the different genotypes were statistically significant ($P < 0.01$), except between wild type mice of the CLIP-L strain and mice of the CLIP-T strain and between wild type and heterozygous CLIP-L mice. ***e,*** 3D surface rendering of the segmented ventricles in the brain of a wild type (wt) and *Cyln2*$^{-/-}$ mouse. The 3D reconstruction is viewed from above with the anterior at the right. All major ventricles appear enlarged. ***f,*** Ventricle size of adult wild type (wt; $n = 4$), CLIP-L$^{+/-}$ (*Cyln2*$^{+/-}$; $n = 4$), CLIP-L$^{-/-}$ (*Cyln2*$^{-/-}$; $n = 4$) and CLIP-T mice ($n=4$) as determined by high resolution MRI. Ventricle volumes (mean ± s.e.m.) of homozygous knockout CLIP-L mice were enlarged compared with wild type mice ($P < 0.05$). The ventricular volume of heterozygous CLIP-L mice (or CLIP-T mice) was not significantly different from that of wild type littermates. ***g,*** Size of the corpus callosum in wild type (wt; $n=5$), CLIP-L$^{+/-}$ (*Cyln2*$^{+/-}$; $n=4$), CLIP-L$^{-/-}$ (*Cyln2*$^{-/-}$; $n=6$) and CLIP-T mice ($n=3$). Corpus callosum volumes of the homozygous and heterozygous knock out mice are significantly smaller than those of wild type mice ($P < 0.01$). Sizes of the corpus callosum in wild type mice of the CLIP-L and CLIP-T strains did not differ significantly from each other.

of competition. The dynactin component p150^{Glued} was also displaced in these cells (Fig. 6*c*), consistent with the notion that CLIP-170 and the dynein-dynactin motor system work in concert at microtubule plus-ends (Valetti et al., 1999; Vaughan et al., 1999). In line with these observations, overexpression of GFP-CLIP-170 recruited p150^{Glued} to distal microtubule segments (Fig. 6*e, f*). Overexpression of a mutant GFP-CLIP170 (named GFP-CLIP-170 (-tail)), in which the last 79 amino acids were removed resulted in removal of dynactin from the microtubule plus-ends as a result of the dislocation of endogenous CLIP-170 by mutant GFP-CLIP-170 (Fig. 6*g, h*). Thus, overexpressed GFP-CLIP-170 (-tail) behaved like GFP-CLIP-115 in its effect on p150^{Glued}, supporting the hypothesis that the C-terminal metal-binding motif of CLIP-170 is important in the interaction with dynactin (Valetti et al., 1999; Vaughan et al., 1999). By contrast, when the final 159 amino acids of the C-terminal domain of CLIP-170 were transferred to the end of GFP-CLIP-115 (GFP-CLIP-115 (+tail)), this fusion protein recruited the dynactin complex to plus-ends (Fig. 6*i, j*). These results indicate that the last 159 amino acids of CLIP-170 were sufficient to confer to CLIP-115 the capacity to relocalize dynactin.

Notably, we detected greater CLIP-170 staining at microtubule tips in *Cyln2*-knockout fibroblasts than in wild type cells (Fig. 7*b, d*). The average CLIP-170 staining per microtubule tip is 1.6 times greater in knockout than in wild type cells (Fig. 7*h*), but varied considerably between individual microtubule ends. In contrast, the distribution of EB1, a specific marker of growing microtubule plus-ends with no similarity to the CLIPs, was similar in wild type and knockout cells (Fig. 7*a, c*). The localization of the dynactin complex, as measured with antibodies against p150^{Glued} and p50 (dynamitin), was markedly different in knockout and wild type cells. Average dynactin staining per microtubule tip in *Cyln2*-knockout cells was 2.8 times greater than in wild type fibroblasts (Fig. 7*e, f, h*). The higher level of dynactin at microtubule tips was not due to different cell culture conditions, because the differential staining pattern was clearly visible in experiments where *Cyln2*-knockout fibroblasts were mixed with wild type cells (Fig. 7*e, f*). Similar observations were made in embryonic and adult *Cyln2*-knockout fibroblasts (data not shown). The greater staining at microtubule tips was not due to greater total levels of CLIP-170 or dynactin in knockout fibroblasts, as demonstrated by western blotting (Fig. 7*i* and data not shown). To our knowledge, this is the first documentation of differences in protein distribution at microtubule distal ends in cells with endogenous levels of protein (that is, without overexpression).

Discussion

Although the deletion region common in Williams syndrome has been characterized in detail (Francke, 1999; Osborne, 1999) and a firm linkage between mutations in *ELN* and cardiovascular abnormalities has been established (Olson et al., 1995; Tassabehji et al., 1997), the genes that, when mutated, contribute to neurodevelopmental aspects of Williams syndrome have not been clearly defined. The neurological symptoms and behavioral profile of individuals affected with Williams syndrome are very similar between individuals, and finding the genes associated with this phenotype is of considerable interest, as they might reveal molecular mechanisms underlying basic neuronal functioning. Here, we show that a reduced level of CLIP-115 in mice results in a mild growth deficit, brain abnormalities and specific behavioral and neurophysiological deficits. As discussed below, defects in *Cyln2*-knockout mice resemble deficiencies in individuals with Williams syndrome. As in Williams syndrome, these deficits are apparent in heterozygous knockout mice. Taken together, our data strongly suggest that haploinsufficiency for *CYLN2* in humans underlies some of the developmental, neurological and behavioral abnormalities

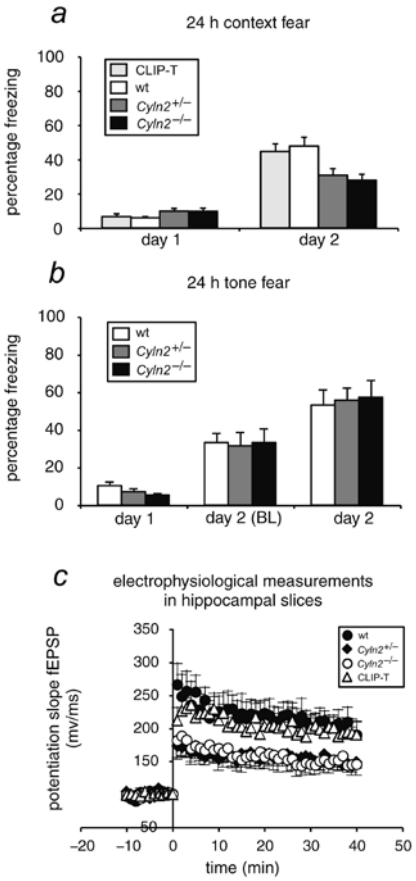

Figure 4. Hippocampal deficits in Cyln2-knockout mice

a, 24 h contextual fear-conditioning test in CLIP-T ($n = 10$), wild type (wt; $n = 17$), *Cyln2*$^{+/-}$ ($n = 19$) and *Cyln2*$^{-/-}$ ($n = 16$) mice. Percentage freezing time (mean ± s.e.m.) is shown at day 1 (baseline activity before foot shock) and day 2 (24 h after foot shock). There is no significant difference in freezing behavior among groups of mice during the baseline period. At 24 h after the foot shock, all mice freeze significantly more than on day 1 ($P < 0.05$), yet both heterozygous and homozygous CLIP-L mice exhibit a significant deficit in freezing relative to wild type mice ($P < 0.05$). Wild type mice from the CLIP-L strain and mice from the CLIP-T strain show no significant difference in freezing time. ***b,*** 24 h cued fear-conditioning test in wild type (wt; $n = 7$), *Cyln2*$^{+/-}$ ($n = 11$) and *Cyln2*$^{-/-}$ ($n = 11$) mice. Percentage freezing time (mean ± s.e.m.) is shown at day 1 (before foot shock and tone) and at day 2 before (baseline, BL) and after tone. There is no significant difference in the percentage freezing time between different genotypes at any time point measured. ***c,*** Hippocampal long-term potentiation induced by theta-burst stimulation. Hippocampal slices from CLIP-T mice ($n=10$) and wild type (wt; $n=7$), *Cyln2*$^{+/-}$ ($n=6$) and *Cyln2*$^{-/-}$ ($n=8$) mice were stimulated at 0.0166 Hz while fEPSPs were recorded from CA1 dendritic fields. After 10 min of baseline, slices were stimulated using a theta-burst stimulation paradigm followed by 40 min of 0.0166 Hz recording. Synaptic plasticity in the hippocampal CA1 area is lower in heterozygous and homozygous knockout mice than in wild type mice ($P < 0.05$). Wild type mice from the CLIP-L strain and mice from the CLIP-T strain show no significant differences from one another.

observed in Williams syndrome. This conclusion is supported by studies of rare individuals with small deletions in the WSCR (Francke, 1999; Osborne, 1999; Tassabehji et al., 1999).

Differences in genetic background are known to cause significant variations in behavior and brain physiology (Silva and et al., 1997; Tarantino et al., 2000). This complicated the interpretation of behavioral and electrophysiological results in our mouse gene-targeting studies, in which the genetic background surrounding the targeted allele (129sv-derived) is different from that surrounding the wild type allele (C57Bl6-derived). Because the gene number and order of the WSCR in humans is conserved in mice (Valero et al., 2000), a mutation impairing the function of any gene in the 129sv-derived genomic region surrounding the *Cyln2* locus might theoretically give rise to a Williams syndrome-like phenotype in the CLIP-L mice. To avoid misinterpretations, we have generated an inducible, rather than a conventional, *Cyln2*-knockout allele. This strategy has allowed us to use as controls not only wild type littermates of the CLIP-L mice, but also mice of the CLIP-T strain, in which *Cyln2* is expressed but the genomic region surrounding the *Cyln2* locus is 129sv-derived as in the CLIP-L strain. Thus, the phenotypes we observe are not due to genetic background differences in the region surrounding the *Cyln2* locus, but can be directly attributed to the absence of CLIP-115.

Although CLIP-115 is not essential for life, the growth deficiency in *Cyln2*$^{+/-}$ and *Cyln2*$^{-/-}$ mice indicates that this protein may be necessary for proper mouse development. A postnatal growth deficiency has been documented in individuals affected with Williams syndrome (Morris et al., 1988; Pankau et al., 1992). The MRI data from *Cyln2*-knockout mice indicate that a reduction in CLIP-115 levels also affects the morphology of the adult mouse brain. Whether this is due to

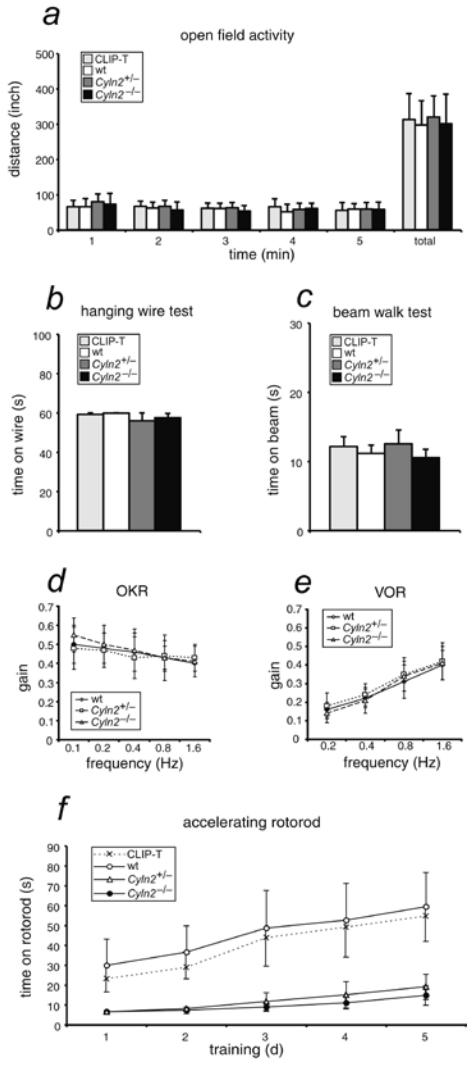

Figure 5. Motor coordination in Cyln2-knockout mice

a, Spontaneous locomotion. Movements of CLIP-T (*n* = 13), wild type (wt; *n* = 11), CLIP-L$^{+/-}$ (*Cyln2*$^{+/-}$; *n* = 24) and CLIP-L$^{-/-}$ (*Cyln2*$^{-/-}$; *n* = 13) mice were monitored during 1-min intervals (mean ± s.e.m.) in an open-field activity test. No differences among mouse lines were observed. ***b,*** Hanging wire test. To measure balance and grip strength of CLIP-T (*n* = 7), wild type (wt; *n* = 7), CLIP-L$^{+/-}$ (*Cyln2*$^{+/-}$; *n* = 10) and CLIP-L$^{-/-}$ (*Cyln2*$^{-/-}$; *n* = 8) mice, a hanging wire test was carried out. Time on the wire was recorded up to a maximum of 60 s. No difference among mouse lines is observed. ***c,*** Beam-walk test. CLIP-T (*n* = 7), wild type (wt; *n* = 7), CLIP-L$^{+/-}$ (*Cyln2*$^{+/-}$; *n* = 10) and CLIP-L$^{-/-}$ (*Cyln2*$^{-/-}$; *n* = 8) mice were tested for basic motor coordination and balance by measuring their ability to cross a wooden beam. The time required to cross the beam was equivalent between the groups of mice. ***d, e,*** Compensatory eye movements. The compensatory eye movements of wild type (wt; *n*= 4), CLIP-L$^{+/-}$ (*Cyln2*$^{+/-}$; *n*= 2) and CLIP-L$^{-/-}$ (*Cyln2*$^{-/-}$; *n*= 4) mice were tested during visual or vestibular stimulation at frequencies varying from 0.1 to 1.6 Hz. At a peak velocity of 8° s^{-1}, the average gain of the optokinetic reflex ranged from 0.40 to 0.50 in the wild type mice, from 0.43 to 0.48 in the homozygous knockout mice, and from 0.41 to 0.55 in the heterozygous mice. At an amplitude of 10°, the average gain of the vestibulo-ocular reflex ranged from 0.16 to 0.40 in the wild type mice, from 0.18 to 0.42 in the homozygous knockout mice, and from 0.14 to 0.41 in the heterozygotes. Thus, the gain values of the various strains do not differ for any stimulus paradigm tested. ***f,*** Accelerating rotarod test. To measure more complicated motor behaviors and a form of motor learning, CLIP-T (*n* = 7), wild type (wt; *n* = 7), CLIP-L$^{+/-}$ (*Cyln2*$^{+/-}$; *n* = 10) and CLIP-L$^{-/-}$ (*Cyln2*$^{-/-}$; *n* = 8) mice were subjected to the rotarod test, in which they were tested for their ability to stay on the rotarod. A repeated-measures ANOVA, including all four genotypes, showed a significant block effect for genotype ($P < 0.05$). Pairwise comparisons showed that both the heterozygous and homozygous CLIP-L mice had a significant performance deficit, relative to wild type mice of the CLIP-L strain and mice of the CLIP-T strain ($P < 0.05$). Whereas the latter strains improved their performance during the training period ($P < 0.05$), both the heterozygous and homozygous CLIP-L mice did not significantly increase performance levels.

aberrant development, absence of CLIP-115 in the adult brain, or both remains to be investigated. It is noteworthy that the volume of cerebrospinal fluid in individuals with Williams syndrome increases with age relative to controls (Reiss et al., 2000). This result correlates with the enlarged ventricle size detected in adult *Cyln2*-knockout mice. MRI studies have also documented a smaller total brain volume in individuals with Williams syndrome relative to controls, with

white matter affected more than gray matter (Reiss et al., 2000). We do not find evidence for smaller brains in adult *Cyln2*-knockout mice, either by MRI or by weighing the brains. It is remarkable, however, that the corpus callosum (which represents one of the main white-matter tracts of the brain) is smaller in homozygous *Cyln2*-knockout mice than in wild type mice. A recent report documents the same phenotype in individuals with Williams syndrome(Schmitt et al., 2001). Together, these data suggest that the deficiency of CLIP-115 underlies a considerable proportion of the neurodevelopmental problems associated with Williams syndrome.

Tests of behavioral and electrophysiological performance indicate that functions controlled by the hippocampus are disturbed in the CLIP-L mice. These results correlate with behavioral data on individuals with Williams syndrome, which score poorly on spatial cognition tests (Bellugi et al., 2000). In addition, both *Cyln2*-knockout mice and individuals with Williams syndrome have difficulties executing specific motor tasks, although neither group is ataxic. Thus, in the behavioral models tested, we find a correlation between the dysfunctions of *Cyln2*-knockout mice and individuals with Williams syndrome. Furthermore, there is a good correlation between impaired behavior in mice and the level of expression of CLIP-115 in the specific brain region that controls this behavior. Studies using crosses between CLIP-T mice and tissue-specific Cre-recombinase transgenes should allow a more detailed analysis of the developmental, acute and spatial consequences of CLIP-115 deficiency in mice.

Immunocytochemistry studies on mouse brain sections using CLIP-170-specific antibodies revealed that in many areas of the brain, including the CA areas of the hippocampus, CLIP-115 and CLIP-170 were co-expressed (C.C.H, A.A., C.I.D.Z., F.G. and N.G., manuscript in preparation). To explain the brain phenotype of the *Cyln2*-knockout mice, one must therefore consider that CLIP-170 may partially compensate for the absence of CLIP-115. This would help explain, for example, why CLASP localization and microtubule dynamics are not disrupted in *Cyln2*-knockout cells. On the other hand, our data from cultured fibroblasts indicate that deletion of *Cyln2* actually results in an accumulation of CLIP-170 and dynactin at microtubule tips. Thus, CLIP-115 normally competes with CLIP-170 and dynactin for binding sites at the distal ends of growing microtubules. Dynactin distribution at microtubule tips may be influenced both by direct competition with CLIP-115 (it has CLIP-like microtubule-binding domains) and by indirect effects on CLIP-170 (refs. 14, 15).

Our data indicate that the cytoplasmic concentration of CLIP–170 in normal cells is in excess of the total amount of available plus-end binding sites, such that when CLIP-115 is absent, there is sufficient cytoplasmic CLIP-170 to occupy more binding sites. It has been proposed that the microtubule-tip localization of CLIP-170 and dynactin enables dynein-bound cargo to attach to microtubules and be transported to the minus-ends (Vaughan et al., 1999). We have recently shown that CLIP-170 interacts with LIS1 through its metal-binding C-terminal domain (Coquelle et al., 2002). Mutations in the gene *LIS1* give rise to lissencephaly, a severe brain disorder (Reiner et al., 1993), and detailed analysis of the LIS1 protein has shown that it is essential for nuclear migration and, like dynactin, modulates dynein function (Vallee et al., 2001). Our data suggest that, although direct interactions of CLIP-115 with CLIP-170, LIS1 or dynactin have not been documented, the actions of these proteins might still be compromised in *Cyln2*-knockout cells. It will therefore be of interest to consider dynein motor perturbations, in addition to a loss of CLIP115-specific functions, when further investigating disturbed molecular processes in *Cyln2*-knockout mice and individuals with Williams syndrome.

Methods

Generation of CLIP-T and CLIP –L mutant mice

We have previously described the characterization of mouse *Cyln2* from an AB1 embryonic stem (ES) cell DNA-derived cosmid library (Hoogenraad et al., 1998). Based on these data, we used a 6.1-kb *Xba*I-*Sal*I genomic subclone encompassing exon 3 with an *Xba*I site in intron 2 to target the 5' end of *Cyln2*. An 8-kb *Nco*I-*Bam*HI fragment containing exons 15, 16 and 17 and a *Hin*dIII site downstream of the last exon was used to target the 3' end (Fig. 1*a*). We made the 5' end-targeting construct by inserting a neomycin-resistance gene, driven by a thymidine kinase promoter and flanked by *lox*P sequences, into the *Xba*I site in intron 2. The 3'end-targeting construct was made by inserting a puromycin-resistance gene, driven by the phosphon glycerate kinase (*Pgk*) promoter and flanked by *lox*P sequences, together with a *lacZ* reporter sequence, in the *Hin*dIII site downstream of *Cyln2*. We constructed the *lacZ* reporter with a splice acceptor site at its 5' end, a 3' untranslated region (UTR) and polyadenylation signal at its 3'end, and sequences encoding a triple HA tag and nuclear localization signal (NLS) sequence at the amino terminus of the lacZ protein. In both the 5'-end construct (called NEO) and in the 3'-end construct (PURO-HA-NLS-lacZ), a negative selection marker gene (thymidine kinase) was inserted in the polylinker of the vector.

E14 ES cells were electroporated first with a linearized 3' end-targeting construct and cultured in BRL-cell conditioned medium as described (Jaegle et al., 1996). After selection with puromycin (0.7 µg ml^{-1}), colonies were isolated and expanded.

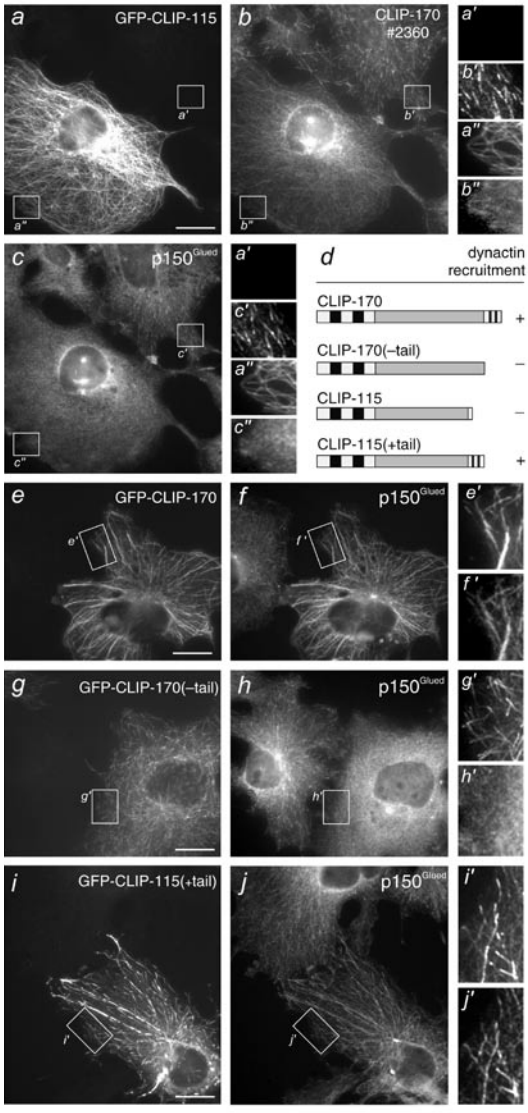

Figure 6. Competition between CLIP-115 and CLIP-170 at microtubule plus-ends

a-c, COS-1 cells were transfected with GFP-CLIP-115 (GFP signal in *a*) and cells were stained with antibodies against CLIP-170 (no. 2360; *b*) and an antibody against p150^{Glued} (*c*). Both endogenous proteins are displaced from microtubule tips by GFP-CLIP-115. ***d,*** Summary of endogenous dynactin recruitment to (+) or displacement from (-) microtubule tips by the different overexpression constructs as demonstrated by staining with an antibody against p150^{Glued}. ***e-j,*** COS-1 cells were transfected with GFP-CLIP-170 (*e, f*), GFP-CLIP-170(-tail) (*g, h*), or GFP-CLIP-115 (+tail) (*i, j*). GFP signals are shown in *e, g, i.* Cells were stained for endogenous dynactin (*f, h, j*). In all panels, insets are enlarged, to better show the presence or absence of microtubule plus-end staining. Bar, 10 µm in all panels

We analyzed the karyotypes of puromycin-resistant ES cell lines targeted at the *Cyln2* locus, and electroporated one line with the correct number of chromosomes with the 5' end-targeting construct. After selection with G418 (200 μg ml^{-1}) for neomycin resistance, we identified homologous recombination at *Cyln2* by Southern-blot analysis. We carried out FISH, using the NEO and PURO-*lacZ* cassettes as probes, to find cell lines with both constructs targeted to the same allele (CLIP-T). We then electroporated ES cells with the correct karyotype with a construct containing the *Cre* recombinase gene, driven by a thymidine kinase promotor, in a vector backbone with a *Pgk* hygromycin-resistance gene. After selection with hygromycin B (100 μg ml^{-1}), we detected deletion of the *Cyln2* region between the outer most *lox*P sites by Southern-blot analysis.

We injected CLIP-T and CLIP-L ES cell lines with correct karyotypes into C57Bl/6 blastocysts. Male chimeric mice were mated with female C57Bl/6 mice to transmit the modified *Cyln2* alleles to the germ line. We determined the genotypes of the CLIP-T and CLIP-L mice by either Southern-blot or PCR analysis using the probes and primer sets indicated in Fig.1*a* (primer sequences are available upon request).

RNA and protein analyses

We prepared total RNA or protein from mouse brain as described (De Zeeuw et al., 1997; Hoogenraad et al., 2000) and performed northern- and western-blot analyses using standard protocols (Sambrook et al., 1989). The *Cyln2*, *lacZ*, *Gapdh*, *Eif4h*, *Rfc2* and *Gtf2ird1* probes (the latter three obtained from IMAGE clones 1276725, 1396169 and 555547, respectively) were radioactively labeled using PCR or random prime methods. The antibodies against CLIP-115 (no. 2238), CLIP-115/170 (no. 2221) and CLIP-170 (no. 2360) used for western blotting, have been described (Coquelle et al., 2002; Hoogenraad et al., 2000).

Histology and electron microscopy

Immunohistochemistry and electron microscopy on mouse brain sections were performed as published (De Zeeuw et al., 1997). For X-gal staining, we fixed dissected brains for 30 min at room temperature in 2% paraformaldehyde, 0.2% glutaraldehyde, in PBS buffer containing 2 mM $MgCl_2$, 5 mM EGTA (pH 8.0) and 0.02% Nonidet P-40 (NP-40). We subsequently washed brains 3 times for 10 min each at room temperature, in 0.02% NP-40 in PBS-buffer and stained whole mount brains and sections for 2 h (or overnight) at 37° in PBS-buffer containing 1 mg ml^{-1} X-gal, 5 mM $K3Fe(CN)_6$, 5 mM $K_4Fe(CN)_6$, 2 mM $MgCl_2$, 0.01% SDS and 0.02% NP-40. For electron microscopy, two homozygous *Cyln2*-knockout, two heterozygous and two wild type mice were transcardially perfused with 1% glutaraldehyde and 3% paraformaldehyde in 0.18 M cacodylate buffer. We dissected the brainstem, including the inferior olive, as well as the cerebellum and hippocampus and cut these brain regions on a Vibratome into sections 100 μm thick. We subsequently osmicated, stained and blocked sections with 3% uranyl acetate and embedded sections in Araldite. We made pyramids of the various olivary subnuclei and cut ultrathin sections that were counterstained with 1% lead citrate and 2% uranyl acetate and examined under a Philips CM-100 electron microscope.

Mouse strains, weights and calcium levels

Generation of the *Cyln2*-knockout strains of mice was approved by the local animal experimental committee at the Erasmus University Rotterdam. Mice were housed at ambient temperature and

subjected to a 12 h day:12 h night circadian cycle with constant access to food and water. When necessary, mice were allowed to accommodate to a new environment for an appropriate period of time before behavioral experiments were done.

We sacrificed mice at different ages (P1, P14 and adult) and immediately analyzed body weights (including brain), total brain weight (including cerebellum, cerebrum, cerebrospinal fluid and brainstem) and calcium levels. Serum calcium concentrations were determined colorimetrically (600 nm, Arsenazo III) as described by the supplier (Sigma diagnostics). For determination of the growth curves groups, we analyzed mice of different genotypes twice per week from two to ten weeks of age at fixed time points during the day.

Magnetic resonance imaging (MRI)

For the MRI analysis, we selected 5-month homozygous, heterozygous and wild type littermates from the CLIP-L strain and age-matched CLIP-T mice. We anesthetized mice using 5% isoflurane induction and 1-1.5% isoflurane maintenance. Isoflurane was administered in a mixture of 30% oxygen and 70% NO_2. We firmly fixed the head of each mouse in a stereotactic device consisting of earplugs and a tooth bar. During MRI, we kept the temperature of the mouse constant at 37.0 ± 0.5 °C. Using Visual Basic code, we monitored the temperature with a rectal probe (PT100), which fed back to a temperature-controlled electrical heating pad (Uty Nelson). The MRI imaging was performed at 300 MHz on an SMIS MR microscope (MRRS) with a 7T horizontal bore magnet and 8 cm aperture self-shielded gradients with a strength of 0.1 T m^{-1} (Oxford Instruments). We positioned the stereotactical apparatus in the center of a 30-mm wide RF bird-cage coil used for both transmitting and receiving. Scouting gradient-echo images in the three orthogonal directions were acquired to guide the reproducible positioning of the three-dimensional (3D) slab of the mouse head. We obtained high resolution coronal slices of the mouse brain using a 3D Fast Spin Echo sequence (Fransen et al., 1998; Kooy et al., 1999; Yuan et al., 1993) with an echo-train length of four, reducing the imaging time by a factor of four.

We acquired MR signals of a 3D volume of 20 x 20 x 20 mm^3 within a 256 x 128 x 64 matrix. The images were taken with a repetition time of 2,500 ms and a first echo time of 35 ms with an inter-echo delay of 25 ms (with echo times of 35, 60, 85, 110 ms). The central line of the k-space was sampled at the first echo. We chose these parameters to obtain 3D images of the brain with optimal contrast between the different brain structures within an acceptable time period. The imaging procedure took about 85 min and allowed a short anesthesia period. We reconstructed the MR data to an image matrix of 256 x 256 x 256, containing 256 coronal slices of 78 µm with in-plane resolution of 78 x 78 $µm^2$. Volumes from different brain structures were estimated to find differences between CLIP-T, wild type, *Cyln2*$^{+/-}$ and *Cyln2*$^{-/-}$mice. We defined brain and ventricular structures on coronal MR images according to the Mouse Brain atlas and their positions in terms of antero-posterior distance to the interaural line (IA).

To extract quantitative volumes of the total brain including the cerebellum (starting from IA –2.00 mm) from a set of images of the mouse obtained *in vivo*, we applied a semi-automatic 3D segmentation technique(Sijbers et al., 1997) on the 3D MR images data set using Visual C routines and Interactive Data Language (IDL, Research Systems). We used Surfdriver software to segment the volumes of the hippocampus (located from IA 2.86 mm to IA 0.72 mm), amygdala (located from IA 2.86 to 1.26 mm), corpus callosum (located from IA 1.50 mm to 3.00 mm) and the entire ventricular system. We later divided the entire ventricular system into the fourth ventricle, the aqueduct of Sylvius, the third ventricle and the lateral ventricles, according to the stereotactic atlas of Paxinos.

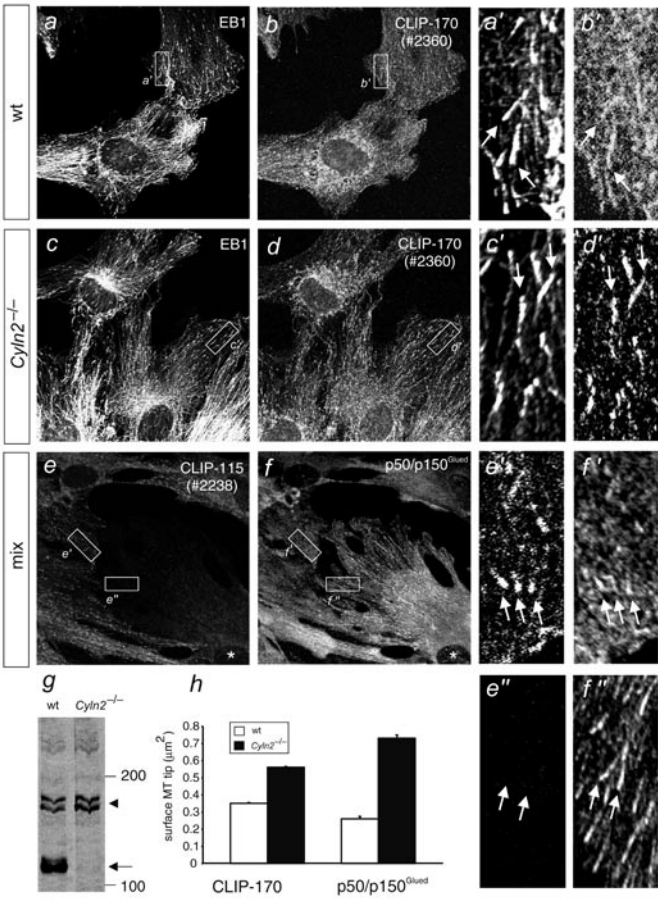

Figure 7. Accumulation of CLIP-170 and dynactin at microtubule tips in Cyln2-knockout fibroblasts

a-f, Fibroblasts derived from *Cyln2*$^{-/-}$ mice or wild type (wt) littermates were seeded separately (*a-d*) or as a mix (*e, f*), and stained for endogenous EB1 (*a, c*), CLIP-170 (no. 2360; *b, d*), CLIP-115 (no. 2238; *e*) or dynactin (p50/p150^{Glued}; *f*) using specific antibodies. Increased accumulation increased accumulation of CLIP-170 and the dynactin complex at microtubule tips is visible in *Cyln2*-knockout cells. This is more obvious in the enlarged insets in each panel.

g, Western blot of protein lysates from wild type (wt) or *Cyln*$^{-/-}$ fibroblasts, separated by 6 % SDS-PAGE and probed with an antibody that recognizes both CLIP-115 and CLIP-170 (no. 2221). The positions of CLIP-170 (arrowhead, doublet band) and CLIP-115 (arrow) are indicated.

h, Quantification of microtubule plus-end staining intensities. The intensity of fluorescent signals at microtubule plus-ends was quantified by measuring the fluorescent surface area of individual microtubules (in μm^2) in which the pixel intensity exceeded a preset threshold value. For staining with antibodies against CLIP-170 (no. 2360), we measured 939 microtubules from wild type fibroblasts and 1,569 microtubules from *Cyln2*-knockout cells. For staining with antibodies against p50 and p150 (p50/p150), we measured 147 microtubules from wild type fibroblasts and 159 MTs from knockout cells. Data are expressed as mean ± s.e.m. Differences in staining intensity between genotypes were highly significant ($P < 0.001$).

Behavioral tests

We carried out all behavioral experiments in a double-blind manner and analyzed wild type and mutant mice for motor coordination as described (De Zeeuw et al., 1998a; Storm et al., 1998). We performed the elevated zero-maze test as described previously (Heisler et al., 1998; Tarantino et al., 2000), using a circular runway (46 cm in diameter, 5.5 cm wide and elevated by 40 cm) divided into two opposing open quadrants without walls and 2 opposing closed quadrants with walls 11 cm high. We placed male mice in the closed quadrant of the maze and allowed them to investigate for 5 min. We monitored the amount of time spent in the open quadrants with a stopwatch and counted the number of entries into open quadrant.

For the computer-assisted 24 h contextual fear-conditioning experiment (Anagnostaras et al., 2000), we placed mice (5-6 months of age) in the conditioning chamber and administered a foot shock (2 s duration, 1.0 mA) after a 2-min baseline period. After 24 h, we placed the mice back into the same conditioning chamber for a 2-min contextual freezing test. In the cued fear-conditioning experiment (Anagnostaras et al., 2000), we placed mice in the conditioning chamber, and after 2 min they received the cue (a tone of 10 s duration, 75 dB, 2.8 kHz). During the final 2 s, mice received a foot shock (1.0 mA). After 24 h, we placed mice in a different

chamber and, after a 2-min baseline period, played the original training tone for 2 min. In both experiments, we scored freezing by computer, using a web cam at 5Hz and customary written software (Matlab). In this manner we could score freezing and activity frame by frame, similar to a previously published method (Anagnostaras et al., 2000).

In the open-field activity tests (50x50 cm), mice were tested for spontaneous locomotor activity. Mice always started from the same corner of the arena, and we recorded them for 5 min using a computerized video tracking system to measure walking distance, moving episodes and moving time at the horizontal and vertical planes and entries of the mice in different imaginary parts of the field.

The compensatory eye-movement test investigates the role of the vestibulocerebellum in controlling the gain and phase of the optokinetic reflex and the vestibulo-ocular reflex (De Zeeuw et al., 1998a). The mice received a head pedestal and an eyecoil under halothane anesthesia, and after recovery were subjected to visual and vestibular stimulation with the use of a drum and turntable at a wide variety of amplitudes (3-15°) and frequencies (0.1-1.6 Hz). We collected the eye movement data before and after visuovestibular training paradigms using Spike-2 (CED) and analyzed these data offline using Matlab programs.

In the hanging wire test (to measure balance and grip strength), we placed mice on top of a wire cage lid taped around the edge and suspended 30 cm above the cage. The lid was shaken three times and then turned upside down and the amount of time that each mouse held on to the lid was recorded, up to a maximum of 60 s.

We assessed motor coordination and balance of mice by measuring the ability of the mice to cross a wooden beam 1 cm wide and 30 cm long, placed horizontally above the bench surface. During training, we allowed mice to explore the beam for 5 min. During the test, we placed each mouse on one end of the beam and recorded the amount of time needed to walk across the beam, up to a maximum of 60 s. Four trials were carried out for each mouse. If a mouse fell off the beam, we scored the trial as 60 s.

The accelerating rotarod test analyzes more complicated motor behaviors and motor learning. The rotarod consists of a smooth plastic roller (8 cm in diameter and 14 cm long) flanked by two large round plates (30 cm in diameter) to prevent mice from escaping. We placed each mouse on the roller for 10 s at a constant rotation (2 rpm) and then gradually increased the rotational speed to 12 rpm over the course of 2 min. We trained mice on day 1 using a stationary rotarod and then tested them over the next 5 days by carrying out three trials for each mouse every day, measuring the amount of time each mouse remained on the rotarod, up to a maximum of 60 s.

The circadian running-wheel test measures the cage activity of mice over 24 h (van der Horst et al., 1999). After an acclimatization period, we tested the circadian rhythms of wild type (n = 4), *Cyln2*$^{+/-}$(n = 4) and *Cyln2*$^{-/-}$ (n = 4) mice using a normal cage with a running wheel. All groups of mice had normal circadian rhythms (data not shown). We noted, however, that *Cyln2*$^{-/-}$ and *Cyln2*$^{+/-}$ mice showed strikingly poor coordination in the running wheel during the initial accommodation period. Although this behavior is not part of a standard test for movement and coordination, it was so notable that we recorded films of wild type and *Cyln2*$^{-/-}$ mice and quantified their behavior. Whereas wild type mice ran in the wheel with smooth coordination, *Cyln2*$^{-/-}$ mice had highly variable motions. This became obvious when interruptions of smooth running behavior were quantified for the four mice of each genotype during a period of 30 s. Wild type mice averaged 2.0 ± 0.7 interruptions per 30 s, whereas *Cyln2*-knockout mice averaged 9.3 ± 1.3 interruptions per 30 s; the difference was statistically significant ($P < 0.005$). Both *Cyln2*$^{-/-}$ and *Cyln2*$^{+/-}$ mice improved their running-wheel performance throughout the acclimatization period, which explains their normal circadian activity patterns afterward.

Electrophysiological recordings

For electrophysiological measurements, we decapitated mice, quickly removed the brains and chilled them in carbogenated (95% O_2 and 5% CO_2) artificial cerebrospinal fluid (aCSF: 120 mM NaCl, 3.5 mM KCl, 1.3 mM $MgSO_4$, 1.25 mM NaH_2PO_4, 2.5 mM $CaCl_2$, 10 mM D-glucose, 25 mM $NaHCO_3$). We prepared hippocampal slices (400 µm) from dissected brain with a tissue chopper and maintained these at room temperature in carbogenated aCSF. After an equilibration period of at least 1 h, we transferred one slice at a time to a recording chamber, which was continuously perfused with carbogenated aCSF (2-3 ml min^{-1}) and kept at 30-32 °C. We fixed and submerged the slice between two nylon meshes and placed a bipolar stimulation electrode (delivering 150 µs pulses) in the Schaffer collateral-commissural fibers and low resistance glass microelectrodes (2-5 MΩ, filled with aCSF) in the CA1 dendritic layer to record field evoked post-synaptic potential (fEPSP).

In each experiment, we first determined the maximal fEPSP amplitude by gradually increasing the stimulus intensity (using an interstimulus interval of 10 s) until the responses reached a saturating level. We fit the relationship between stimulus intensity and the evoked response to a sigmoidal function, and determined which stimulus intensity evoked a response that was ~50% of the maximal EPSP amplitude. In all experiments, we monitored baseline synaptic transmission for at least 10 min with stimuli delivered at an interval of 60 s. After this period, we administered theta-burst stimulation in a pattern consisting of two 30-ms bursts with four pulses at 100 Hz separated by 200 ms; the pattern was applied five times at intervals of 30 s. After theta-burst stimulation, we measured synaptic response for 40 min at 0.0166 Hz (Krugers et al., 1997).

Cell biological analysis

We have previously described GFP-CLIP-115 and GFP-CLIP-170 constructs, as well as methods for culturing and transfection of COS-1 cells (Hoogenraad et al., 2000). To generate GFP-CLIP-170(-tail), we deleted the last 79 amino acids of rat brain-derived CLIP-170. The GPF-CLIP-115(+tail) construct contains the C-terminal 159 amino acids of CLIP-170 linked in-frame to CLIP-115. We obtained primary mouse fibroblasts either from the trunk region of E13.5 day mouse embryos or from adult skin. Fibroblasts were grown for 3-6 passages before analysis. We carried out immunofluorescence studies (Akhmanova et al., 2001) with the following primary and secondary antibodies and dilutions: rabbit antibody against CLIP-170 (antiserum no. 2360; 1:300), rabbit antibody against CLIP-115 (no. 2238; 1:300), rabbit antibody against CLIP-115/170 (no. 2221; 1:300), mouse antibody against $p50^{dynamitin}$, mouse antibody against $p150^{Glued}$ and mouse antibody against EB1 (Transduction Laboratories, 1:100), rhodamine-labeled sheep antibody against mouse (Boehringer, 1:25), fluorescein isothiocyanate (FITC)-conjugated goat antibody against rabbit (Nordic Laboratories; 1:100), Alexa-594-conjugated goat antibody against rabbit (Molecular probes, 1:500) and Alexa-350-conjugated sheep antibody against mouse (Molecular probes, 1:250). We mounted slides using Vectashield mounting medium (Vector laboratories) containing 4',6'-diamidino-2-phenylindoehydrochloride (DAPI) (Sigma) and acquired microscopic images as described (Akhmanova et al., 2001). To quantify the fluorescent signal on microtubule plus-ends, we exported images and analyzed pixel intensities using Image SXM, an extended version of the NIH Image public-domain software program. In Image SXM, we set identical threshold levels for each image and then calculated the surface of individual fluorescent plus-end signals in μm^2 per microtubule plus-end by manually selecting the ends with the wand tool. For CLIP-170 fluorescent intensity, we analyzed ten images each from *Cyln2*-knockout and

wild type fibroblasts (>20 cells per genotype), and for dynactin signals we analyzed five images from the mixed cell cultures (>10 cells).

We analyzed microtubule dynamic behavior by injection of Cy3-labelled tubulin into fibroblasts, as described previously (Kaverina et al., 1999). Microtubule growth and shrinkage rates, as well as catastrophe and rescue events, were calculated by exporting movies of microtubules in living cells to Image SXM. Individual microtubules were followed frame by frame to record their behavior and generate life-history plots. The behavior of growing microtubule plus-ends was analyzed in live transfected cells as described previously (Akhmanova et al., 2001). Mouse fibroblasts (*Cyln2*-knockout and wild type cells) were transfected with EB3-GFP, which is the best marker for visualization of growing microtubule ends in transfected cells (T. Stepanova, A.A., C.C.H., F.G. and N.G., manuscript in preparation).

Statistical analysis

We compared genotypes at fixed time points using either a two-tailed Student *t*-test (to compare data from two groups) or a one-way ANOVA (to compare data from more than two groups). In the latter case, if we obtained a significant difference, Dunnett's multiple comparison was used as a *post-hoc* test with wild type littermates of CLIP-L mice as the reference group. We compared genotypes over time using a two-way repeated-measures ANOVA, with a correction for differences in variance over time. Analysis of the interaction terms (genotype-time) failed to show significant differences in growth curves or rotarod behavior over time between the different genotypes. Thus, the shape of the curves shown in the figures is not significantly different between the genotypes. We analyzed data using Microsoft Excel, GraphPad Prism and SAS for Windows.

Acknowledgements

We would like to thank G. van Cappellen for his help with the quantification of the fluorescence data and live imaging analysis, M. Rutteman for x-gal staining experiments and A. Langeveld for FISH experiments. This research was supported by the Netherlands Organization for Scientific Research (NWO) and the Royal Dutch Academy of Sciences (KNAW).

References

Akhmanova, A., C.C. Hoogenraad, K. Drabek, T. Stepanova, B. Dortland, T. Verkerk, W. Vermeulen, B.M. Burgering, C.I. De Zeeuw, F. Grosveld, and N. Galjart. 2001. Clasps are CLIP-115 and -170 associating proteins involved in the regional regulation of microtubule dynamics in motile fibroblasts. *Cell.* 104:923-35.

Anagnostaras, S.G., S.A. Josselyn, P.W. Frankland, and A.J. Silva. 2000. Computer-assisted behavioral assessment of Pavlovian fear conditioning in mice. *Learn Mem.* 7:58-72.

Armstrong, D.M. 1986. Supraspinal contributions to the initiation and control of locomotion in the cat. *Prog Neurobiol.* 26:273-361.

Bellugi, U., L. Lichtenberger, W. Jones, Z. Lai, and M. St George. 2000. I. The neurocognitive profile of Williams Syndrome: a complex pattern of strengths and weaknesses. *J Cogn Neurosci.* 12:7-29.

Bellugi, U., L. Lichtenberger, D. Mills, A. Galaburda, and J.R. Korenberg. 1999. Bridging cognition, the brain and molecular genetics: evidence from Williams syndrome. *Trends Neurosci.* 22:197-207.

Bloedel, J.R., and J. Courville. 1981. Handbook of physiology vol II: Motor Control. A review of cerebellar afferent systems. Williams & Wilkins, Baltimore. 735-830 pp.

Bourtchuladze, R., B. Frenguelli, J. Blendy, D. Cioffi, G. Schutz, and A.J. Silva. 1994. Deficient long-term memory in mice with a targeted mutation of the cAMP- responsive element-binding protein. *Cell*. 79:59-68.

Brunner, D., and P. Nurse. 2000. CLIP170-like tip1p spatially organizes microtubular dynamics in fission yeast. *Cell*. 102:695-704.

Coquelle, F.M., M. Caspi, F.P. Cordelieres, J.P. Dompierre, D.L. Dujardin, C. Coifmann, P. Martin, C.C. Hoogenraad, A. Akhmanova, N. Galjart, J.R. De Mey, and O. Reiner. 2002. LIS1: CLIP-170's Key to the Dynein/Dynactin Pathway. *Mol. Cell. Biol.* (in press).

De Zeeuw, C.I., C. Hansel, F. Bian, S.K. Koekkoek, A.M. van Alphen, D.J. Linden, and J. Oberdick. 1998a. Expression of a protein kinase C inhibitor in Purkinje cells blocks cerebellar LTD and adaptation of the vestibulo-ocular reflex. *Neuron*. 20:495-508.

De Zeeuw, C.I., C.C. Hoogenraad, E. Goedknegt, E. Hertzberg, A. Neubauer, F. Grosveld, and N. Galjart. 1997. CLIP-115, a novel brain-specific cytoplasmic linker protein, mediates the localization of dendritic lamellar bodies. *Neuron*. 19:1187-99.

De Zeeuw, C.I., J.I. Simpson, C.C. Hoogenraad, N. Galjart, S.K. Koekkoek, and T.J. Ruigrok. 1998b. Microcircuitry and function of the inferior olive. *Trends Neurosci.* 21:391-400.

Francke, U. 1999. Williams-Beuren syndrome: genes and mechanisms. *Hum Mol Genet*. 8:1947-54.

Frangiskakis, J.M., A.K. Ewart, C.A. Morris, C.B. Mervis, J. Bertrand, B.F. Robinson, B.P. Klein, G.J. Ensing, L.A. Everett, E.D. Green, C. Proschel, N.J. Gutowski, M. Noble, D.L. Atkinson, S.J. Odelberg, and M.T. Keating. 1996. LIM-kinase1 hemizygosity implicated in impaired visuospatial constructive cognition. *Cell*. 86:59-69.

Fransen, E., R. D'Hooge, G. Van Camp, M. Verhoye, J. Sijbers, E. Reyniers, P. Soriano, H. Kamiguchi, R. Willemsen, S.K. Koekkoek, C.I. De Zeeuw, P.P. De Deyn, A. Van der Linden, V. Lemmon, R.F. Kooy, and P.J. Willems. 1998. L1 knockout mice show dilated ventricles, vermis hypoplasia and impaired exploration patterns. *Hum Mol Genet*. 7:999-1009.

Heisler, L.K., H.M. Chu, T.J. Brennan, J.A. Danao, P. Bajwa, L.H. Parsons, and L.H. Tecott. 1998. Elevated anxiety and antidepressant-like responses in serotonin 5-HT1A receptor mutant mice. *Proc Natl Acad Sci U S A*. 95:15049-54.

Hoogenraad, C.C., A. Akhmanova, F. Grosveld, C.I. De Zeeuw, and N. Galjart. 2000. Functional analysis of CLIP-115 and its binding to microtubules. *J Cell Sci*. 113:2285-97.

Hoogenraad, C.C., B.H. Eussen, A. Langeveld, R. van Haperen, S. Winterberg, C.H. Wouters, F. Grosveld, C.I. De Zeeuw, and N. Galjart. 1998. The murine CYLN2 gene: genomic organization, chromosome localization, and comparison to the human gene that is located within the 7q11.23 Williams syndrome critical region. *Genomics*. 53:348-58.

Jaegle, M., W. Mandemakers, L. Broos, R. Zwart, A. Karis, P. Visser, F. Grosveld, and D. Meijer. 1996. The POU factor Oct-6 and Schwann cell differentiation. *Science*. 273:507-10.

Kaverina, I., O. Krylyshkina, and J.V. Small. 1999. Microtubule targeting of substrate contacts promotes their relaxation and dissociation. *J Cell Biol*. 146:1033-44.

Kim, J.J., and M.S. Fanselow. 1992. Modality-specific retrograde amnesia of fear. *Science*. 256:675-7.

Kooy, R.F., E. Reyniers, M. Verhoye, J. Sijbers, C.E. Bakker, B.A. Oostra, P.J. Willems, and A. Van Der Linden. 1999. Neuroanatomy of the fragile X knockout mouse brain studied using in vivo high resolution magnetic resonance imaging. *Eur J Hum Genet*. 7:526-32.

Krugers, H.J., M. Mulder, J. Korf, L. Havekes, E.R. de Kloet, and M. Joels. 1997. Altered synaptic plasticity in hippocampal CA1 area of apolipoprotein E deficient mice. *Neuroreport*. 8:2505-10.

Morris, C.A., S.A. Demsey, C.O. Leonard, C. Dilts, and B.L. Blackburn. 1988. Natural history of Williams syndrome: physical characteristics. *J Pediatr.* 113:318-26.

Olson, T.M., V.V. Michels, Z. Urban, K. Csiszar, A.M. Christiano, D.J. Driscoll, R.H. Feldt, C.D. Boyd, and S.N. Thibodeau. 1995. A 30 kb deletion within the elastin gene results in familial supravalvular aortic stenosis. *Hum Mol Genet*. 4:1677-9.

Osborne, L.R. 1999. Williams-Beuren syndrome: unraveling the mysteries of a microdeletion disorder. *Mol Genet Metab*. 67:1-10.

Osborne, L.R., D. Martindale, S.W. Scherer, X.M. Shi, J. Huizenga, H.H. Heng, T. Costa, B. Pober, L. Lew, J. Brinkman, J. Rommens, B. Koop, and L.C. Tsui. 1996. Identification of genes from a 500-kb region at 7q11.23 that is commonly deleted in Williams syndrome patients. *Genomics*. 36:328-36.

Pankau, R., C.J. Partsch, A. Gosch, H.C. Oppermann, and A. Wessel. 1992. Statural growth in Williams-Beuren syndrome. *Eur J Pediatr.* 151:751-5.

Peoples, R., Y. Franke, Y.K. Wang, L. Perez-Jurado, T. Paperna, M. Cisco, and U. Francke. 2000. A physical map, including a BAC/PAC clone contig, of the Williams- Beuren syndrome--deletion region at 7q11.23. *Am J Hum Genet*. 66:47-68.

Perez, F., G.S. Diamantopoulos, R. Stalder, and T.E. Kreis. 1999. CLIP-170 highlights growing microtubule ends in vivo. *Cell*. 96:517-27.

Phillips, R.G., and J.E. LeDoux. 1992. Differential contribution of amygdala and hippocampus to cued and contextual fear conditioning. *Behav Neurosci*. 106:274-85.

Reiner, O., R. Carrozzo, Y. Shen, M. Wehnert, F. Faustinella, W.B. Dobyns, C.T. Caskey, and D.H. Ledbetter. 1993. Isolation of a Miller-Dieker lissencephaly gene containing G protein beta-subunit-like repeats. *Nature*. 364:717-21.

Reiss, A.L., S. Eliez, J.E. Schmitt, E. Straus, Z. Lai, W. Jones, and U. Bellugi. 2000. IV. Neuroanatomy of Williams syndrome: a high-resolution MRI study. *J Cogn Neurosci*. 12:65-73.

Sambrook, J., E.F. Fritsch, and T. Maniatis. 1989. Molecular cloning: a laboratory manual, 2 Edition. Cold Spring Harbor Laboratory Press, New York.

Schmitt, J.E., S. Eliez, I.S. Warsofsky, U. Bellugi, and A.L. Reiss. 2001. Corpus callosum morphology of Williams syndrome: relation to genetics and behavior. *Dev Med Child Neurol*. 43:155-9.

Schuyler, S.C., and D. Pellman. 2001. Microtubule "plus-end-tracking proteins": The end is just the beginning. *Cell*. 105:421-4.

Sijbers, J., P. Scheunders, M. Verhoye, A. van der Linden, D. van Dyck, and E. Raman. 1997. Watershed-based segmentation of 3D MR data for volume quantization. *Magn Reson Imaging*. 15:679-88.

Silva, a.j., and et al. 1997. Mutant mice and neuroscience: recommendations concerning genetic background. Banbury Conference on genetic background in mice. *Neuron*. 19:755-9.

Storm, D.R., C. Hansel, B. Hacker, A. Parent, and D.J. Linden. 1998. Impaired cerebellar long-term potentiation in type I adenylyl cyclase mutant mice. *Neuron*. 20:1199-210.

Tarantino, L.M., T.J. Gould, J.P. Druhan, and M. Bucan. 2000. Behavior and mutagenesis screens: the importance of baseline analysis of inbred strains. *Mamm Genome*. 11:555-64.

Tassabehji, M., K. Metcalfe, D. Donnai, J. Hurst, W. Reardon, M. Burch, and A.P. Read. 1997. Elastin: genomic structure and point mutations in patients with supravalvular aortic stenosis. *Hum Mol Genet*. 6:1029-36.

Tassabehji, M., K. Metcalfe, A. Karmiloff-Smith, M.J. Carette, J. Grant, N. Dennis, W. Reardon, M. Splitt, A.P. Read, and D. Donnai. 1999. Williams syndrome: use of chromosomal microdeletions as a tool to dissect cognitive and physical phenotypes. *Am J Hum Genet*. 64:118-25.

Valero, M.C., O. de Luis, J. Cruces, and L.A. Perez Jurado. 2000. Fine-scale comparative mapping of the human 7q11.23 region and the orthologous region on mouse chromosome 5G: the low-copy repeats that flank the Williams-Beuren syndrome deletion arose at breakpoint sites of an evolutionary inversion(s). *Genomics*. 69:1-13.

Valetti, C., D.M. Wetzel, M. Schrader, M.J. Hasbani, S.R. Gill, T.E. Kreis, and T.A. Schroer. 1999. Role of dynactin in endocytic traffic: effects of dynamitin overexpression and colocalization with CLIP-170. *Mol Biol Cell*. 10:4107-20.

Vallee, R.B., C. Tai, and N.E. Faulkner. 2001. LIS1: cellular function of a disease-causing gene. *Trends Cell Biol*. 11:155-60.

Van der Horst, G.T., M. Muijtjens, K. Kobayashi, R. Takano, S. Kanno, M. Takao, J. de Wit, A. Verkerk, A.P. Eker, D. van Leenen, R. Buijs, D. Bootsma, J.H. Hoeijmakers, and A. Yasui. 1999. Mammalian Cry1 and Cry2 are essential for maintenance of circadian rhythms. *Nature*. 398:627-30.

Vaughan, K.T., S.H. Tynan, N.E. Faulkner, C.J. Echeverri, and R.B. Vallee. 1999. Colocalization of cytoplasmic dynein with dynactin and CLIP-170 at microtubule distal ends. *J Cell Sci*. 112:1437-47.

Voogd, J., and M. Glickstein. 1998. The anatomy of the cerebellum. *Trends Neurosci*. 21:370-5.

Yuan, C., U.P. Schmiedl, E. Weinberger, W.R. Krueck, and S.D. Rand. 1993. Three-dimensional fast spin-echo imaging: pulse sequence and in vivo image evaluation. *J Magn Reson Imaging*. 3:894-9.

Chapter 3

CLIP-115 and -170 are microtubule rescue factors that regulate cell spreading and prevent dynein-dynactin aggregation

Manuscript in preparation

Chapter 3

CLIP-115 and -170 are microtubule rescue factors that regulate cell spreading and prevent dynein-dynactin aggregation

Marja Miedema[1], Yulia Komarova[2], Catherine Robin[1], Jeffrey van Haren[1], Casper Hoogenraad[1*], Anna Akhmanova[1], Marvin Tanenbaum[3], Rene Medema[3], Frank Grosveld[1], and Niels Galjart[1]

[1] Department of Cell Biology and Genetics, P.O. Box 2040, 3000 CA Rotterdam, The Netherlands. [2] Department of Cell and Molecular Biology, Northwestern University Medical School, 303 E. Chicago Avenue, Chicago, Illinois 60611-3008. [3] Department of Medical Oncology, University Medical Center, Stratenum 2.118, Universiteitsweg 100, 3584 CG Utrecht, The Netherlands.

* Present address:
Department of Neuroscience, P.O. Box 2040, 3000 CA Rotterdam, The Netherlands

Abstract

The cytoplasmic linker proteins CLIP-115 and -170 were originally proposed to link vesicular cargo to microtubules. Later studies showed that both CLIPs are microtubule 'plus-end-tracking proteins', or +TIPs, with a redundant role as microtubule rescue factors in CHO cells. To further investigate CLIP function, we derived CLIP-115/170 double knockout (DKO) fibroblasts from DKO mice. These cells are devoid of CLIP-115 and -170, which results in reduced microtubule rescue frequencies. Expression of a truncated form of CLIP-170, that contains the N-terminal microtubule binding motifs, restores rescue frequencies to wild type levels. Surprisingly, DKO fibroblasts spread abnormally; when attached they are much larger than wild type cells, yet in suspension they have a similar volume. In addition, DKO cells accumulate large aggregates of dynein-dynactin in microtubule-free, extremely flat areas of cells. These accumulations also contain BicD2, a CLIP-115-interacting protein. Thus, CLIPs are microtubule rescue factors that regulate cell spreading. Since CLIPs control the proper microtubule plus-end accumulation of a number of other +TIPs involved in motor-mediated transport, we propose that cycling at microtubule ends prevents aggregation of these proteins.

Introduction

Microtubules form a highly dynamic intracellular network and are essential in several fundamental processes such as cell morphogenesis, cell motility, cell division and intracellular transport. They are polar fibers with a fast growing 'plus'-end and a slower growing 'minus'-end. In many cell types microtubules form radial arrays with their minus ends anchored near the centrosome, which is the major microtubule organizing center (MTOC). Microtubule plus-ends grow persistently towards the cell periphery (Komarova et al., 2002b), where they undergo frequent transitions from steady growth to rapid shrinkage (catastrophe) and vice versa (rescue), a behavior known as dynamic instability (Mitchison and Kirschner, 1984).

Numerous proteins have been shown to associate and interact with microtubules and thereby regulate this network. Among them are factors that localize specifically to the ends of microtubules. In mammalian cells this group of so called 'plus-end-tracking proteins', or +TIPs (Schuyler and Pellman, 2001), actually only associates with the ends of growing microtubules. 'Plus-end tracking' behavior was first demonstrated for CLIP-170, a cytoplasmic linker protein of 170 kDa (Perez et al., 1999; Rickard and Kreis, 1990). Since this original and important observation, both the number and diversity of +TIPs has extended steadily (Akhmanova and Hoogenraad, 2005).

CLIP-170 was initially thought to be essential for the binding of endocytic vesicles to microtubules (Pierre et al., 1992), hence its name. Later studies showed that CLIP-170 influences microtubules dynamics, serving as an anti-catastrophe factor in fission yeast, yet as a rescue factor in mammalian cells (Brunner and Nurse, 2000; Komarova et al., 2002a). The closest mammalian homologue of CLIP-170, CLIP-115, also binds the ends of growing microtubules (Hoogenraad et al., 2000). The two CLIPs are structurally similar, with microtubule-binding (MTB) domains at their NH_2-terminus, that consist of two CAP_GLY motifs, surrounded by basic, serine-rich stretches. CAP_GLY regions have been shown to recognize COOH-terminal EEY/F motifs, which are present in EB1-like proteins and alpha-tubulin, and in CLIP-170 itself (Honnappa et al., 2006). The C-terminal tyrosine of alpha-tubulin is actually essential for microtubule-end accumulation of CLIPs in mammalian fibroblasts (Peris et al., 2006).

In both CLIPs the MTB domains are followed by several, long coiled coil regions, which allows homo-dimerization. In line with their structural similarity, studies in CHO cells showed that CLIP-115 and -170 act as redundant rescue factors and that microtubule rescue activity was located in the N-terminal domain (Komarova et al., 2002a). However, as these studies were done using a so-called dominant-negative approach (i.e. the overexpression of a C-terminal mutant of CLIP-170, that lacks the MTB regions and sequesters endogenous CLIPs in the cytoplasm of cells), the risk existed that the observed microtubule rescue defect was due to titration of essential cellular factors other than the CLIPs.

Another protein that shares the basic structure of the CLIPs (a MTB domain consisting of a CAP_GLY motif and basic amino acids, followed by a coiled-coil region) is $p150^{Glued}$, the largest subunit of the protein complex dynactin (Schroer, 2004). This complex was shown to be required for proper functioning of the molecular motor dynein. More recent data have, however, implicated dynactin in kinesin function as well (Berezuk and Schroer, 2007). CLIP-170 and dynactin have been shown to interact directly and overexpression of CLIP-170 enhances the accumulation of $p150^{Glued}$ at microtubule plus-ends, while CLIP-170 downregulation reduces $p150^{Glued}$ accumulation (Goodson et al., 2003; Lansbergen et al., 2004). These results suggest that CLIP-170 regulates dynactin function by localizing this complex.

The COOH-terminal region of CLIP-170 has been shown to be responsible for its interaction with endocytic vesicles and kinetochores (Dujardin et al., 1998; Perez et al., 1999; Pierre et al.,

1992), for binding to the dynein regulators LIS1 (Coquelle et al., 2002; Tai et al., 2002) and p150Glued (Goodson et al., 2003; Lansbergen et al., 2004), and for intra- and inter-molecular CLIP interactions (Lansbergen et al., 2004). CLIP-115 lacks such a COOH-terminal region, however, in mouse embryonic fibroblasts (MEFs) this protein was shown to mediate dynactin localization at microtubule ends indirectly, by competing with CLIP-170 (Hoogenraad et al., 2002).

Our group has previously generated mice with targeted mutations at the *Cyln2* (Hoogenraad et al., 2002) and *Rsn* (Akhmanova et al., 2005) loci, which encode CLIP-115 and CLIP-170, respectively. CLIP-115 deficiency results in a mild growth deficit, specific behavioral and neurophysiological problems and brain abnormalities, including enlarged ventricles and a smaller corpus callosum. Homozygous CLIP-170 deficient mice produce virtually no offspring due to abnormal sperm morphology. However, analysis of cultured fibroblasts derived from single knockout mice did not show a profound dysfunction.

To analyze CLIP function in more detail, we recently generated CLIP-115 and CLIP-170 double knockout (DKO) mice and derived both embryonic and adult fibroblasts from these mice. Using the DKO cells, we confirm a role for CLIPs as rescue factors (Komarova et al., 2002a). We further demonstrate that attached DKO fibroblasts have an increased surface area compared to wild type cells, while the volume of unattached cells is unaltered. These data indicate a role for the CLIPs in cell spreading. Finally, we observe large and extremely flat areas in DKO cells, which are microtubule-free and often contain aggregates of dynactin, dynein, and BicD2, a CLIP-115 interaction partner. Our data suggest that CLIPs are not only involved in the regulation of microtubule dynamics, but have an essential additional function in cell morphology. We propose that this role is linked to the microtubule end localization of the CLIPs.

Results

Double CLIP-115 and CLIP-170 knockout fibroblasts

Mouse lines deficient for either CLIP-115 or CLIP-170 were previously generated by our group (Akhmanova et al., 2005; Hoogenraad et al., 2002). Figure 1B shows how these two knockouts were generated. CLIP-115 and CLIP-170 double knockout (DKO) mice were made by crossing the single knockout lines. Since the genes encoding CLIP-115 (*Cyln2*) and CLIP-170 (*Rsn*) are located approximately 11 Mb apart on murine chromosome 5 (Fig. 1A), generation of the DKO line required a meiotic cross-over event (Miedema et al., 2007).

To study the cellular effect of a combined CLIP-115 and CLIP-170 deficiency, we derived dermal fibroblasts (MDFs) from young (5 to 10 weeks) adult homozygous DKO animals and their wild type (wt) littermates and mouse embryonic fibroblasts (MEFs) from embryonic day 13.5 (E13.5) pups. Genotypes were verified by PCR analysis (Fig. 1C).

In MDFs and MEFs no CLIP-115 and CLIP-170 could be detected on Western blot, using antibodies recognizing CLIP-115 (#2238), CLIP-170 (#2360) or both CLIP-115 and CLIP-170 (#2221) (Fig. 1D). The absence of CLIPs did not affect the cellular levels of tubulin or actin (Fig.1D). There is also no difference in the levels of other +TIPs such as dynactin ($p150^{Glued}$), dynein (dynein intermediate chain), CLASP1, CLASP2 and EBs (Fig. 1D and data not shown).

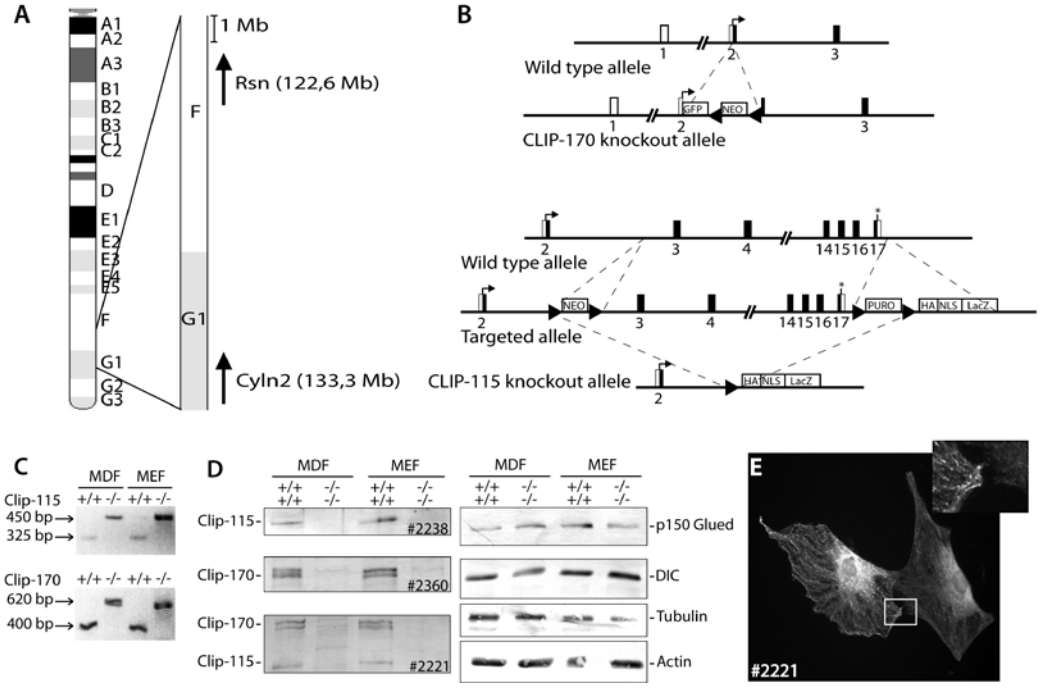

Figure 1. Double Clip-115 and Clip-170 knockout fibroblasts
A, B. Positions of the genes encoding Clip-115 (Cyln2) and Clip-170 (Rsn) on mouse chromosome 5 (**A**) and the gene loci with the respective targeting strategies (**B**). For Cyln2 the doubly targeted allele is shown below the wild type allele, containing neomycin (NEO) and puromycin (PURO) resistance genes flanked by loxP sites (arrowheads, not to scale) and a HA-NLS-lacZ cassette. Cre-mediated recombination in ES-cells at the outermost loxP-sites generates the knockout allele by removal of the vast majority of the coding sequences of Cyln2. Contrarily, the Clip-170 knockout allele was generated by targeting GFP and a loxP-flanked NEO to the ATG, leaving the rest of the gene intact. **C.** Genotyping of embryonic (MEF) and dermal (MDF) fibroblasts derived from wild type (wt) and homozygous double CLIP-115 and CLIP-170 knockout (dko) mice was done by PCR. **D.** Protein extracts of wt and dko MEFs and MDFs were analyzed by Western blot. Blots were incubated with polyclonal antibodies against Clip-115 (#2238), Clip-170 (#2360) and both Clip-115 and Clip-170 (#2221) to show the absence of the Clip-proteins in the dko cells. Incubations with monoclonal antibodies against dynactin (p150 Glued), dynein intermediate chain (DIC), tubulin and actin show no change in the levels of these proteins between wt and dko cells. **E.** Mixed wt and dko MEF cultures were incubated with antibody #2221, recognizing both Clip-115 and Clip-170, to show the absence of plus-ends in dko cells.

Immunofluorescence analysis using the antibody recognizing both CLIPs confirmed the absence of CLIPs at the plus-ends of microtubules (Fig. 1E).

We transfected MDFs with EB3-GFP in order to measure the speed of displacement of this marker of growing microtubules. As control we examined wild type and CLIP-170 single knockout MDFs. Rates of EB3-GFP movements were similar in the three cell types (Table 1). Taken together these results strongly suggest that DKO MDFs and MEFs are suitable model systems to study cellular effects of a combined CLIP deficiency.

CLIP deficiency decreases microtubule rescue frequency

CLIPs have been shown to serve as rescue factors in CHO-K1 cells (Komarova et al., 2002a). Since these studies were done using a dominant negative approach, we wanted to test the same parameters of microtubule dynamics in DKO cells using fluorescently labeled, microinjected

tubulin. Analysis of individual microtubules at the cell margin of wild type cells demonstrates the specific fluctuating behavior, with alternating episodes of shortening and growth (k_{res} = 0.10 s^{-1}) (Fig. 2A, B). The asymmetric distribution of shortening phases throughout the cell results in an increase in the number of growing plus-ends towards the periphery of the cell, as shown by staining for EB3 (Fig. 2C, D).

Table 1. Velocity of EB3-GFP displacements

Group	N	Mean (± S.E.M.)
wild type	24	0.37 ± 0.021
DKO	49	0.43 ± 0.013
CLIP-170 KO	52	0.40 ± 0.014

Data analyzed in MDFs, displacements are in micrometers/second, N; number of plus-ends measured.

In cells deficient for the CLIPs microtubule dynamics were profoundly altered. Although there was no change in growth and shortening rate and the catastrophe frequency was unaffected, there was a significant decrease in rescue frequency. Instead of fluctuating at the cell margin, most microtubules shrank persistently after catastrophe (Fig. 2E, F). The rescue frequency was calculated from the life history plots, indicating a fivefold decrease (Table 2). Without the fluctuating behavior of the microtubules, growing plus-ends do not concentrate near the cell edge, leading to an even distribution of growing microtubules throughout the cytoplasm, shown by the staining for EB3 (Fig. 2G,H). These results confirm the earlier conclusion that CLIPs function as rescue factors in regulating microtubule dynamics, thereby causing an accumulation of dynamic microtubule plus-ends at the cell periphery.

Microtubule rescue frequency can be restored by CLIP-170 head domain

Whereas the COOH-terminal domain of CLIP-170 serves as a dominant negative protein by removing endogenous CLIPs from the plus-ends, the monomeric NH_2-terminus has been shown to bind tubulin oligomers with high affinity and localize to microtubule plus-ends (Diamantopoulos et al., 1999; Folker et al., 2005; Scheel et al., 1999). We previously demonstrated that overexpression of EGFP-tagged CLIP-170 head was sufficient to restore microtubule dynamics when endogenous CLIPs had previously been removed by the CLIP-170 COOH-terminus (Komarova et al., 2002a).

We overexpressed the EGFP-CLIP monomeric head in DKO MEFs to determine whether we could restore microtubule dynamics in these cells as well. The EGFP-CLIP head decorates microtubules along the length, concentrating at the growing plus-ends (Fig. 3A), showing long episodes of persistent growth in the internal cytoplasm (Fig. 3C). It restores the fluctuating behavior that was abolished because of the CLIP deficiency, leaving microtubules to undergo frequent transitions between growth and shrinkage again (Fig. 3B,D). Analysis of the microtubule dynamics showed that the rescue frequency was restored to the level in wild type cells (Table 2). These results demonstrate that the abolishment of microtubule rescue in DKO cells is specifically caused by the absence of CLIP-115 and CLIP-170.

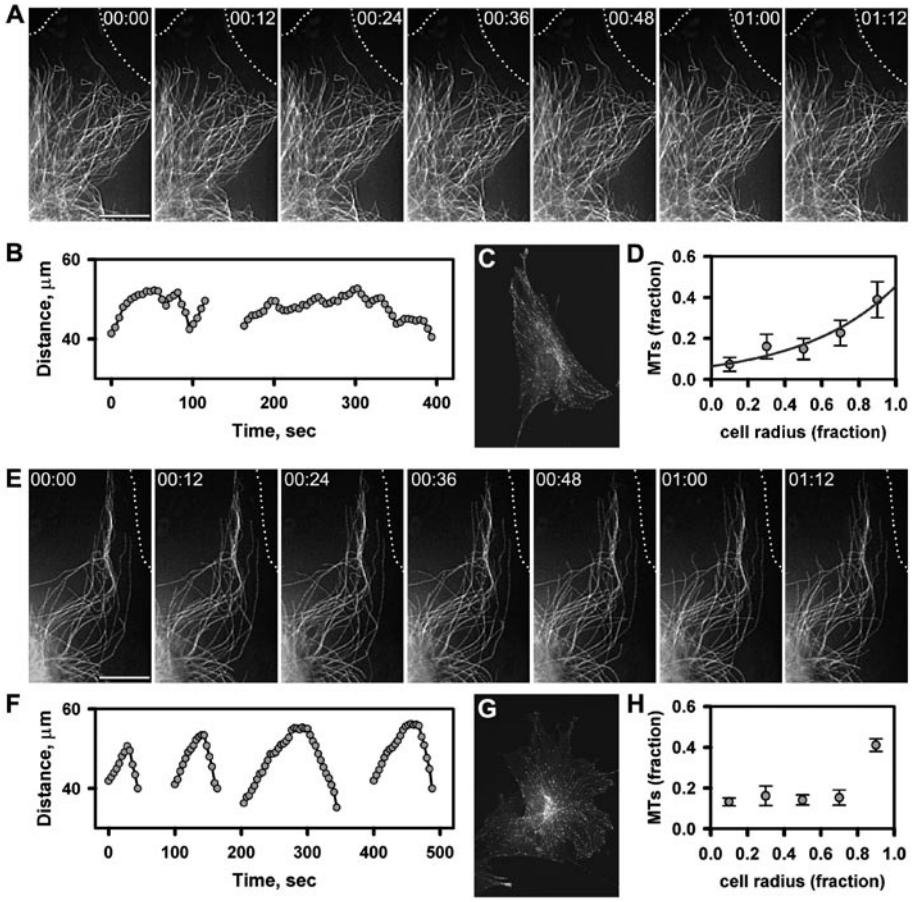

Figure 2. CLIPs promote microtubule rescue
A, E. Time-lapse images of microtubules in MDF (mouse dermal fibroblasts) cells derived form wild type (**A**) and double CLIP-170 and CLIP-115 knockout mice (**E**). Microtubules undergo rapid transitions from shrinkage to growth at the cell edge in the cells derived from wild type mice (two microtubule plus-ends are indicated by arrowhead, **A**). **B.** The representative life history plots of two microtubules demonstrate that microtubules retain fluctuating at the cell periphery. **C, D.** The high rescue frequency maintains steeply ascending distribution of the growing microtubule plus-ends along the cell radius as shown by EB3 staining. The best curve fitting y=aebx gives value for a=0.064±0.017 and b=1.96±0.33 (**D**). 1786 EB3 positive microtubule ends were scored in 5 cells. **E.** In the cells derived from double CLIPs knockout mice microtubules undergo persistent shrinkage from the cell cortex. **F.** Life history plots show that microtubules persistently grow toward and persistently shrink from the cell edge for the distance over 20 μm. **G, H.** The distribution of growing microtubule plus-ends is descending (**G**); EB3 positive ends are distributed evenly along the cell radius (**H**). 1263 EB3 positive MT ends were scored in 5 cells. Dotted lines indicate the cell edge. Time is shown in seconds in the upper corners. Bar, 10 μm.

CLIP deficiency does not influence mitosis

Since microtubule dynamics is essential for the attachment of chromosomes to the mitotic spindle and this dynamic behavior is clearly altered in CLIP deficient cells in interphase, we analyzed the DKO MEFs for possible mitotic defects. Surprisingly, DKO MEF cultures show the same cell cycle distribution as wild type cultures (Fig. 4A, B), with the same time spent between the breakdown of the nuclear envelope and the onset of anaphase (Fig. 4C). This indicates that

the attachment of the chromosomes to the microtubules is not disturbed by the alteration of microtubule dynamics. Analysis of the growth curves of both MEFs and MDFs confirms these results (Fig. 4 D, E). Taken together, these data indicate that CLIP deficiency does not cause mitotic defects in MEFs or MDFs.

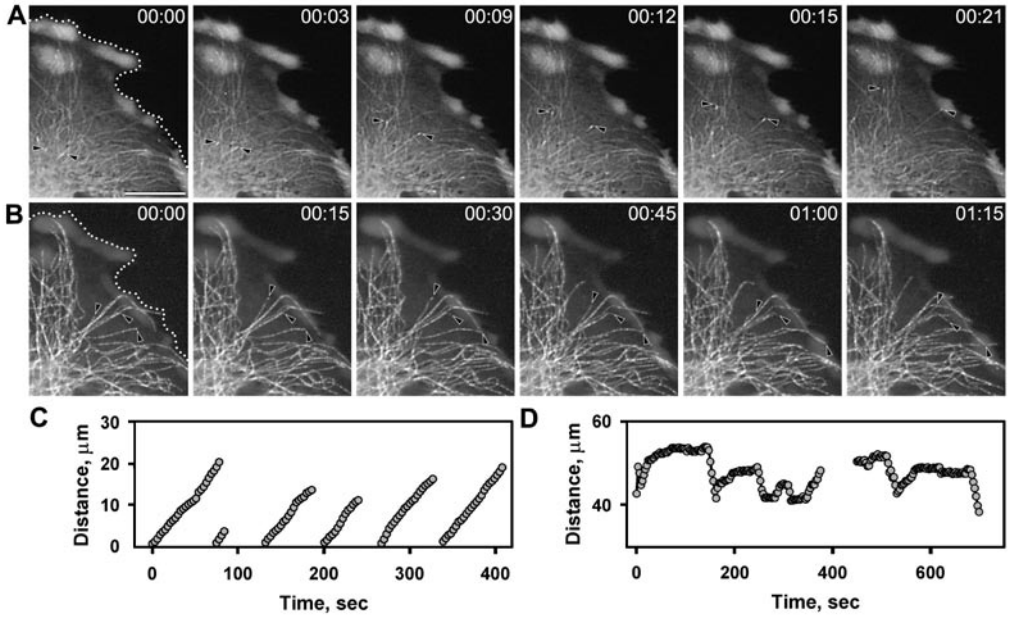

Figure 3. Expression of GFP-CLIP monomeric head restores microtubule dynamics in cells derived from double knockout mice

A, B. Time-lapse images of GFP-CLIP head (**A**) and microtubules (**B**). GFP-CLIP head decorates microtubules along the length and is concentrated at the microtubule growing ends; two GFP-positive microtubule tips are indicated by arrowheads (**A**). Microtubules undergo frequent transitions from growth to shortening (catastrophe) and from shortening to growth (rescue) at the cell edge; three microtubule plus-ends are indicated by arrowheads (**B**). **C.** Representative live history plots of CLIP head tracks demonstrate persistent growth of microtubules in the internal cytoplasm. The average length of the persistent growth is 11.64±5.5 μm (50 microtubules). **D.** Life history plots of microtubules demonstrate the restoration of the microtubule rescue frequency after expression of CLIP head. Microtubules retain fluctuating at the cell edge. Dotted lines indicate the cell edge. Time is shown in seconds in the upper corners. Bar, 10 μm.

CLIP deficiency disturbs microtubule distribution and causes dynactin aggregation

In interphase fibroblasts microtubules are typically organized in a radial array, emanating from the MTOC near the cell nucleus. In most cells the microtubules growing towards the cell periphery are distributed evenly, covering all areas of the cell. We examined the distribution of the microtubules in fixed wild type and CLIP-115 and CLIP-170 double knockout (DKO) MDFs and MEFs. Although most wild type cells indeed show an even distribution of their microtubules, approximately 30% (MDF) and 6% (MEF) of the cells showed microtubule-free areas, of which some contained aggregates of $p150^{Glued}$ (Fig. 5A-C).

In DKO cultures we noticed a significant increase in the number of cells with an uneven distribution of microtubules and $p150^{Glued}$-containing aggregates (fig. 5D, E). Approximately 70% of the MDFs and 33% of the MEFs had one or more of these aggregate-positive, microtubule-

free areas (Fig. 5F). Staining for other proteins revealed the presence of dynein intermediate chain (DIC) in the aggregates (Supplemental Figure 1), as well as dynamitin (p50) and Arp1 (data not shown). Thus, these aggregates contain both dynactin and dynein.

In wild type cells microtubule-free areas were rare and predominantly located near the cell cortex. However, in the DKO population we often found cells with a 'star-shaped' microtubule distribution. In these cells, groups of microtubules growing away from the MTOC reached all sides of the cell, but the areas in between were devoid of microtubules. Thus, compared to wild type cells, DKO cells had larger microtubule-free areas and more aggregation of $p150^{Glued}$ and other proteins.

Table 2. Microtubule dynamics parameters

	Growth rate[a], μm/min	Catastrophe frequency[b], s^{-1}	Shortening rate[a], μm/min	Rescue frequency[b], s^{-1}
Wt	22.8±8.6 100 MTs in 6 cells	0.017±0.008 100 MTs in 6 cells	37.4±13.3 120 MTs in 6 cells	0.10±0.02 120 MTs in 6 cells
CLIPs ko	21.5±6.8 100 MTs in 6 cells	0.02±0.007 100 MTs in 6 cells	42.7±15.3 120 MTs in 6 cells	0.02±0.006 120 MTs in 6 cells
CLIP ΔXmn rescue	23.2±7.2 57 MTs in 5 cells	0.02±0.007 57 MTs in 5 cells	35.5±15.8 120 MTs in 6 cells	0.15±0.02 120 MTs in 6 cells

[a] rates were calculated from the histogram of instantaneous displacements. [b] frequencies were calculated as a number of events integrated over time of the individual phases; in wt cells - 41 catastrophes and 112 rescues were observed for 2654 s and for 1255.2 s respectively; in dko cells - 54 catastrophes and 57 rescues were observed for 2662.4 s and for 2939.2 s; CLIP head rescue - 35 catastrophes and 118 rescues were observed for 1548 s and for 794.2 s. MT, microtubules.

By labeling cells with 5-Carboxyfluorescein Diacetate Succinimidyl Ester (CFSE), we were able to image the thickness of cells. Microtubule-free areas in DKO fibroblasts turned out to be extremely flat, containing hardly any cytoplasm (data not shown). Analysis of vesicular transport in these areas demonstrated they are practically devoid of lipid-enriched vesicles; the limited number of vesicles present was completely immobile (data not shown).

Overexpression of CLIP-115 and CLIP-170, but not of CLIP-170 Xmn, removes aggregates

To determine whether the disturbed distribution of microtubules and subsequent aggregation of dynactin and related proteins is due to the alteration in microtubule dynamics, we overexpressed EGFP fusions of CLIP-115 and CLIP-170 as well as the CLIP monomeric head. In almost all cells overexpressing either EGFP-CLIP115 or EGFP-CLIP170, irrespective of the expression level, microtubule distribution was restored and dynactin aggregates could not be detected (Fig. 5G, H, J, K; Table 3).

In none of the MDFs and MEFs overexpressing EGFP-CLIP170 aggregates were observed, while in approximately 7% of the MDFs (1/15 cells) overexpressing EGFP-CLIP115 remnants of aggregates were observed. In contrast, 92% of the MDFs and 73% of the MEFs overexpressing EGFP-CLIP-head still contained aggregates (Fig. 5I, L; Table 3). Taken together, these data suggest that the altered distribution of microtubules and the presence of dynactin-containing aggregates are due to the absence of both CLIP-115 and CLIP-170. Restoration of microtubule

dynamics, however, does not rescue this morphological phenotype, indicating that the CLIPs have a function in addition to their regulatory role in microtubule dynamics.

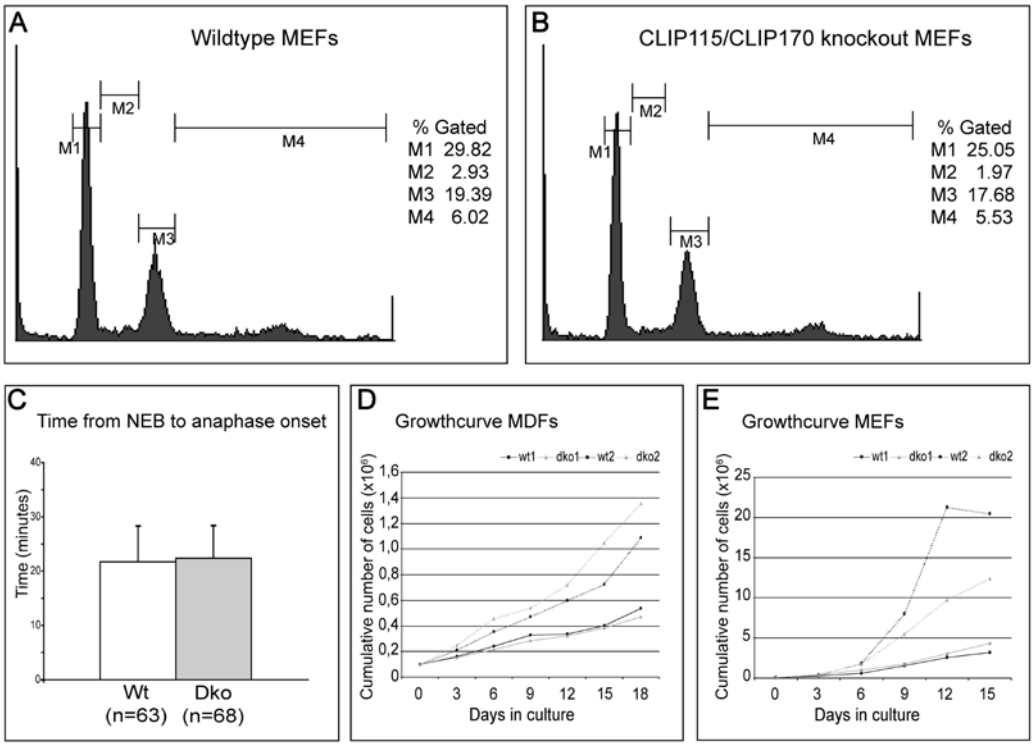

Figure 4. CLIP deficiency does not alter cell cycle or growth
A, B. FACS analysis of wt (**A**) and double CLIP-115 and CLIP-170 knockout MEFs (**B**) shows no difference in cell cycle distribution. **C.** Time from NEB to anaphase onset is unaltered in dko cells relative to wild type. **D, E.** Growth curves of MDFs (**D**) and MEFs (**E**) show that cell growth is similar in wild type and double knockout cultures.

BicD2 interacts with CLIP-115 and is also found in aggregates of DKO fibroblasts

To isolate proteins that interact with CLIP-115, we previously performed a yeast two-hybrid screen. We identified the CLASPs (Akhmanova et al., 2001) and also reported on an association between CLIP-115 and the dynein-dynactin regulatory factor BICD2 (Hoogenraad et al., 2001). The latter interaction was not worked out in detail, but because dynein-dynactin function appears affected in CLIP DKO cells, this interaction was pursued further.

Four criteria indicate that the interaction between the CLIP-115 bait (amino acids 287-591) and BICD2 (amino acids 706-810, i.e. the last 114 amino acids of the C-terminus) is specific. First, when fish and bait domains are swapped, the interaction still occurs (data not shown). Second, BICD2 does not interact with other parts of the CLIP-115 coiled-coil region or a tropomyosin control bait, which contains a long coiled coil structure (Supplemental Figure 2); third, CLIP-115 does not interact with other BICD2 regions or with the tropomyosin control bait (data not shown); fourth, the region of CLIP-170 (amino acids 277-588), which is very similar to the positive CLIP-115 bait, does not associate with BICD2 (Supplemental Figure 2).

To localize the binding site for BICD2 on CLIP-115, CLIP-115 was divided in three overlapping clones (Supplemental Figure 2), which were each tested in the yeast two-hybrid system. The results of these experiments show that binding of CLIP-115 to BICD2 is dependent on the presence of residues 353-591, i.e. the initial coiled-coil segment of CLIP-115. CLIP-115 is also able to interact with BICD1 (amino acids 707-820) in a yeast two hybrid assay (Supplemental Figure 2), which is not surprising since BICD1 and BICD2 are highly conserved, especially in their C-terminal regions (Hoogenraad et al., 2001). No interactions of BICD1 with other parts of CLIP-115, or the homologous region of CLIP-170 were detected. Together these data indicate that both BICD1 and BICD2 interact with CLIP-115 and not with CLIP-170.

Table 3. Rescue efficiency in dko fibroblasts

Cell type	GFP-CLIP-115 FL[a]		GFP-CLIP-170 FL[a]		GFP-CLIP-170 head[a]	
	Cells with aggregates[b]	Relative (%)	Cells with aggregates[b]	Relative (%)	Cells with aggregates[b]	Relative (%)
MDF	1/15 n=3	6,7	0/16 n=3	0	12/13 n=3	92,3
MEF	N.D.	N.D.	0/17 n=3	0	11/15 n=3	73,3

[a] FL = full length, head = N-terminal domain aa 4–309. [b] Aggregates were visualized by $p150^{Glued}$ staining. All GFP expressing cells were scored irrespective of the expression level. High overexpression of GFP-CLIP-170 results in bundling of microtubules and local concentration of GFP-CLIP-170 in aggregates that are not comparable to the aggregates observed in dko cells. These were not scored.

The direct nature of the interactions between CLIP-115 and BICD2 was confirmed by in vitro binding assays. Equal amounts of various glutathione S-transferase (GST) fusion proteins (see Fig. 6A for a schematic representation), purified on glutathione beads (Fig. 6B), were added to in vitro transcribed and translated CLIP-115 (Fig. 6C, left lane). After washing, radioactive proteins were detected using SDS-PAGE and autoradiography (Fig. 6C). The results show that CLIP-115 binds to GST-BICD2 but not to GST, supporting the conclusion that CLIP-115 and BICD2 interact directly. Our results also indicate that CLIP-115 interacts with itself via coiled-coil domains (Fig. 6C), corroborating previous experiments that CLIP-115 dimerizes via its coiled-coil region (Hoogenraad et al., 2000).

The association of BICD2 with CLIP-115 was further examined in co-immunoprecipitation studies from transfected COS-1 cells. One set of transfections was done with full length BICD2 and/or CLIP-115 (Fig. 6D). The second set of transfections was with full length BICD2 and CLIP-115 or, as a negative control, BICD2 and CLIP-170 (Fig. 6E). Immunoprecipitations were carried out with an antiserum against BICD2 (#2293), CLIP-115 (#2338,) or an antiserum that recognizes both CLIPs (#2221). Western blots of the immunoprecipitated proteins were incubated with BICD2, CLIP-115 or CLIP-115/170 (CLIP) antibodies. As shown in Figure 6D, the CLIP-115 antiserum is able to coprecipitate BICD2. The reciprocal immunnoprecipitation shows that anti-BICD2 antiserum is able to coprecipitate CLIP-115 (Fig. 6E). The anti-BICD2 antibodies do not, however, coprecipitate CLIP-170, despite the fact that this protein is expressed at the same level as CLIP-115 (Fig. 6E). Taken together, these results support the yeast two-hybrid finding of a specific and direct interaction between BICD2 and CLIP-115.

To obtain *in vivo* evidence for these interactions, we performed co-immunoprecipitation

experiments from mouse brain extracts. BICD1 (#2296) and BICD2 antibodies (#2293, #2298) were used for the co-immunoprecipitations. In addition to BICD itself, All three BICD antisera were able to coprecipitate not only BICD, but CLIP-115 as well (Fig 6F). None of these proteins were immunoprecipitated by non-specific control rabbit antiserum (Fig 6F). These results indicate that both BICD1 and BICD2 can bind to CLIP-115 *in vivo*.

Our data indicate that CLIP-115, like CLIP-170, might be involved in regulating dynein function, by interacting with one of the important accessory factors of this motor complex. Since dynein-dynactin aggregates only occur in CLIP-115- and CLIP-170-depleted cells, we examined if BICD2 also accumulated in DKO cells. Staining with BICD2 antiserum indeed revealed that this factor is indeed present in the aggregates in DKO cells (Supplemental Figure 1G and data not shown). These results suggest that when both CLIPs are absent essential components of vesicular motility start to form protein aggregates in microtubule-free areas of cells.

Increased cell surface size of attached CLIP deficient fibroblasts

Although cultured fibroblasts are typically very heterogeneous in size and appearance, we observed more extremely large cells in the DKO cultures than in the wild type cells. We calculated the surface area of attached wild type and DKO MEFs and MDFs from images of $p150^{Glued}$ stained cells. Our results indicate that in both types of fibroblasts the surface area of DKO cells is two-fold increased relative to wild type controls (Fig. 7A). DKO MDFs expressing full length GFP-CLIP-115 and -170, but not GFP-CLIP-170 XmnI, had normal cell surface values (Fig. 7B). However, the latter assay may be biased towards smaller cells, which might be more easily transfected than large cells. The increase in surface area observed in DKO fibroblast cultures can have two causes. Either the DKO cells have a larger volume than wild type cells, or the DKO cells spread more when they attach to a matrix such as the culture dish. In the latter case cells should also be flatter. To investigate which of these options applied to DKO cells, we determined the sizes of unattached cells using fluorescent-activated cell sorting (FACS). Comparison of the plots of both MDFs and MEFs showed no difference in volume between wild type and DKO cells (Fig. 7C). This suggests that size differences in attached cells are due to altered cell spreading.

Spreading of fibroblasts involves the protrusion of filopodia and lamellipodia and the attachment to the extracellular matrix through focal adhesions. We therefore investigated the appearance of focal adhesions using antibodies against different focal adhesion proteins. Although we could not find significant differences in the focal adhesion proteins paxillin and vinculin or in the focal adhesion-associated tyrosine kinase (FAK, data not shown), we did observe an increase in intensity when we stained focal adhesions for phosphotyrosine (PT66, Fig. 8A, B). This suggests that a CLIP-deficiency does not affect the level of the proteins present in the focal adhesions, but rather their phosphorylation status.

CLASP distribution in DKO fibroblasts

Both CLIP-115 and -170 interact with the CLASPs (Akhmanova et al., 2001) and we therefore examined the localization of these proteins in DKO cells. We did not detect CLASPs in dynein-dynactin-BicD2 aggregates in DKO cells (Figure 8 and data not shown). Thus, not every CLIP-interaction partner accumulates in aggregates when the CLIPs are absent.

In fission yeast peg1 (the CLASP-homologue) does not require mal3p (EB1) nor tip1p (CLIP-170) for localization at microtubule ends (Grallert et al., 2006). However, in DKO fibroblasts we noted a significant reduction in microtubule end staining of CLASP1 (Fig. 8E, F) compared to

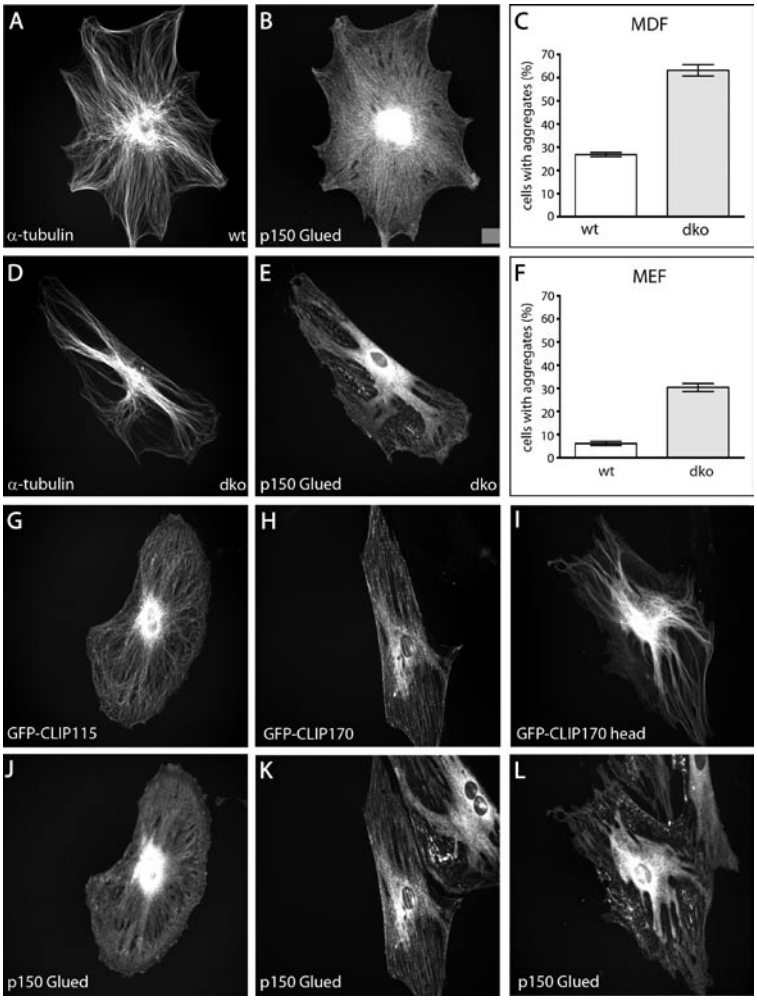

Figure 5. CLIP deficiency disturbs microtubule distribution and causes dynactin to aggregate
A-F. Distribution of microtubules and dynactin in wild type (**A-C**) and double CLIP-115 and CLIP-170 knockout MDFs (**D-F**). Microtubules and dynactin were detected using antibodies against α-tubulin and p150Glued, respectively. In MDF cultures, 63% of the DKO cells have an uneven distribution of microtubules, leaving microtubule-free areas in which dynactin is found in aggregates, compared to 26% in wild type cultures (**C**). In MEF cultures, this is 30% (dko) and 6% (wt) (**D**). **G-L.** Rescue of microtubule distribution and dynactin aggregation. Overexpression of full length GFP-CLIP115 (**G, J**) and GFP-CLIP170 (**H, K**) removes dynactin aggregates in both MDFs and MEFs, as shown by $p150^{Glued}$ staining, while expression of GFP-CLIP head does not remove the aggregates (**I, L**).

normal cultured fibroblasts (Fig. 8C, D). These data demonstrate, for the first time, that CLIPs are required for proper microtubule plus-end distribution of CLASPs on dynamic microtubules. By contrast, the localization of CLASPs at leading edges of cells, where these proteins are involved in microtubule stabilization (Akhmanova et al., 2001), and are bound to the cell cortex by complexing with LL5beta (Lansbergen et al., 2006), was not significantly altered in DKO cells (data not shown). Consequently, we did not detect a decrease in leading edge oriented stable microtubules in the DKO cells.

Discussion

The ends of growing microtubules are decorated with a large number of proteins that belong to the group of +TIPs (Schuyler and Pellman, 2001). Most of these proteins can associate with microtubules directly, but their concentration at the distal ends is also thought to depend on interactions between +TIPs, resulting in a complex network (Akhmanova and Hoogenraad, 2005; Honnappa et al., 2006). Two of these plus-end-binding proteins are the cytoplasmic linker proteins CLIP-115 and CLIP-170. Several attempts have been made to elucidate the *in vivo* function of the mammalian CLIPs utilizing different approaches. Using the dominant-negative properties of a C-terminal CLIP-170 mutant, it was shown that removal of the CLIPs from the microtubule plus-ends reduces the rescue of microtubule growth at the cell periphery, resulting in persistent depolymerization after catastrophe instead of dynamic instability. This indicates that the CLIPs play a role in regulating microtubule dynamics (Komarova et al., 2002a). Our data in DKO cells fully support this conclusion.

Using a gene-targeting strategy, our group generated a CLIP-115 deficient mouse line which was shown to suffer from brain abnormalities and particular behavioral deficits (Hoogenraad et al., 2002). More recently, a CLIP-170 knockout allele was generated (Akhmanova et al., 2005). Although this knockout turned out to be leaky, resulting in residual protein in adult lung and the embryo, it could be shown that CLIP-170 plays an essential role in spermatogenesis. The phenotypes of cultured dermal and embryonic fibroblasts derived from both mouse lines, however, are surprisingly mild. Given their high structural similarity, the CLIPs are thought to have redundant functions, which might explain the relatively mild cellular phenotypes. In order to prove the existence of the redundancy and to analyze the effect of the absence of both CLIPs, we crossed both single knockout lines to obtain a CLIP-115 and CLIP-170 double knockout mouse line. Dermal and embryonic fibroblasts derived from these mice were used to study the cellular effect of the CLIP deficiency.

We show that double CLIP-115 and CLIP-170 deficient fibroblasts contain many more microtubule-free areas, with dynein-dynactin-BICD2 aggregates, than fibroblasts derived from wild type and single CLIP deficient mice. There is a remarkable correlation between the number of aggregate-containing areas and the surface area of the cell, i.e. DKO MDFs are very large and contain most aggregates, whereas wild type MEFs are the smallest cells measured here and contain fewest aggregates. These data suggest that aggregate formation depends in part on cell spreading.

Although microtubules are thought to constantly occupy all areas of the cell, their dynamic properties allow certain areas to be transiently devoid of microtubules. In wild type cells, such a microtubule-free area will in most cases be immediately occupied by new microtubules. In double knockout cells, however, dynamic instability is decreased because of the lack of rescue factors. When microtubules shrink persistently towards the cell center instead of being rescued near the cell periphery, it will take more time for new microtubules to grow into an area that is transiently unoccupied. Without microtubules such an area might not able to hold its form, and hence it collapses. After collapse, microtubule ingrowth is no longer possible due to mechanical obstruction leaving the area permanently microtubule-free. Without microtubules the dynactin components and the other proteins present in the area can no longer bind to the growing microtubule ends and because of the cell collapse they cannot relocate to other areas of the cell. As a consequence they aggregate.

However, the observed morphological phenotype can not be the result of the altered microtubule dynamics alone, since we show that overexpression of a GFP-fusion of the N-terminal domain of CLIP-170, which is able to bind to microtubules but lacks the C-terminal

metal binding domain that has been shown to interact with p150^{Glued}, restores microtubule dynamics but does not remove the microtubule-free areas. In contrast, overexpression of full length GFP-CLIP-115 or GFP-CLIP-170 does remove the aggregate-containing microtubule-free areas. Taken together, these data suggest that CLIP-115 and CLIP-170 are redundant factors and that both have another function independent of their regulative role in microtubule dynamics.

Because of the intricate network of proteins present at the microtubule plus-end, it is likely that removal of the CLIPs affects other microtubule plus-end-binding proteins. The observation that p150^{Glued}, together with other components of the dynactin complex, forms aggregates in double CLIP deficient cells suggests that the additional function of the CLIPs involves dynactin. This possibility is especially obvious for CLIP-170, which has been shown to be required for

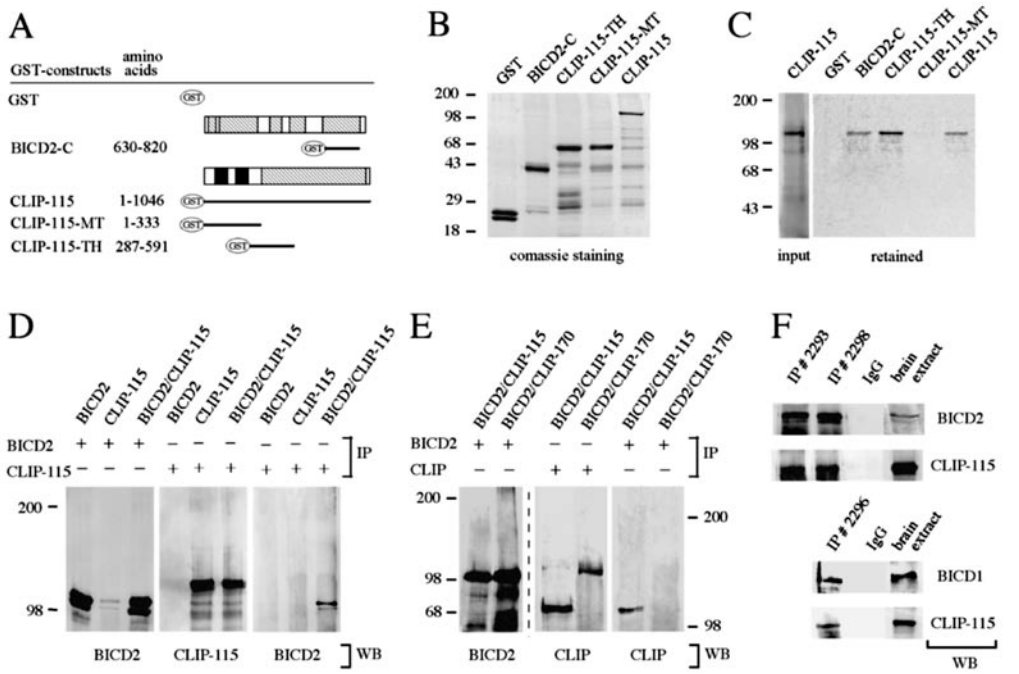

Figure 6. BICD1 and -2 association with CLIP-115
A. Structure of GST fusion proteins. Amino acid residues of CLIP-115 and BICD2, which were cloned in frame with GST, are indicated. **B** Analysis of the purified fusion proteins by SDS-PAGE and coomassie blue staining. All purified have the expected size. Molecular weight markers are indicated. **C.** *In vitro* binding of CLIP-115 by bacterial fusion proteins. 35S-labeled CLIP-115 (marked "input") was incubated with the different GST fusion proteins shown. Purified radioactive proteins were analyzed by X-ray film exposure of dried SDS-gels (marked "retained"). Molecular weight markers are indicated. **D.** Co-immunoprecipitation of BICD2 with CLIP-115. COS-1 cells were transfected with BICD2, CLIP-115 or a combination of these proteins. Immunoprecipitations (IPs) were performed using an anti-BICD2 antibody (#2298), or anti-CLIP-115 antibody (#2238). Western blots (WBs) of the precipitated material were incubated with anti-BICD2 antibodies (#2298), or with anti-CLIP-115 antibodies (#2238). Molecular weight markers are indicated. **E.** Co-immunoprecipitation of CLIP-115 with BICD2. COS-1 cells were transfected with BICD2 and CLIP-115, or with BICD2 and CLIP-170. Precipitation and detection of BICD2 was as in (**D**). Precipitation and detection of CLIP-115 and CLIP-170 was done using an antibody, which recognizes both proteins (#2221, CLIP). While BICD2 was detected on an 8 % gel, the CLIPs were detected on 6 % gels, since they are larger proteins. A dotted line distinguishes the different gels. **F.** Co-immunoprecipitations from mouse brain extracts. All three BICD antibodies (#2293, #2298 and #2296) were able to co-precipitate CLIP-115. Molecular weight markers are indicated.

the localization of p150^{Glued} at growing microtubule ends (Lansbergen et al., 2004). Depletion of CLIP-170 results in a loss of dynactin from the microtubule plus-ends, while overexpression of CLIP-170 enhances its plus-end accumulation (Goodson et al., 2003; Lansbergen et al., 2004; Valetti et al., 1999; Watson and Stephens, 2006). Although the decrease in plus-end localization of p150^{Glued} is already visible in single CLIP-170 deficient cells, aggregate-containing microtubule-free areas are not being formed in these cells. Hence, the relocalization of the microtubule-bound fraction of dynactin to the cytoplasm is not sufficient to cause aggregation. Besides, the fraction of dynactin that is not bound to microtubules in wild type cells does not form aggregates. Only when both CLIPs are absent, aggregates are formed. This suggests that either of the CLIPs is able to affect unbound dynactin in such a way that it prevents dynactin from aggregating. The interaction between CLIP-170 and dynactin does not depend on microtubules, as shown by coprecipitation experiments after nocodazole treatment (Lansbergen et al., 2004), suggesting that CLIP-170 could prevent dynactin from aggregating by interacting with p150^{Glued} independently of microtubule binding.

In contrast to the direct interaction between dynactin and CLIP-170, the effect of CLIP-115 on dynactin has to be indirect since CLIP-115 does not interact with dynactin. Here we show that CLIP-115 binds to BICD1 and BICD2, the mammalian homologues of the *Drosophila* Bicaudal D protein. BICD proteins have been shown to recruit dynein to membranes positive for the small GTPase Rab6, through simultaneous binding to Rab6 and to dynein and dynactin complexes (Hoogenraad et al., 2001; Matanis et al., 2002; Short et al., 2002). Since BICD2 is also present in the dynactin containing aggregates, it seems likely that in the absence of CLIP-170, CLIP-115 protects dynactin from aggregation through its interaction with the BICD proteins.

Although fibroblast cultures are known to be very heterogeneous with respect to cell size and shape, cell surface area of the double knockout population was approximately twice that of wild type cells. The total level of tubulin did not increase and neither did the speed of microtubule polymerization. Since this speed depends on the level of free tubulin in the cell, and the length of polymerized microtubules in the large cells must have increased, these data implicate a decrease in the total number of microtubules. In larger cells we often observe a star-shaped distribution of microtubules with microtubule-free areas in between. This distribution could be an adaptation of the cell to the decreased number of microtubules.

The mechanism, by which DKO fibroblasts are able to spread more than wild type fibroblasts, is perhaps via an altered regulation of focal adhesion dynamics. Indeed phosphorylated tyrosines in focal adhesions of CLIP-deficient cells appear to be increased. There is no apparent change, however, in paxillin, vinculin and focal adhesion kinase staining. This suggests that the absence of CLIP-115 and CLIP-170 exerts an effect on the phophorylation status of focal adhesions, rather than on the localization of the focal adhesion proteins itself. Tyrosine phosphorylation of focal adhesion proteins such as paxillin (Turner, 2000), tensin (Bockholt and Burridge, 1993) and the signaling molecule focal adhesion kinase (FAK) (Schaller, 2001) is involved in the formation and turnover of matrix adhesions. Inhibition of tyrosine kinases and enhanced activity of phosphotyrosine phosphatases respectively blocks the development of focal adhesions (Burridge et al., 1992; Ridley and Hall, 1994) or disrupts them (Schneider et al., 1998), while inhibition of these phosphatases can stimulate focal adhesion assembly (Retta et al., 1996). Since we observe no differences in the level of the signaling molecule focal adhesion kinase, it is not likely that the increase in tyrosine phosphorylation is caused by increased activity of this kinase, although we cannot exclude this possibility completely. It seems more likely to be the result of a decrease in dephosphorylation leading to a reduced focal adhesion turnover.

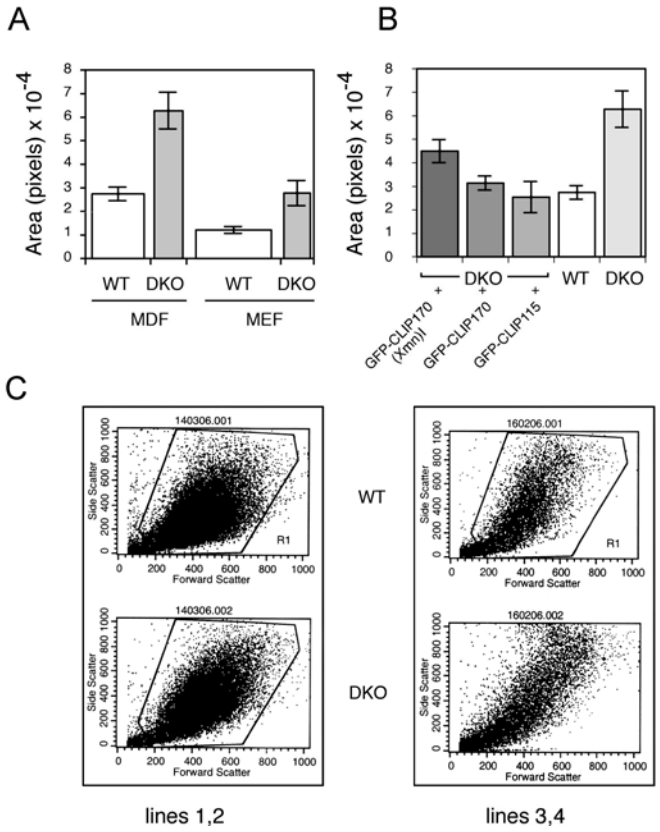

Figure 7. CLIPs are involved in cell spreading
A. Cell surface measurements. MDFs and MEFs were plated on glass coverslips and after 2 days cell surface areas were measured. **B.** Cell surface measurements before and after transfection. Non-transfected and transfected MDFs were plated on glass coverslips and cell surface areas were measured. **C, D.** Cell volume measurements. MDFs were harvested by trypsinization and forward and side scatter was measured by FACS. Two experiments were performed (left and right hand panels).

Proper formation and maintenance of focal adhesions requires intact networks of both actin filaments and microtubules, revealing a functional interplay between these two cytoskeletal networks in the control of cell morphology (Gavin, 1997; Goode et al., 2000). Disruption of microtubules induces enlargement of focal adhesions (Bershadsky et al., 1996; Enomoto, 1996) and direct microtubule targeting to substrate contact sites promotes the turnover or detachment of focal adhesions (Kaverina et al., 1999; Kaverina et al., 1998). It has been shown that this modulation of focal adhesion dynamics via microtubule targeting requires kinesin-1, not for the targeting itself but for the focal delivery of one or more components that promote their disassembly (Krylyshkina et al., 2002). Since the targeting of the microtubules to the adhesion sites specifically involves the plus-end, and microtubules can be captured and stabilized by adhesion sites (Kaverina et al., 1998), a role for microtubule plus-end interacting proteins in this process is likely.

It has already been shown that dissociation of the dynein-dynactin complex had no effect on adhesion site dynamics (Krylyshkina et al., 2002). Other potential players are CLIP-115 and CLIP-170, since we show that removal of these proteins decreases the dynamics of microtubules, thereby reducing the probability of microtubules targeting focal adhesion sites. In addition, CLASPs might very well be involved since they has been shown to regionally attach microtubule plus-ends to the cell cortex and stabilize them (Drabek et al., 2006; Lansbergen et al., 2006). We show that the removal of both CLIP-115 and CLIP-170 decreases the amount

of CLASP1 and CLASP2 at the microtubule plus-end, but not the accumulation at the leading edge of motile fibroblasts. Although in particular this latter accumulation makes the CLASPs interesting candidates for capture of microtubules at sites of substrate adhesion, we can not rule out the possibility that the decrease of CLASP accumulation at the plus-end has an effect on this process. In summary, our data suggest that CLIP-115 and CLIP-170 are involved in the regulation of focal adhesion turnover, either directly through their function inmicrotubule dynamics, or indirectly through their interaction with the CLASPs.

Methods

Molecular biology and antibodies

The yeast two-hybrid assay system has been described previously (Akhmanova et al., 2001). For direct binding studies, glutathione S-transferase (GST) fusion proteins were made in BL21 E. coli cells as described (Hoogenraad et al., 2000; Hoogenraad et al., 2001), using plasmids pGEX-2T and pGEX-3X (Pharmacia). The following proteins were purified: GST; GST-BICD2 (amino acids 706-812), GST-CLIP-115 (amino acids 287-591), GST-CLIP-115 (amino acids 1-333), GST-CLIP-115 (amino acids 1-1046), GST-CLIP-115 (amino acids 755-899/1026-1046).

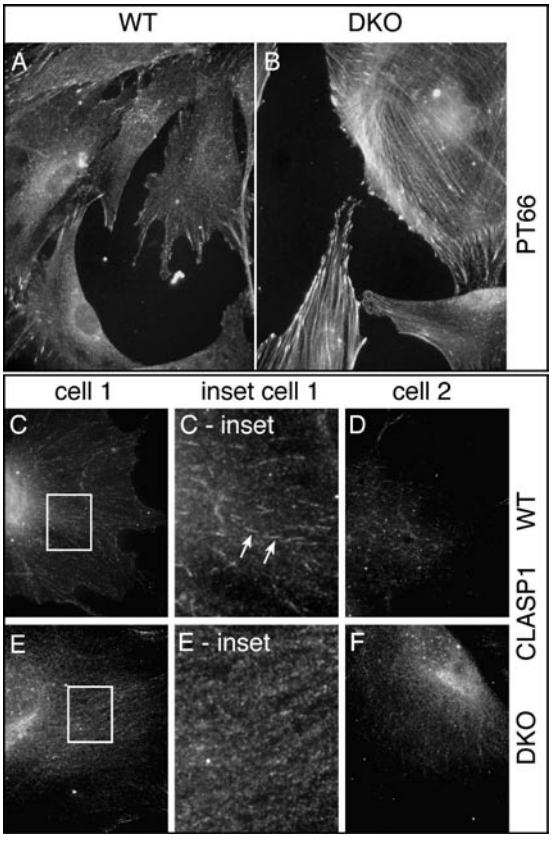

Figure 8. CLIPs regulate focal adhesions and CLASP localization
A, B. Phosphorylated proteins in focal adhesions. MDFs were plated and stained for PT66. Notice the more intense staining in DKO MDFs. **C-F.** CLASP1 distribution. MDFs were plated and stained for CLASP1 (#402 antiserum). In wild type cells CLASP1 localizes at microtubule ends (indicated by arrows). Notice the less intense staining of CLASP1 at microtubule ends in DKO MDFs.

CLIP-115 was transcribed and translated using the TnT coupled transcription-translation system (Promega) and 35S-methionine (Trans35S label, ICN, >1000 Ci/mmol). Aliquots of radiolabeled proteins were incubated with different GST fusion proteins in NETT buffer (100 mM NaCl, 50 mM Tris (pH 7.5), 5 mM EDTA, 0.5 % Triton X-100), for 2 hr at room temperature. Afterwards, samples were washed 5 times in NETT buffer. Proteins were eluted by boiling in sample buffer and analyzed by SDS-PAGE. Dried gels were exposed to film (Akhmanova et al., 2001; Hoogenraad et al., 2001).

In the co-immunoprecipitation experiments, extracts were lysed in buffer containing 30 mM HEPES (pH 7.4), 100 mM KCl, 1 % NP40, supplemented with protease inhibitors (Boehringer) and incubated at 4˚C for 30 min, to depolymerize microtubules. All subsequent steps were also carried out at 4˚C. Cell lysates were centrifuged at 13,000 rpm for 10 min, and the supernatant was precleared with protein A beads for 30 min, after which beads were removed by low speed centrifugation. Precleared supernatants were incubated with the different antibodies for 2 hr, in the presence of protein A beads. Immunoprecipitated material was collected on the beads, washed extensively and purified proteins were eluted in sample buffer. Precipitated proteins were analyzed on western blot as described before (Hoogenraad et al., 2000).

Polyclonal rabbit antisera against EB1 and -3, BICD2 (#2293), CLIP-115 (#2238), CLIP-115 and -170 (#2221), CLIP-170 (#2360), CLASP1 (#402) and CLASP2 (#2358) have been described (Akhmanova et al., 2001; Coquelle et al., 2002; Hoogenraad et al., 2000; Hoogenraad et al., 2001; Stepanova et al., 2003). Polyclonal rabbit antibodies against p150glued were made as described previously (Hoogenraad et al., 2000). Antibodies against detyrosinated alpha-tubulin were a kind gift of Dr. C. Bulinski. Monoclonal antisera were against GFP (Clontech), actin, beta-tubulin, gamma-tubulin, acetylated alpha-tubulin, vinculin, paxillin (Sigma), mDia1, p150Glued and GM130 (BD Biosciences). Secondary goat anti-rabbit and anti-mouse antibodies were coupled to alkaline phosphatase (Sigma, 1:7000) for western blotting, or to Alexa-350, -488 or -594 (Molecular Probes, 1:300 or 1:500) for immunofluorescent studies.

Cell culture and immunofluorescent analysis

The generation of CLIP-115 deficient mice and CLIP-170 deficient mice has been described previously (Akhmanova and Hoogenraad, 2005; Hoogenraad et al., 2002). We crossed heterozygous animals of both mouse lines, to obtain compound heterozygotes. Subsequent breeding with C57/Bl6 wild type animals resulted in DKO mice. We obtained primary mouse fibroblasts either from the trunk region of E13,5 embryos or from the skin of young adult animals (5-10 weeks).

For immunofluorescent analysis, MDFs or MEFs were seeded onto glass coverslips and grown to 30-60% density. Cells were fixed for 10 minutes in ice cold MeOH containing 1 mM EGTA or for 15 minutes in 4% paraformaldehyde in PBS at room temperature or sequentially in MeOH and 4% PFA. After permeabilization for 10 minutes in PBS/0,15% Triton X-100, cells were blocked for 30 minutes in PBS/1% BSA/0,05% Tween-20. Antibody incubations were performed for 1 hour at room temperature or overnight at 4°C using a 1:300 dilution of the rabbit polyclonals, and a 1:100 dilution of mouse monoclonals against $p150^{Glued}$ (Transduction Laboratories), p50, Arp1 and dynein intermediate chain (DIC) and 1:500 for the rat monoclonal against α-tubulin YL1/2 (Abcam). We used the following secondary antibodies: fluorescein isothiocyanate (FITC)-conjugated goat anti rabbit (Nordic Laboratories; 1:100), Alexa-594-conjugated goat anti mouse (Molecular Probes; 1:250), Alexa-350-conjugated goat anti rabbit (Molecular Probes; 1:250) and Alexa-350-conjugated goat anti rat (Molecular Probes; 1:250).

Coverslips were mounted onto chamberslides using Vectashield mounting medium with or without 4',6'-diamidino-2-phenylindolehydrochloride (DAPI) (Vector Laboratories).

Microscopic images were captured as described (Akhmanova et al., 2001; Drabek et al., 2006). MDFs and MEFs were transfected with GFP constructs that have been described (De Zeeuw et al., 1997; Hoogenraad et al., 2000). Cells were transfected using AMAXA MEF Nucleofector kit 2.

For the generation of the growth curves of MDF and MEF cultures, 10^5 cells of each line were seeded in triplo in a six-well plate and allowed to grow. On day three, cells were trypsinized and counted using an automated cell counter (Z2 Coulter Particle Count and Size Analyzer, Beckman Coulter). Cell numbers of the triplos we averaged and 10^5 cells were replated in triplo. Graphs were generated by plotting the cumulative cell number against the number of days in culture.

Analysis of microtubule dynamics

The following parameters of microtubule dynamics were determined: instantaneous rates of growth and shortening, frequency of rescue and catastrophe transitions, and length of microtubule shortening from the cell edge. Data measurements were performed using 16-bit images in Metamorph software. SigmaPlot software (Jandel Scientific Corp.) was used for statistical analysis and plotting of graphs as described elsewhere (Komarova et al., 2002). Briefly, the lengths of individual microtubules were measured from the centrosome (0,0 position of a centrosome), and life histories of microtubules were plotted as length (μm) versus time (s). Instantaneous velocities were calculated as displacement of the plus-end between successive images (3 s) in a time-lapse series. The threshold of measurement was 2 pixels in the digital image, corresponding to 0.18 μm in the cell. Histograms of instantaneous velocities were generated for the microtubule population, and the mean values and SDs were computed. Cell margin was defined as a 3-μm zone from the cell boundary. The rate of the shortening was calculated from the histogram of instantaneous displacements of shortening microtubules. For estimation of rescue and catastrophe frequencies, analyses of direct or subtracted images of microtubules were used (Vorobjev et al., 1999). The transition probabilities were estimated as the ratio of number of transition events divided by the time of growth or shortening phase before a transition occurred. If an microtubule growing from the centrosome reached the cell edge without any transition to shortening, the time of the growth phase was included into overall data but not transition (catastrophe) was scored. The same method of estimation was used for determining rescue frequency of microtubules shortening back from the cell margin (Komarova et al., 2002). The extent of microtubule shortening was expressed as the absolute distance shortened from the cell edge until the microtubule was rescued, and the data were presented in a frequency histogram.

Quantification of the microtubule length distribution along the cell radius was performed as described previously (Komarova et al., 2002). Briefly, the cell radius was divided into five zones (each zone was a 0.2 fraction of the length of cell radius), and number of active ends, growing (black segments) and shortening (white segments) were scored for each zone. The result is represented as percent of the microtubules within each zone where 100% is a total number of scored active plus-ends of microtubules in experiment or control. The data were fitted by least squares regression to a single exponential.

Fluorescence-activated cell sorting (FACS)

In order to compare the cell volumes of wt and dko MDFs and MEFS, cells were analyzed using a FACScan (Beckton Dickinson). Subconfluent cells were detached using trypsin-EDTA, washed with Dulbecco's phosphate buffered saline (DPBS, Cambrex) and analyzed in PBS/1% fetal calf serum (FCS). To exclude dead cells, we incubated the cells for 5 min with 7AAD (7-Amino-Actinomycin-D).

References

Akhmanova, A., and C.C. Hoogenraad. 2005. Microtubule plus-end-tracking proteins: mechanisms and functions. *Curr Opin Cell Biol*. 17:47-54.

Akhmanova, A., C.C. Hoogenraad, K. Drabek, T. Stepanova, B. Dortland, T. Verkerk, W. Vermeulen, B.M. Burgering, C.I. De Zeeuw, F. Grosveld, and N. Galjart. 2001. Clasps are CLIP-115 and -170 associating proteins involved in the regional regulation of microtubule dynamics in motile fibroblasts. *Cell*. 104:923-35.

Akhmanova, A., A.L. Mausset-Bonnefont, W. van Cappellen, N. Keijzer, C.C. Hoogenraad, T. Stepanova, K. Drabek, J. van der Wees, M. Mommaas, J. Onderwater, H. van der Meulen, M.E. Tanenbaum, R.H. Medema, J. Hoogerbrugge, J. Vreeburg, E.J. Uringa, J.A. Grootegoed, F. Grosveld, and N. Galjart. 2005. The microtubule plus-end-tracking protein CLIP-170 associates with the spermatid manchette and is essential for spermatogenesis. *Genes Dev*. 19:2501-15.

Berezuk, M.A., and T.A. Schroer. 2007. Dynactin enhances the processivity of Kinesin-2. *Traffic*. 8:124-9.

Bershadsky, A., A. Chausovsky, E. Becker, A. Lyubimova, and B. Geiger. 1996. Involvement of microtubules in the control of adhesion-dependent signal transduction. *Curr Biol*. 6:1279-89.

Bockholt, S.M., and K. Burridge. 1993. Cell spreading on extracellular matrix proteins induces tyrosine phosphorylation of tensin. *J Biol Chem*. 268:14565-7.

Brunner, D., and P. Nurse. 2000. CLIP170-like tip1p spatially organizes microtubular dynamics in fission yeast. *Cell*. 102:695-704.

Burridge, K., C.E. Turner, and L.H. Romer. 1992. Tyrosine phosphorylation of paxillin and pp125FAK accompanies cell adhesion to extracellular matrix: a role in cytoskeletal assembly. *J Cell Biol*. 119:893-903.

Coquelle, F.M., M. Caspi, F.P. Cordelieres, J.P. Dompierre, D.L. Dujardin, C. Koifman, P. Martin, C.C. Hoogenraad, A. Akhmanova, N. Galjart, J.R. De Mey, and O. Reiner. 2002. LIS1, CLIP-170's key to the dynein/dynactin pathway. *Mol Cell Biol*. 22:3089-102.

De Zeeuw, C.I., C.C. Hoogenraad, E. Goedknegt, E. Hertzberg, A. Neubauer, F. Grosveld, and N. Galjart. 1997. CLIP-115, a novel brain-specific cytoplasmic linker protein, mediates the localization of dendritic lamellar bodies. *Neuron*. 19:1187-99.

Diamantopoulos, G.S., F. Perez, H.V. Goodson, G. Batelier, R. Melki, T.E. Kreis, and J.E. Rickard. 1999. Dynamic localization of CLIP-170 to microtubule plus ends is coupled to microtubule assembly. *J Cell Biol*. 144:99-112.

Drabek, K., M. van Ham, T. Stepanova, K. Draegestein, R. van Horssen, C.L. Sayas, A. Akhmanova, T. Ten Hagen, R. Smits, R. Fodde, F. Grosveld, and N. Galjart. 2006. Role of CLASP2 in Microtubule Stabilization and the Regulation of Persistent Motility. *Curr Biol*. 16:2259-64.

Dujardin, D., U.I. Wacker, A. Moreau, T.A. Schroer, J.E. Rickard, and J.R. De Mey. 1998. Evidence for a role of CLIP-170 in the establishment of metaphase chromosome alignment. *J Cell Biol*. 141:849-62.

Enomoto, T. 1996. Microtubule disruption induces the formation of actin stress fibers and focal adhesions in cultured cells: possible involvement of the rho signal cascade. *Cell Struct Funct*. 21:317-26.

Folker, E.S., B.M. Baker, and H.V. Goodson. 2005. Interactions between CLIP-170, tubulin, and microtubules: implications for the mechanism of Clip-170 plus-end tracking behavior. *Mol Biol Cell*. 16:5373-84.

Gavin, R.H. 1997. Microtubule-microfilament synergy in the cytoskeleton. *Int Rev Cytol*. 173:207-42.

Goode, B.L., D.G. Drubin, and G. Barnes. 2000. Functional cooperation between the microtubule and actin cytoskeletons. *Curr Opin Cell Biol*. 12:63-71.

Goodson, H.V., S.B. Skube, R. Stalder, C. Valetti, T.E. Kreis, E.E. Morrison, and T.A. Schroer. 2003. CLIP-170 interacts with dynactin complex and the APC-binding protein EB1 by different mechanisms. *Cell Motil Cytoskeleton*. 55:156-73.

Grallert, A., C. Beuter, R.A. Craven, S. Bagley, D. Wilks, U. Fleig, and I.M. Hagan. 2006. S. pombe CLASP needs dynein, not EB1 or CLIP170, to induce microtubule instability and slows polymerization rates at cell tips in a dynein-dependent manner. *Genes Dev.* 20:2421-36.

Honnappa, S., O. Okhrimenko, R. Jaussi, H. Jawhari, I. Jelesarov, F.K. Winkler, and M.O. Steinmetz. 2006. Key Interaction Modes of Dynamic +TIP Networks. *Mol Cell.* 23:663-71.

Hoogenraad, C.C., A. Akhmanova, F. Grosveld, C.I. De Zeeuw, and N. Galjart. 2000. Functional analysis of CLIP-115 and its binding to microtubules. *J Cell Sci.* 113:2285-2297.

Hoogenraad, C.C., A. Akhmanova, S.A. Howell, B.R. Dortland, C.I. De Zeeuw, R. Willemsen, P. Visser, F. Grosveld, and N. Galjart. 2001. Mammalian Golgi-associated Bicaudal-D2 functions in the dynein-dynactin pathway by interacting with these complexes. *Embo J.* 20:4041-54.

Hoogenraad, C.C., B. Koekkoek, A. Akhmanova, H. Krugers, B. Dortland, M. Miedema, A. Van Alphen, W.M. Kistler, M. Jaegle, M. Koutsourakis, N. Van Camp, M. Verhoye, A. Van Der Linden, I. Kaverina, F. Grosveld, C.I. De Zeeuw, and N. Galjart. 2002. Targeted mutation of Cyln2 in the Williams syndrome critical region links CLIP-115 haploinsufficiency to neurodevelopmental abnormalities in mice. *Nat Genet.* 32:116-27.

Kaverina, I., O. Krylyshkina, and J.V. Small. 1999. Microtubule targeting of substrate contacts promotes their relaxation and dissociation. *J Cell Biol.* 146:1033-44.

Kaverina, I., K. Rottner, and J.V. Small. 1998. Targeting, capture, and stabilization of microtubules at early focal adhesions. *J Cell Biol.* 142:181-90.

Komarova, Y.A., A.S. Akhmanova, S. Kojima, N. Galjart, and G.G. Borisy. 2002a. Cytoplasmic linker proteins promote microtubule rescue in vivo. *J Cell Biol.* 159:589-99.

Komarova, Y.A., I.A. Vorobjev, and G.G. Borisy. 2002b. Life cycle of MTs: persistent growth in the cell interior, asymmetric transition frequencies and effects of the cell boundary. *J Cell Sci.* 115:3527-39.

Krylyshkina, O., I. Kaverina, W. Kranewitter, W. Steffen, M.C. Alonso, R.A. Cross, and J.V. Small. 2002. Modulation of substrate adhesion dynamics via microtubule targeting requires kinesin-1. *J Cell Biol.* 156:349-59.

Lansbergen, G., I. Grigoriev, Y. Mimori-Kiyosue, T. Ohtsuka, S. Higa, I. Kitajima, J. Demmers, N. Galjart, A.B. Houtsmuller, F. Grosveld, and A. Akhmanova. 2006. CLASPs attach microtubule plus ends to the cell cortex through a complex with LL5beta. *Dev Cell.* 11:21-32.

Lansbergen, G., Y. Komarova, M. Modesti, C. Wyman, C.C. Hoogenraad, H.V. Goodson, R.P. Lemaitre, D.N. Drechsel, E. van Munster, T.W. Gadella, Jr., F. Grosveld, N. Galjart, G.G. Borisy, and A. Akhmanova. 2004. Conformational changes in CLIP-170 regulate its binding to microtubules and dynactin localization. *J Cell Biol.* 166:1003-14.

Matanis, T., A. Akhmanova, P. Wulf, E. Del Nery, T. Weide, T. Stepanova, N. Galjart, F. Grosveld, B. Goud, C.I. De Zeeuw, A. Barnekow, and C.C. Hoogenraad. 2002. Bicaudal-D regulates COPI-independent Golgi-ER transport by recruiting the dynein-dynactin motor complex. *Nat Cell Biol.* 4:986-92.

Miedema, M., N. Keijzer, N. van Camp, A.-L. Bonnefont, M. Rutteman, E. Haasdijk, A. Akhmanova, C.C. Hoogenraad, A. van der Linden, F. Grosveld, and N. Galjart. 2007. Progressive hydrocephalus and abnormal neuronal migration in mice lacking the microtubule plus end tracking proteins CLIP-115 and -170. *manuscript in preparation*.

Mitchison, T., and M. Kirschner. 1984. Dynamic instability of microtubule growth. *Nature.* 312:237-42.

Perez, F., G.S. Diamantopoulos, R. Stalder, and T.E. Kreis. 1999. CLIP-170 highlights growing microtubule ends in vivo. *Cell.* 96:517-27.

Peris, L., M. Thery, J. Faure, Y. Saoudi, L. Lafanechere, J.K. Chilton, P. Gordon-Weeks, N. Galjart, M. Bornens, L. Wordeman, J. Wehland, A. Andrieux, and D. Job. 2006. Tubulin tyrosination is a major factor affecting the recruitment of CAP-Gly proteins at microtubule plus ends. *J Cell Biol.* 174:839-49.

Pierre, P., J. Scheel, J.E. Rickard, and T.E. Kreis. 1992. CLIP-170 links endocytic vesicles to microtubules. *Cell.* 70:887-900.

Retta, S.F., S.T. Barry, D.R. Critchley, P. Defilippi, L. Silengo, and G. Tarone. 1996. Focal adhesion and stress fiber formation is regulated by tyrosine phosphatase activity. *Exp Cell Res.* 229:307-17.

Rickard, J.E., and T.E. Kreis. 1990. Identification of a novel nucleotide-sensitive microtubule-binding protein in HeLa cells. *J Cell Biol.* 110:1623-33.

Ridley, A.J., and A. Hall. 1994. Signal transduction pathways regulating Rho-mediated stress fibre formation: requirement for a tyrosine kinase. *Embo J.* 13:2600-10.

Schaller, M.D. 2001. Biochemical signals and biological responses elicited by the focal adhesion kinase. *Biochim Biophys Acta*. 1540:1-21.

Scheel, J., P. Pierre, J.E. Rickard, G.S. Diamantopoulos, C. Valetti, F.G. van der Goot, M. Haner, U. Aebi, and T.E. Kreis. 1999. Purification and analysis of authentic CLIP-170 and recombinant fragments. *J Biol Chem*. 274:25883-91.

Schneider, G.B., A.P. Gilmore, D.L. Lohse, L.H. Romer, and K. Burridge. 1998. Microinjection of protein tyrosine phosphatases into fibroblasts disrupts focal adhesions and stress fibers. *Cell Adhes Commun*. 5:207-19.

Schroer, T.A. 2004. Dynactin. *Annu Rev Cell Dev Biol*. 20:759-79.

Schuyler, S.C., and D. Pellman. 2001. Microtubule "plus-end-tracking proteins": The end is just the beginning. *Cell*. 105:421-4.

Short, B., C. Preisinger, J. Schaletzky, R. Kopajtich, and F.A. Barr. 2002. The Rab6 GTPase regulates recruitment of the dynactin complex to Golgi membranes. *Curr Biol*. 12:1792-5.

Stepanova, T., J. Slemmer, C.C. Hoogenraad, G. Lansbergen, B. Dortland, C.I. De Zeeuw, F. Grosveld, G. van Cappellen, A. Akhmanova, and N. Galjart. 2003. Visualization of microtubule growth in cultured neurons via the use of EB3-GFP (end-binding protein 3-green fluorescent protein). *J Neurosci*. 23:2655-64.

Tai, C.Y., D.L. Dujardin, N.E. Faulkner, and R.B. Vallee. 2002. Role of dynein, dynactin, and CLIP-170 interactions in LIS1 kinetochore function. *J Cell Biol*. 156:959-68.

Turner, C.E. 2000. Paxillin and focal adhesion signalling. *Nat Cell Biol*. 2:E231-6.

Valetti, C., D.M. Wetzel, M. Schrader, M.J. Hasbani, S.R. Gill, T.E. Kreis, and T.A. Schroer. 1999. Role of dynactin in endocytic traffic: effects of dynamitin overexpression and colocalization with CLIP-170. *Mol Biol Cell*. 10:4107-20.

Watson, P., and D.J. Stephens. 2006. Microtubule plus-end loading of p150(Glued) is mediated by EB1 and CLIP-170 but is not required for intracellular membrane traffic in mammalian cells. *J Cell Sci*. 119:2758-67.

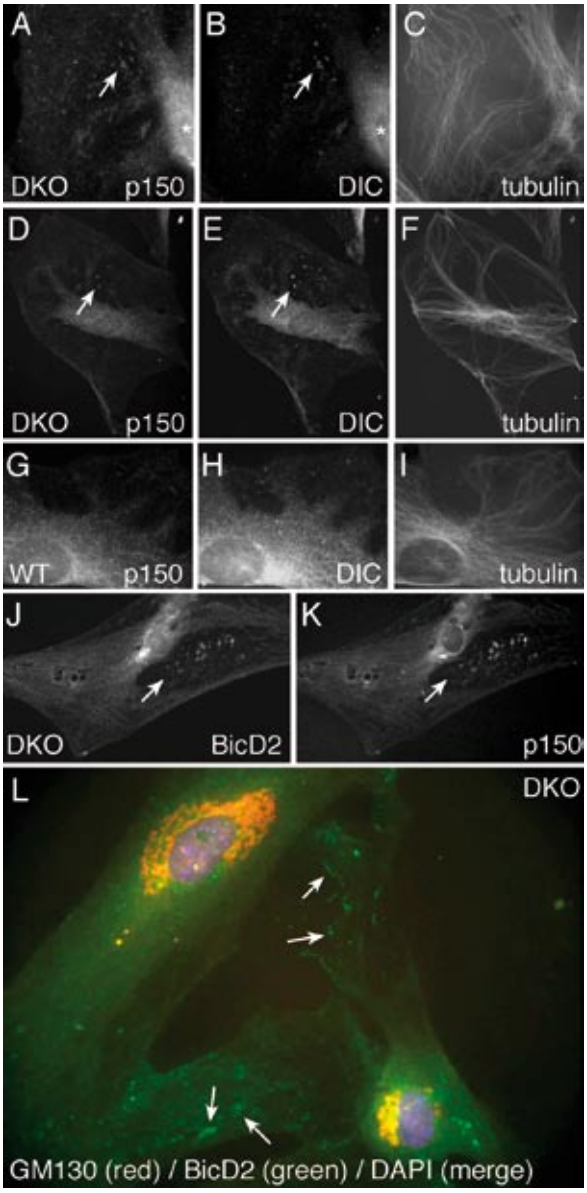

Supplemental Figure 1. CLIP deficiency causes dynein-dynactin-BicD2 aggregates
A-I. Distribution of p150^{Glued}, dynein intermediate chain (DIC) and MTs in DKO (**A-F**) and wild type (WT, **G-I**) MDFs. To simultaneously stain for DIC and p150^{Glued} (dynactin) a polyclonal antiserum against the latter was used. These antibodies are less efficient in recognizing dynactin aggregates than the monoclonal antiserum that is normally used. Still, in microtubule-free areas of DKO MDF cultures dynactin is found in aggregates with DIC (arrows). In microtubule-free areas of WT cells these accumulations are not observed. **J-L.** Distribution of BicD2 and GM130 in DKO fibroblasts. Notice the accumulations of BicD2 (arrows) in the cytoplasm of DKO cells, where p150^{Glued} also accumulates. GM130, an ER-Golgi marker, is not found in these aggregates. Wild type fibroblasts do not show these aggregates (not shown).

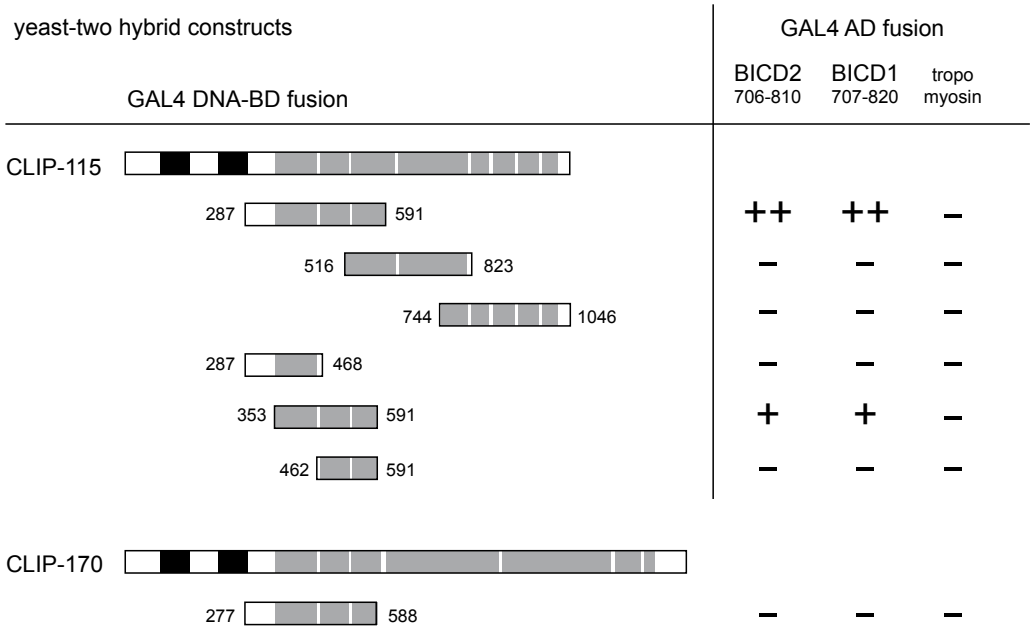

Supplemental Figure 2. Yeast two hybrid interaction of BICD1 and BICD2 with CLIP-115.
Interaction between CLIP-115 and BICD1 and BICD2. The domain structure of CLIP-115 and CLIP-170, including the two microtubule binding motifs (black bars) and coiled coil regions (hatched bars; the regions are interrupted by small stretches of coil-breaking residues) is shown. Below these are the fragments of CLIP-115 and CLIP-170 that are fused to DNA-binding domain (DNA-BD) used in the yeast two-hybrid experiments. Fragment 287-591 of CLIP-115 was used to screen an E14.5 day mouse cDNA library. From this screen the BICD2 cDNA was isolated, that encodes amino acids 706-820 from murine BICD2. This fragment was truncated (residue 706-810) and tested in direct yeast two hybrid assays with the other CLIP-115 and -170 encoding domains. Next, the homologues region of BICD1 (707-820) and tropomyosin were fused to activation domain (AD) and used in the same experiment. Results of β-galactosidase activity, measured in yeast lysate, are expressed as (++), which indicates high activation (50-100 units); (+), which indicates moderate activity (5-50 units); and (–), which indicates low or no activity (0-5 units).

Chapter 4

Progressive hydrocephalus and abnormal neuronal migration in mice lacking the microtubule plus-end-tracking proteins CLIP-115 and -170

Manuscript in preparation

Chapter 4

Progressive hydrocephalus and abnormal neuronal migration in mice lacking the microtubule plus-end-tracking proteins CLIP-115 and -170

Marja Miedema[1], Nanda Keijzer[1], Nadja van Camp[2], Anne-Laure Bonnefont[1], Mandy Rutteman[3], Elize Haasbeek[3], Anna Akhmanova[1], Casper C. Hoogenraad[3], Annemie van der Linden[2], Frank Grosveld[1], and Niels Galjart[1]

[1] MGC Department of Cell Biology and Genetics, Erasmus University, P.O. Box 2040, 3000 CA Rotterdam, The Netherlands. [2] Bio-Imaging Lab, University of Antwerp (RUCA), Belgium. [3] MGC Department of Neuroscience, Erasmus University, P.O. Box 2040, 3000 CA Rotterdam, The Netherlands.

Abstract

CLIP-115 and CLIP-170 are microtubule "plus-end-tracking" proteins, or +TIPs, with redundant roles as microtubule rescue factors in cultured fibroblasts. In CLIP double knockout (DKO) fibroblasts large cytoplasmic aggregates of dynactin and the minus-end directed motor dynein are observed. Since a dysfunctional microtubule cytoskeleton, dynactin aggregates and decreased dynein activity have been associated with accelerated aging in motor neurons, we analyzed mice deficient for CLIP-115 and -170 for age-dependent defects in motor performance. We find that CLIP DKO mice have an abnormal posture and show hind limb clasping throughout life. Surprisingly, we initially observe an age-related improvement of motor coordination, while performances on certain tasks start to deteriorate in older mice. Using magnetic resonance imaging and histological analysis a progressive form of hydrocephalus is detected in the DKO mice, which occasionally results in a highly increased volume of the lateral and third ventricles. In young DKO mice obstruction of the aqueduct of Sylvius is seen, and accumulation of cerebellar neurons in other parts of the brain. We propose that CLIP-115 and -170 are involved in neuronal migration by regulating dynein-dynactin-mediated transport processes and microtubule dynamics in neurons.

Introduction

Microtubules form one of the three major cytoskeletal networks in a cell. These dynamic elements are involved in essential cellular processes, including mitosis, cell motility and intracellular transport. Microtubules are long, hollow and polar fibers, with a fast growing plus-end and a slow growing minus end (Desai and Mitchison, 1997). The polarity is used by opposing motor proteins to move cargo in a bi-directional manner. Microtubules are especially important for neuronal functioning, among others because neurons carry long and thin dendritic and axonal extensions, which completely depend on microtubule-based motor proteins for long-range transport and delivery of organelles to appropriate locations (Terada and Hirokawa, 2000). In addition, neuronal migration depends on microtubule-based motor proteins. In particular the role of dynein and its activator LIS1 have been extensively studied (Lambert de Rouvroit and Goffinet, 2001; Mesngon et al., 2006).

The behavior of the microtubule network is controlled by microtubule-associated proteins (MAPs). Among them are the so-called 'plus-end-tracking' proteins, or +TIPs (Schuyler and Pellman, 2001), a group of (mostly unrelated) proteins that specifically associate with the plus-ends of microtubules. CLIP-115 and CLIP-170 are 'cytoplasmic linker proteins' of 115 and 170 kDa, respectively (Hoogenraad et al., 2000; Pierre et al., 1992). CLIPs are structurally and functionally related +TIPs, both forming homodimers through long α-helical domains that are predicted to fold into coiled-coils (reviewed in (Galjart, 2005)). Both CLIPs contain a highly similar N-terminal region of approximately 300 amino acids, which binds microtubules and consists of two CAP_GLY motifs (Riehemann and Sorg, 1993), surrounded by basic serine-rich stretches. This domain is responsible for a very prominent function of the CLIPs, namely that as MT rescue factors (Komarova et al., 2002).

CLIP-170 contains a C-terminal metal-binding motif, initially presumed to be the cargo-binding domain responsible for the interaction of CLIP-170 with endocytic vesicles (Pierre et al., 1992). Later analysis has shown that this domain mediates interaction of CLIP-170 with several other proteins, including LIS1 (Coquelle et al., 2002) and $p150^{Glued}$ (Lansbergen et al., 2004). Interestingly, $p150^{Glued}$ is a component of the dynactin complex (Schroer, 2004), which regulates the activity of microtubule-based motor proteins and thereby organelle transport (Deacon et al., 2003). LIS1 is a multifunctional protein, which also controls dynein function (Xiang, 2003). These results suggest that CLIP-170 might indirectly regulate motor protein function, in particular that of dynein.

CLIP-115 lacks the metal-binding motifs of CLIP-170, hence does not interact with dynactin. However, it does interact with the protein BicD2 in a yeast two-hybrid assay (Hoogenraad et al., 2001). Since BicD2 is also a regulator of dynein (Hoogenraad et al., 2001; Hoogenraad et al., 2003), CLIP-115, like CLIP-170, might have an indirect function in the control of this motor protein. We have shown that a combined deficiency of the CLIPs leads to the formation of dynactin-BicD2-dynein aggregates in double CLIP-115 and CLIP-170 knockout (DKO) fibroblasts **(**Miedema *et al*, see chapter 3**)**. This phenotype is linked to increased cell spreading and the presence of extremely flat areas in DKO cells, in which no organelle motility can be detected. We hypothesized that CLIPs are microtubule rescue factors and dynein motor protein regulators and that both functions are required for normal cell homeostasis **(**Miedema *et al*, see chapter 3**)**. Since dynactin aggregates and dynein dysfunctioning have been linked to neuronal degeneration (Holzbaur, 2004), and both CLIP-115 and -170 are expressed in the brain (Hoogenraad et al., 2002), one would predict that a combined deficiency of the CLIPs leads to accelerated aging in the central nervous system (CNS).

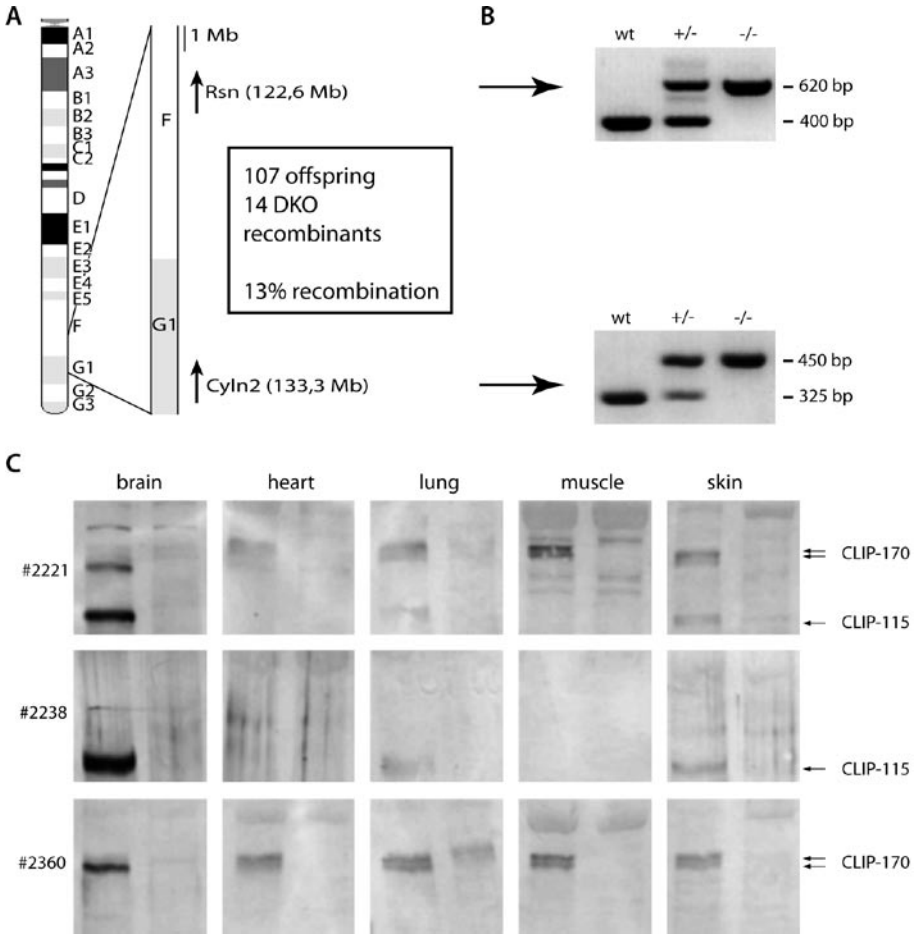

Fig. 1. Characterization of CLIP DKO mice
A. Location of *Cyln2* and *Rsn* genes in mouse. The genes are on chromosome 5, approximately 10 Mb apart. We obtained 107 offspring from breedings of compound heterozygotes with wild type mice, 14 of which had a DKO allele. **B.** PCR analysis. Tail DNA from wild type (wt), heterozygous (+/-), and homozygous (-/-) knockout mice was analyzed by PCR. **C.** Western blot analysis. Total protein extract from the indicated tissues was analyzed on Western blot using antibodies against CLIP-115 and -170 (#2221), against CLIP-115 only (#2238) or against CLIP-170 only (#2360).

We have previously described mild brain abnormalities in mice lacking CLIP-115 (encoded by the *Cyln2* gene), including reduced corpus callosum size and enlarged ventricle volumes (Hoogenraad et al., 2002). To study the function of CLIP-170, we generated a mouse line in which we targeted the encoding gene (*Restin, Rsn*) allele (Akhmanova et al., 2005). Despite the targeting, expression of CLIP-170 was still detected in lung and embryos of these mice, indicating that the targeted allele is leaky (Akhmanova et al., 2005). CLIP-170 was absent from all other tissues we examined. In order to study the consequences of a combined deficiency of CLIP-115 and CLIP-170 in the brain we generated CLIP DKO mice. Surprisingly, we observe hydrocephalus in a significant percentage of the mice. The enlargement of brain ventricles,

which accumulate cerebrospinal fluid (CSF), appears to be due to a blockage of the aqueduct of Sylvius, in which we find cerebellar Purkinje and granule cells. These data indicate that the combined deficiency for CLIP-115 and -170 in the brain leads to neuronal migration defects. We propose that this is due to a misregulation of motor protein activity and altered microtubule dynamics.

Results

Generation of CLIP-115 and CLIP-170 double knockout (DKO) mice

Our group previously generated mouse lines deficient for either CLIP-115 or CLIP-170 (Akhmanova et al., 2005; Hoogenraad et al., 2002). Generation of the CLIP-115 knockout mice (encoded by *Cyln2*) included a Cre-mediated recombination event, which removed the vast majority of coding sequences. By contrast, the CLIP-170 knockout mice (encoded by *Rsn*) was generated by insertion of a GFP-loxP-pMC1neo-loxP cassette in the first ATG translation initiation codon, leaving the rest of the coding sequences intact. This knockout allele was shown to be leaky, with residual CLIP-17p protein in adult lung and in the embryo (Akhmanova et al., 2005). CLIP double knockout (DKO) mice were made by crossing the two single knockout lines.

Table 1. Offspring and genotype from CLIP-115 and -170 heterozygous DKO crosses

genotype	female mice		male mice		all mice	
Cyln2* / *Rsn	**N[a]**	**Percentage[b]**	**N**	**percentage**	**N**	**percentage**
wt;wt	59	21,9	52	17,7	111	19,7
+/-;+/-	91	33,8	118	40,1	209	37,1
-/-;-/-	45	16,7	61	20,7	106	18,8
wt;+/-	20	7,4	11	3,7	31	5,5
+/-;wt	17	6,3	21	7,1	38	6,7
wt;-/-	1	0,3	1	0,3	2	0,4
-/-;wt	2	0,7	1	0,3	3	0,5
+/-;-/-	11	4,1	17	5,8	28	5,0
-/-;+/-	23	8,6	12	4,1	35	6,2
Total number	269	99,8	294	99,8	563	99,9
Recombination Frequency[c]		27,5		21,4		24,3

[a]N = number of mice. [b]Percentages were calculated by dividing the number of mice of a certain genotype by the total number of mice. [c]Recombination frequencies for DKO were calculated by dividing the number of recombined pups (= other than wt;wt, +/-;+/- and -/-;-/-) by total number of pups.

Since the genes encoding CLIP-115 (*Cyln2*) and CLIP-170 (*Rsn*) are located approximately 11 Mb apart on mouse chromosome 5 (Fig. 1A), obtaining a DKO allele required a meiotic crossover event. Breedings between heterozygous mice from both lines gave rise to double heterozygous offspring with the targeted genes on separate chromosomes. From subsequent breedings between these double heterozygotes and wild type mice, we obtained double heterozygous CLIP-115 and CLIP-170 offspring with the targeted genes on one chromosome (hereafter referred to as

double heterozygotes) at a recombination efficiency of 13 percent (Fig. 1A), which is within the expected range.
PCR analyses confirmed the presence of the modified *Cyln2* and *Rsn* alleles in double heterozygous and homozygous mice (Fig. 1B). Subsequently, western blot analysis with three different antibodies against CLIP-115 and/or CLIP-170 showed absence of both CLIPs in brain lysates of the DKO mice (Fig. 1C). As expected, residual CLIP-170 was detected in lysates of the lung of the DKO mice. We conclude that the DKO mice are a valid model system to investigate the consequences of a combined deficiency for CLIP-115 and -170 in the brain.

Mild body weight reduction in CLIP DKO mice

To test if a deficiency of CLIP-115 and -170 has an effect on early mouse development, we analyzed offspring number and genotype from heterozygous CLIP DKO crosses (Table 1). The results show that homozygous DKO mice are born in normal numbers, compared to wild type littermates. We again calculated recombination frequencies and obtained values of approximately 24 % (Table 1). Note that these frequencies are about two times higher than the 13% efficiency we observed when generating the double knockout allele. This is because meiotic recombination can now take place in the male and the female germline. Actually, to obtain wt;-/- and -/-;wt pups, recombination has to take place both on the allele from the father as well as the mother, hence frequency of pups born with this genotype is very low (Table 1). We conclude that a combined deficiency for CLIP-115 and CLIP-170 does not severely hamper mouse development.

We subsequently analyzed if CLIP-115 and -170 deficiency has an influence on adult mice. We examined the body weights of 10 male DKO mice and 10 wild type males, at biweekly intervals over a period of approximately 2 years (Fig. 2A). The data show that 3-4 months after birth the DKO animals start lagging behind in weight, resulting in a reduction of total body weight of approximately 15%. This reduction persists throughout the complete period of measurement and is significant (single factor ANOVA, $p < 0{,}01$). Thus, CLIP DKO mice show an age-related difference in body weight gain, lagging behind as compared to wild type mice.

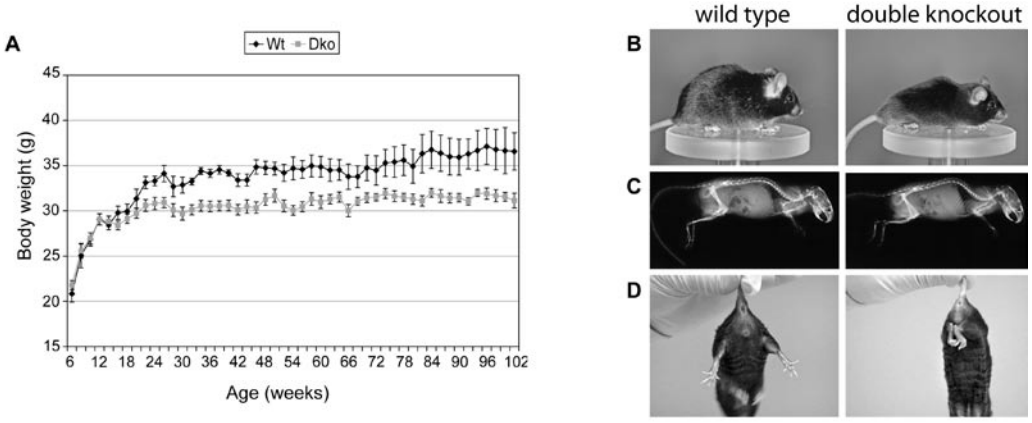

Fig. 2. Weight and appearance of CLIP DKO mice
A. Weight of mice. Adult wild type (WT) and CLIP DKO mice were weighed biweekly for almost two years. Ten mice were analyzed in each group. Values are indicated +/- SEM. **B, C.** Posture of mice. The CLIP DKO mice have a flatter back than wild type littermates, and CLIP DKO mice show a bulge. However, the skeletons of these mice look similar to wild type. **D.** Clasping reflex of mice. The CLIP DKO mice lack the ability to extend their hind legs when suspended by the base of their tail. Instead they clasp their hind legs together.

The data indicate that CLIPs are not essential for mouse development, but are required for normal growth during adult life.

Abnormal posture, clasping reflex and progressive hydrocephalus in CLIP DKO mice

Gross examination of the CLIP DKO mice revealed three obvious phenotypes. First, DKO have an abnormal posture, which appears to be due to flattened hind limbs and back (Fig. 2B). As a result the spinal column appears more bulged at the position of the forelimbs. However, we observed no significant differences in skeletal morphology between the two types of mice (Fig. 2C). These data indicate that CLIP DKO mice might suffer from hind limb weakness. The second phenotype is that the CLIP DKO mice fail to extend their hind limbs when suspended by the base of their tails. Instead they show a hind limb clasping reflex (Fig. 2D), sometimes combined with fore limb clasping. Both phenotypes are observed in all homozygous DKO mice and are therefore fully penetrating.

The third phenotype that we noted was that some CLIP DKO mice died unexpectedly, while others showed signs of severe hydrocephalus, with an obvious bulging skull (Table 2). Therefore, a magnetic resonance imaging (MRI) analysis was performed on 5 DKO mice and 5 wild type and double heterozygous littermates, to document the size of the ventricles in living animals. The results show a wide range of ventricle volumes in the DKO mice, which are significantly increased relative to wild type mice (Fig. 3B). One of the DKO mice suffered from severe hydrocephalus, contributing to the large spread in data (Fig. 3A, B). Notably, the third and lateral ventricles (white arrows in Fig. 3A) appear more enlarged than the fourth ventricle (black arrows in Fig. 3A). This unequal accumulation of CSF in brain ventricles is often associated with a blockage of the aqueduct of Sylvius, which connects the third and fourth ventricle.

To investigate when the hydrocephalus arises during mouse development, we made thionin-stained brain sections and analyzed morphology in brains from 17.5-day embryos and 5-week-old mice. Because of the hippocampal dysfunction observed in CLIP-115 single knockout mice, extra attention was paid to that part of the brain. In the embryos we did not observe any aberrant morphology of the hippocampus (Fig. 3C). Analysis of the 5-weeks-old mice showed that in the wild type animals the aqueduct of Sylvius was open, and lined by ependymal cells (Fig. 3D), but that in the DKO mouse it was almost completely closed in one section (Fig. 3G, H). In adjacent sections we detected an abnormal infiltration of cerebellar Purkinje and granule cells into the ependymal cell layers, and only a small opening in the aqueduct. (Fig. 3F, I).

Next, we analyzed the distribution of cerebellar cells in other brain areas and detected an abnormal accumulation of granule and Purkinje cells in the DKO brain next to the parasubiculum

Table 2. Hydrocephalus and unexplained deaths in CLIP DKO mice and littermates.

genotype (*Cyln2* / *Rsn*)	mice with hydrocephalus[a]	mice found dead[a, b]	total number of mice[c]
wt; wt	0 – 0 %	1 – 0.4 %	263
+/-; +/-	2 – 0.5 %	13 – 3.4 %	382
-/-; -/-	10 – 9.3 %	11 – 10 %	107
other	0 – 0 %	1 – 0.5 %	199

[a]Total number of mice and percentage of mice. [b]Mice found dead in cage, age of DKO mice ranged from 31-377 days.
[c]Total number of mice analyzed.

(Fig. 3E). Together our results suggest that CLIP DKO mice suffer from hydrocephalus because the aqueduct of Sylvius is 'clogged' with cerebellar neurons that have migrated aberrantly.

Age-related increase in motor coordination performance in CLIP DKO mice

The clasping reflex, abnormal posture and aberrant cerebellar migration indicate motor coordination defects (see, for example, (Lalonde, 1987; Trushina et al., 2006)). We therefore set out to test motor performance in the CLIP DKO mice. We tested a group of 10 DKO mice, 5 wild type littermates and 5 C57Bl6 controls over a period of 2 years at intervals of 3 months, to analyze age-related motor performance in CLIP DKO mice.

Muscle strength was examined using a grip strength meter (Fig. 4A) and did not yield any significant difference between wild type and DKO mice. However, in a hanging wire test, that measures strength, balance and endurance, the DKO mice performed significantly worse than the wild type mice at 6 and 9 months of age (Fig. 4B). At 12 months they still performed worse but had improved compared to the earlier time points. At 15 and 18 months the DKO mice performed like the wild types, but at 21 and 24 months their performance deteriorated again relative to wild types (Fig. 4B).

Next we performed a rotarod test as a measure of motor coordination. Similar to the hanging wire experiment, the DKO mice showed an age-related performance improvement when tested at 3-9 months, but deteriorated again at 24 months (Fig. 4C). Together these results indicate that CLIP DKO mice take approximately 9 months to improve their motor coordination to the level of wild type mice. This is not due to a strength deficit. At later age the performance of the DKO mice deteriorates, which indicates an age-related decline in motor function.

To analyze the gait of the CLIP DKO mice, we performed a catwalk analysis. The results show that CLIP DKO mice have a slightly smaller step size than wild type animals and walk slightly slower (data not shown). Taken together, the results obtained in the behavioral analyses suggest a defect in the neuromuscular system, although it is not clear at what level this defect is located.

Discussion

We have generated a new strain of mice with a deletion of the *Cyln2* gene (encoding CLIP-115) and an insertion within the *Rsn* gene (encoding CLIP-170). Although CLIP-170 is still present in lungs of adult DKO mice and in embryos, as was shown in single CLIP-170 knockout mice (Akhmanova et al., 2005), CLIP-115 and CLIP-170 are absent from all other tissues examined. Thus we called this mouse strain the 'CLIP double knockout' (CLIP DKO) line. The residual levels of CLIP-170 in embryos may explain why a combined targeting of the *Cyln2* and *Rsn* alleles does not lead to embryonic lethality in homozygous DKO mice. However, we recently generated another strain of mice in which both the *Cyln2* gene and the *Rsn* gene are completely deleted and we obtained homozygous offspring from this line, although numbers were too low to calculate the Medelian distribution. It will be interesting to compare the phenotype of these true double 'null' mutants with those carrying the leaky *Rsn* mutation.

We observe both constitutive and age-dependent symptoms in the CLIP DKO mice. The constitutive symptoms include male infertility, an abnormal posture and gait, and a clasping reflex. Whereas male infertility has been described in the single CLIP-170 knockout mice (Akhmanova et al., 2005), the abnormal posture, gait and clasping reflex are likely the result of the combined CLIP deficiency. They point to problems in the central nervous system and/or musculature of the DKO mice.

The age-related symptoms include growth retardation, hydrocephalus and decreased motor performance. Although initial growth curves are similar, after approximately 3 months male CLIP DKO mice have reached their maximum body weight, whereas wild type mice continue to grow. Eventually this leads to a difference in body weight of about 15 %. A mild growth retardation has been described in male CLIP-115 knockouts (Hoogenraad et al., 2002), but it was less pronounced than in the DKO mice. One explanation is that the combined deficiency of CLIP-115 and -170 leads to an imbalance in hormone levels that regulate body weight. This imbalance could be due to altered testosterone levels as a result of the male infertility, in combination with affected neuronal signaling pathways. Alternatively, it is the loss of CLIPs in various tissues of the body, which results in their slightly smaller size. To analyze the weight phenotype in more detail we will perform a longitudinal body weight analysis on adult female DKO mice, as well as on aging CLIP-115 and -170 single knockout animals.

Neurons appear to be particularly susceptible to defects in dynein–dynactin function (for review, see (Holzbaur, 2004). Recent data have emphasized a link between aggregates of mutant dynactin and motor neuron disease (Levy et al., 2006). Mice carrying mutations in the dynein heavy chain exhibit progressive loss of motor neurons, leading to muscle weakness and atrophy (Hafezparast et al., 2003). A similar phenotype is observed in transgenic mice with a targeted disruption of dynactin in motor neurons (LaMonte et al., 2002). Since a deficiency in CLIP-115 and -170 causes the appearance of dynein-dynactin aggregates and leads to vesicular transport problems in DKO fibroblasts (Miedema *et al*, see chapter 3), we expected to see motor performance loss in aging CLIP DKO mice as a sign of neuronal dysfunction. We did indeed observe this, at least in the hanging wire and rotarod assays, in mice of 21-24 months of age. Thus, we propose that CLIPs regulate dynein-dynactin function in the central nervous system and that loss of the CLIPs leads to mild neuronal degeneration.

Approximately 10 % of the CLIP DKO mice suffered from severe hydrocephalus, and another 10% of adult DKO mice died prematurely by an unknown cause. Although we did not assess the brain pathology of the dead mice, we assume that these two phenomena are related, i.e. the adult homozygous DKO mice died prematurely as a result of hydrocephalus. The hydrocephalus is progressive but not fully penetrating, indicating that genetic factors besides (lack of) CLIP-115 and -170 play a role in its formation. Moreover, the level of CLIP-115 and -170 appears to be relevant for the apparition of enlarged brain ventricles, since the fraction of double heterozygous mice with hydrocephalus is low, but significantly increased as compared to wild type mice, and an increased ventricle size (but no hydrocephalus) was observed in CLIP-115 single knockout mice (Hoogenraad et al., 2002).

Hydrocephalus is due to the abnormal accumulation of CSF in brain ventricles. In one form, called non-communicating hydrocephalus, CSF flow within the ventricular system is impaired, which is often accompanied by obstructions. Non-communicating hydrocephalus has been ascribed to impaired motility of the cilia of the ependymal cells lining the ventricular system (Banizs et al., 2005). Ciliary movement appears to be essential to maintain the flow of CSF through the ventricular system. The results in the CLIP DKO mice raise the possibility that CLIP-115 and -170 are involved in the formation and/or maintenance of motile cilia. Indeed, we have detected CLIP-170 in cilia of cultured lung epithelium (N.G., unpublished observations).

Alternatively, the brain ventricle enlargement in the CLIP DKO mice could be due to neuronal loss. For example, in mice that express high levels of Cre recombinase in neuronal progenitors, loss of neurons results in a very severe form of hydrocephalus (Forni et al., 2006). In the case of the CLIP DKO mouse model Cre recombinase was used early on in ES cells, to remove CLIP-115 encoding sequences (Hoogenraad et al., 2002). While this may have affected results

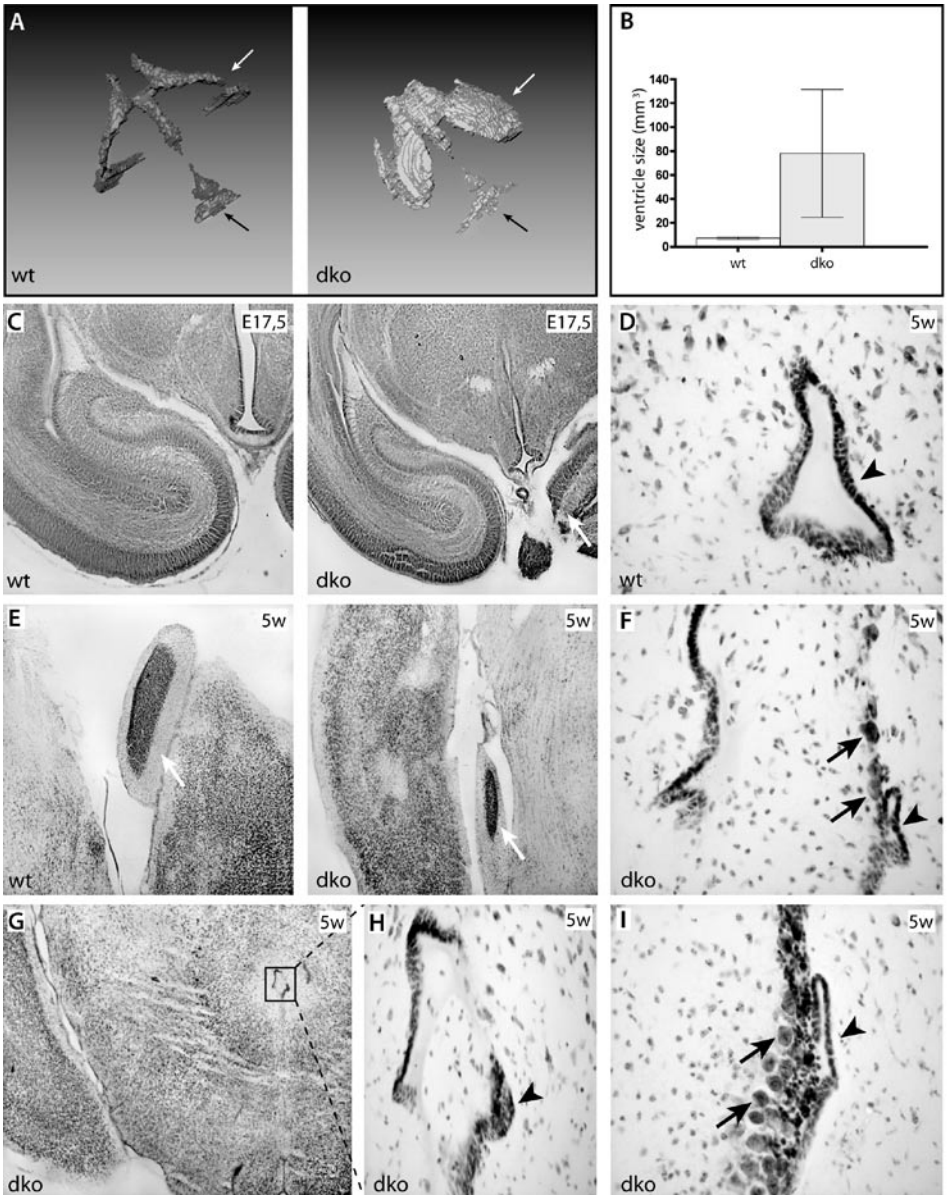

Figure 3. Hydrocephalus in CLIP DKO mice
A, B. MRI analysis. Five CLIP DKO and 5 wildtype or heterozygous littermates were analyzed by MRI. In (A) ventricles are shown of a wild type control mouse (left hand panel) and a DKO mouse suffering from hydrocephalus (right hand panel). In (B) the average ventricle volumes of the two groups are shown (+/- SEM). The volume of the DKO ventricles is significantly increased ($P<0.01$, Mann Whitney Test). **C-I.** Histological analysis. Thionine-stained sections of the indicated genotypes and ages were investigated for hydrocephalus-related phenotypes. Arrow in **C**: unidentified tube-like structure in cerebrum of an E17.5 DKO mouse embryo. Arrows in **E**: cerebellar migration into cerebral areas, in mice of 5 weeks old (5w). In the DKO mouse (right hand panel) the cerebellar neurons are located in an area adjacent to the subiculum, near the entorhinal cortex. In the wild type littermate (left hand panel) the cerebellum commences more posteriorly and ventrally. In panels **D** (control) and **F-I** (DKO) the aqueduct of Sylvius is shown (arrowheads). Notice the abnormal (closed) phenotype in the DKO mouse. Arrows in F, I point to Purkinje cells that have invaded the zone near the aqueduct.

with the CLIP-115-deficient mice, we consider it unlikely that aspecific Cre activity underlies the hydrocephalus phenotype in the DKO mice, since both the single *Cyln2* and *Rsn* knockouts, as well as the DKO mice themselves, were crossed back to C57Bl6 for several generations. Moreover, morphologic analysis of the embryonic brains did not indicate severe neuronal loss.

We believe that the most likely cause of hydrocephalus in CLIP DKO mice is an obstruction of the aqueduct of Sylvius by invading (i.e. aberrantly migrating) cerebellar neurons. Abnormal neuronal migration has been associated with hydrocephalus in other studies (see, for example, (Ma et al., 2006). These data establish a novel role for the CLIPs, namely in the proper migration of cerebellar neurons, a process that occurs largely in the first days after birth. Notably CLIP-115 is very abundantly expressed in these first postnatal days (De Zeeuw et al., 1997). Moreover, CLIP-170 interacts with LIS1 (Coquelle et al., 2002), which plays an important role in neuronal migration, neurodegeneration and male infertility, by regulating dynein activity (Reiner et al., 2006). Our data in fibroblasts and mice are highly suggestive of an important role for the CLIPs in the control of dynein activity, in addition to their established function as regulators of the microtubule network.

Methods

Generation of CLIP-115 and CLIP-170 double knockout mice

The generation of the CLIP-115 and CLIP-170 single knockout lines has been described previously (Akhmanova et al., 2005; Hoogenraad et al., 2002). We crossed heterozygous animals of both mouse lines to obtain compound heterozygotes. Meiotic recombination in the germ line generated the CLIP-115 and CLIP-170 double knockout (DKO) allele. Subsequent breeding of compound heterozygotes (which carried the DKO allele in their germ line) with C57/Bl6 wildtype animals resulted in 14 recombined pups in a total of 107 offspring (recombination efficiency of ~13%).

Molecular biology methods

Mouse genotyping was done by PCR, as described (Akhmanova et al., 2005; Hoogenraad et al., 2002). Protein extraction and western blot analysis methods have been published (Akhmanova et al., 2005; Hoogenraad et al., 2002). We used antibodies against CLIP-115 and/or CLIP-170 (#2221, #2238, #2360), which have been described previously (Coquelle et al., 2002; Hoogenraad et al., 2000).

Morphological and histological analysis of DKO mice

Weight of mice was analyzed every other week, starting at 6 weeks of age. A group of 10 DKO mice was compared with 5 wild type littermates and 5 C57Bl6 mice. The posture of mice was investigated by X-ray analysis. For this analysis 2 wild type and 2 homozygous DKO mice were sacrificed by intraperitoneal application of an overdose of ketamine and rompun placed onto a film cassette (18 x 25 cm) that contained a sheet of Kodak film. X-ray films were taken using a Kodak CGC model SPG-S (500 MA) machine at a distance of 10 inches with a current of 200 MA at 60 for 1/40 s. Hind limb clasping was examined by lifting mice at the base of their tails.

Procedures for the histological analysis of mice have been described (Akhmanova et al., 2005; Hoogenraad et al., 2002). For this analysis we used adult mice of 22 weeks, as well as E17.5 day embryos and young mice of 5 weeks. Sections of 40 micron were stained with thionin.

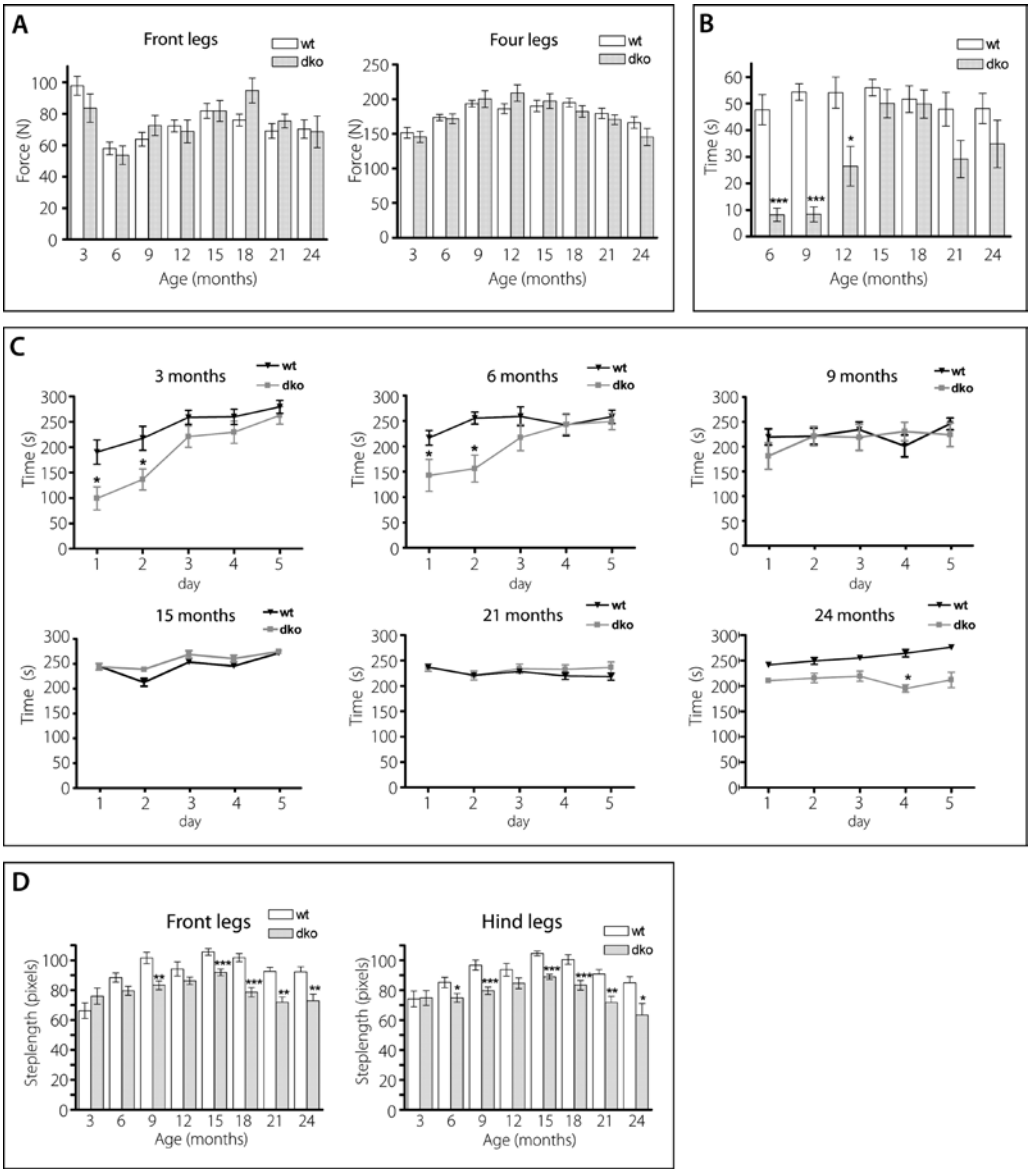

Figure 4. Longitudinal analysis of CLIP DKO mice

A. Grip strength. Muscle strength of the fore limbs (left hand panel) and of all four limbs (right hand panel) was measured on a grip strength meter in 10 DKO mice and 10 wild type mice. Both genotypes show equal strength throughout life. **B.** Hanging wire analysis. Strength and endurance of 10 DKO mice and 10 wild type mice was measured by the hanging wire test. Notice how the DKO group first shows an age-related increase in performance, but that at old ages this deteriorates again. **C.** Rotarod analysis. Motor coordination was analyzed in 10 DKO mice and 10 wild type mice in a rotarod set-up. Notice how the DKO group first shows an age-related increase in performance, but that at old ages this deteriorates again. **D.** Catwalk analysis. The gait of the front legs (left hand panel) and hind legs (right hand panel) of 10 DKO mice and 10 wild type mice was measured in a catwalk set-up. Except for the 3-month time point, the DKO mice have a smaller step size throughout life.

Behavioral analysis of DKO mice

Grip strength measurements were performed with a grip strength meter from Bioseb (Chaville, France). Measurements were performed on the front limbs and on all four limbs.
To measure grip strength combined with balance and endurance, mice were subjected to the hanging wire test, in which each mouse was placed on top of a wire cage lid and suspended 30 cm above the cage. After a short shake, the lid was turned upside down and the latency to fall was recorded, up to a maximum of 60 s.

Motor coordination activity was evaluated in adult mice using an accelerating rotarod treadmill (Ugo Basile 7650). Five mice were tested at a time in individual compartments. Mice were placed on the slowly rotating cylinder (4 rpm). After an initial adaptation period of 10 s, the rotational speed was gradually increased to a maximum of 40 rpm. The latency to fall was measured up to a maximum of 300 s. Animals that turned with the rotarod by hanging on to it were taken off after three rotations. Mice participated in one trial each day for five consecutive days. A total of ten mice were tested for each group.

Mice were tested for spontaneous locomotor activity in the open-field activity test (50x50 cm). Mice were placed in the middle of the arena and were recorded for 30 min using a computerized video tracking system to measure walking distance, moving episodes and moving time at the horizontal and vertical planes and entries of the mice in different imaginary parts of the field.

To gather information on the gait of the mice, we analyzed multiple locomotion parameters using the CatWalk set-up and program (Hamers et al., 2001). Mice traverse a walkway with a glass floor in which white fluorescent light is entirely internally reflected. Only where a paw touches the glass, light exits the floor and illuminates the contact area of the paw. The floor of the corridor is monitored via a video camera. Data analysis yields information about step length, time paws are standing or lifted and base of support.

Magnetic resonance imaging (MRI)

Five DKO and five wild type mice were anaesthetized with 5% isoflurane induction and 1-1.5 % isoflurane maintenance (in a mixture of 30% O2 and 70% NO2) and their temperature (37.0 ± 0.5) °C and breathing rate (100BPM) was kept constant during the experiments. MRI imaging was performed at 300 MHz Bruker system with horizontal bore magnet. A 20mm diameter surface RF coil was used for both transmitting and receiving. Scouting gradient echo images in the 3 orthogonal directions were acquired to guide the positioning of the 3D slab of the stereo tactically positioned mouse head. High-resolution coronal slices of the mouse brain were obtained using a 3D Fast Spin Echo sequence with an echo train length of eight, reducing the imaging time to 43 minutes. MR signals of a 3D volume of (20 x 20 x 20) mm^3 were acquired within a (256 x 128 x 64) matrix, TR = 2500 ms and first TE = 14 ms. MRI data was reconstructed to an image matrix of (256 x 256 x 256), containing 256 coronal slices of 78 μm with an in plane resolution of (78 x 78) μm^2.
The ventricles of mice were manually segmented from MRI 3D data sets and volumes were measured using AMIRA. Subsequently, for each ventricle, a surface-based representation was obtained by triangulating the boundary of the segmentation. Position and orientation normalization was performed through iterative closest point surface alignment of each ventricle with a chosen template ventricle; this in order to analyze only shape and size differences.

Acknowledgements

This work was supported by the Dutch Ministry of Economic Affairs (BSIK), the Netherlands Organization for Scientific Research (NWO Earth and Life Sciences and ZonMw) and the Dutch Cancer Society.

References

Akhmanova, A., A.L. Mausset-Bonnefont, W. van Cappellen, N. Keijzer, C.C. Hoogenraad, T. Stepanova, K. Drabek, J. van der Wees, M. Mommaas, J. Onderwater, H. van der Meulen, M.E. Tanenbaum, R.H. Medema, J. Hoogerbrugge, J. Vreeburg, E.J. Uringa, J.A. Grootegoed, F. Grosveld, and N. Galjart. 2005. The microtubule plus-end-tracking protein CLIP-170 associates with the spermatid manchette and is essential for spermatogenesis. *Genes Dev.* 19:2501-15.

Banizs, B., M.M. Pike, C.L. Millican, W.B. Ferguson, P. Komlosi, J. Sheetz, P.D. Bell, E.M. Schwiebert, and B.K. Yoder. 2005. Dysfunctional cilia lead to altered ependyma and choroid plexus function, and result in the formation of hydrocephalus. *Development.* 132:5329-39.

Coquelle, F.M., M. Caspi, F.P. Cordelieres, J.P. Dompierre, D.L. Dujardin, C. Koifman, P. Martin, C.C. Hoogenraad, A. Akhmanova, N. Galjart, J.R. De Mey, and O. Reiner. 2002. LIS1, CLIP-170's key to the dynein/dynactin pathway. *Mol Cell Biol.* 22:3089-102.

De Zeeuw, C.I., C.C. Hoogenraad, E. Goedknegt, E. Hertzberg, A. Neubauer, F. Grosveld, and N. Galjart. 1997. CLIP-115, a novel brain-specific cytoplasmic linker protein, mediates the localization of dendritic lamellar bodies. *Neuron.* 19:1187-99.

Deacon, S.W., A.S. Serpinskaya, P.S. Vaughan, M. Lopez Fanarraga, I. Vernos, K.T. Vaughan, and V.I. Gelfand. 2003. Dynactin is required for bidirectional organelle transport. *J Cell Biol.* 160:297-301.

Desai, A., and T.J. Mitchison. 1997. Microtubule polymerization dynamics. *Annu Rev Cell Dev Biol.* 13:83-117.

Forni, P.E., C. Scuoppo, I. Imayoshi, R. Taulli, W. Dastru, V. Sala, U.A. Betz, P. Muzzi, D. Martinuzzi, A.E. Vercelli, R. Kageyama, and C. Ponzetto. 2006. High levels of Cre expression in neuronal progenitors cause defects in brain development leading to microencephaly and hydrocephaly. *J Neurosci.* 26:9593-602.

Galjart, N. 2005. CLIPs and CLASPs and cellular dynamics. *Nat Rev Mol Cell Biol.* 6:487-98.

Hafezparast, M., R. Klocke, C. Ruhrberg, A. Marquardt, A. Ahmad-Annuar, S. Bowen, G. Lalli, A.S. Witherden, H. Hummerich, S. Nicholson, P.J. Morgan, R. Oozageer, J.V. Priestley, S. Averill, V.R. King, S. Ball, J. Peters, T. Toda, A. Yamamoto, Y. Hiraoka, M. Augustin, D. Korthaus, S. Wattler, P. Wabnitz, C. Dickneite, S. Lampel, F. Boehme, G. Peraus, A. Popp, M. Rudelius, J. Schlegel, H. Fuchs, M. Hrabe de Angelis, G. Schiavo, D.T. Shima, A.P. Russ, G. Stumm, J.E. Martin, and E.M. Fisher. 2003. Mutations in dynein link motor neuron degeneration to defects in retrograde transport. *Science.* 300:808-12.

Hamers, F.P., A.J. Lankhorst, T.J. van Laar, W.B. Veldhuis, and W.H. Gispen. 2001. Automated quantitative gait analysis during overground locomotion in the rat: its application to spinal cord contusion and transection injuries. *J Neurotrauma.* 18:187-201.

Holzbaur, E.L. 2004. Motor neurons rely on motor proteins. *Trends Cell Biol.* 14:233-40.

Hoogenraad, C.C., A. Akhmanova, F. Grosveld, C.I. De Zeeuw, and N. Galjart. 2000. Functional analysis of CLIP-115 and its binding to microtubules. *J Cell Sci.* 113:2285-2297.

Hoogenraad, C.C., A. Akhmanova, S.A. Howell, B.R. Dortland, C.I. De Zeeuw, R. Willemsen, P. Visser, F. Grosveld, and N. Galjart. 2001. Mammalian Golgi-associated Bicaudal-D2 functions in the dynein-dynactin pathway by interacting with these complexes. *Embo J.* 20:4041-54.

Hoogenraad, C.C., B. Koekkoek, A. Akhmanova, H. Krugers, B. Dortland, M. Miedema, A. Van Alphen, W.M. Kistler, M. Jaegle, M. Koutsourakis, N. Van Camp, M. Verhoye, A. Van Der Linden, I. Kaverina, F. Grosveld, C.I. De Zeeuw, and N. Galjart. 2002. Targeted mutation of Cyln2 in the Williams syndrome critical region links CLIP-115 haploinsufficiency to neurodevelopmental abnormalities in mice. *Nat Genet.* 32:116-27.

Hoogenraad, C.C., P. Wulf, N. Schiefermeier, T. Stepanova, N. Galjart, J.V. Small, F. Grosveld, C.I. De Zeeuw, and A. Akhmanova. 2003. Bicaudal D induces selective dynein-mediated microtubule minus end-directed transport. *Embo J.* 22:6004-6015.

Komarova, Y.A., A.S. Akhmanova, S. Kojima, N. Galjart, and G.G. Borisy. 2002. Cytoplasmic linker proteins promote microtubule rescue in vivo. *J Cell Biol*. 159:589-99.

Lalonde, R. 1987. Motor abnormalities in staggerer mutant mice. *Exp Brain Res*. 68:417-20.

Lambert de Rouvroit, C., and A.M. Goffinet. 2001. Neuronal migration. *Mech Dev*. 105:47-56.

LaMonte, B.H., K.E. Wallace, B.A. Holloway, S.S. Shelly, J. Ascano, M. Tokito, T. Van Winkle, D.S. Howland, and E.L. Holzbaur. 2002. Disruption of dynein/dynactin inhibits axonal transport in motor neurons causing late-onset progressive degeneration. *Neuron*. 34:715-27.

Lansbergen, G., Y. Komarova, M. Modesti, C. Wyman, C.C. Hoogenraad, H.V. Goodson, R.P. Lemaitre, D.N. Drechsel, E. van Munster, T.W. Gadella, Jr., F. Grosveld, N. Galjart, G.G. Borisy, and A. Akhmanova. 2004. Conformational changes in CLIP-170 regulate its binding to microtubules and dynactin localization. *J Cell Biol*. 166:1003-14.

Levy, J.R., C.J. Sumner, J.P. Caviston, M.K. Tokito, S. Ranganathan, L.A. Ligon, K.E. Wallace, B.H. LaMonte, G.G. Harmison, I. Puls, K.H. Fischbeck, and E.L. Holzbaur. 2006. A motor neuron disease-associated mutation in p150Glued perturbs dynactin function and induces protein aggregation. *J Cell Biol*. 172:733-45.

Ma, X., S. Kawamoto, J. Uribe, and R.S. Adelstein. 2006. Function of the neuron-specific alternatively spliced isoforms of nonmuscle myosin II-B during mouse brain development. *Mol Biol Cell*. 17:2138-49.

Mesngon, M.T., C. Tarricone, S. Hebbar, A.M. Guillotte, E.W. Schmitt, L. Lanier, A. Musacchio, S.J. King, and D.S. Smith. 2006. Regulation of cytoplasmic dynein ATPase by Lis1. *J Neurosci*. 26:2132-9.

Pierre, P., J. Scheel, J.E. Rickard, and T.E. Kreis. 1992. CLIP-170 links endocytic vesicles to microtubules. *Cell*. 70:887-900.

Reiner, O., S. Sapoznik, and T. Sapir. 2006. Lissencephaly 1 linking to multiple diseases: mental retardation, neurodegeneration, schizophrenia, male sterility, and more. *Neuromolecular Med*. 8:547-66.

Riehemann, K., and C. Sorg. 1993. Sequence homologies between four cytoskeleton-associated proteins. *Trends Biochem Sci*. 18:82-3.

Schroer, T.A. 2004. Dynactin. *Annu Rev Cell Dev Biol*. 20:759-79.

Schuyler, S.C., and D. Pellman. 2001. Microtubule "plus-end-tracking proteins": The end is just the beginning. *Cell*. 105:421-4.

Terada, S., and N. Hirokawa. 2000. Moving on to the cargo problem of microtubule-dependent motors in neurons. *Curr Opin Neurobiol*. 10:566-73.

Trushina, E., J. Du Charme, J. Parisi, and C.T. McMurray. 2006. Neurological abnormalities in caveolin-1 knock out mice. *Behav Brain Res*. 172:24-32.

Xiang, X. 2003. LIS1 at the microtubule plus end and its role in dynein-mediated nuclear migration. *J Cell Biol*. 160:289-90.

Chapter 5

Discussion

Chapter 5

Discussion

5.1. Introduction

The eukaryotic cytoskeleton is an essential determinant for cellular morphology. Actin filaments, intermediate filaments and microtubules form separate, but interacting intracellular networks that determine the shape of the cell and provide it with strength. These networks are not static structures. On the contrary, they are in general highly dynamic allowing the cell to change its shape in response to extracellular cues such as mechanical forces or changing environmental conditions. In addition, the cytoskeleton is involved in several other essential cellular processes such as cell division and intracellular transport. Microtubules form one of the major components of the cytoskeleton. They are hollow cylindrical tubes built up of α- and β-tubulin heterodimers. Microtubules are polarized structures with a fast growing 'plus'-end and a slower growing 'minus'-end. In fibroblasts they are typically organized into a radial array with their minus ends anchored near the nucleus in the microtubule organizing center (MTOC) and their plus-ends growing towards the cell periphery. The dynamic behavior of the plus-ends at the cell periphery with alternating phases of growth and shrinkage, called dynamic instability, is essential for proper functioning of the microtubule network.

Microtubule plus-ends are specifically targeted by a large number of proteins that only bind during the growing phases. They are called plus-end-tracking proteins, or +TIPs. The different proteins in this group each have their own mode of binding, either directly or via other +TIPs. Their concentration at the relatively small area of the plus-end allows them to interact with each other in a intensive and intricate manner. In this thesis, we focused on two highly similar plus-end binding proteins, the cytoplasmic linker proteins, or CLIPs. Their intriguing binding behavior, appearing as comets on the growing microtubule ends when fused to green fluorescent protein (GFP), suggested a specialized function which was yet unknown.

5.2 CLIP deficient mice

To investigate the functions of the CLIPs we generated knockout mice for both CLIP-115 ((Hoogenraad et al., 2002a); this thesis) and CLIP-170 (Akhmanova et al., 2005). The gene encoding CLIP-115 is located in a chromosomal region that is commonly deleted in patients with Williams (or Williams-Beuren) syndrome, a neurodevelopmental disorder characterized by cardiovascular abnormalities, growth retardation and neurological deficits. Since CLIP-115 is highly expressed in the brain, and can barely be detected in other tissues, it might very well be involved in the neurological features of the disease. Deletion of CLIP-115 in mice results in a mild growth deficiency, brain abnormalities, hippocampal dysfunction and particular deficits in motor coordination, all features reminiscent of Williams syndrome. Unfortunately, the behavioral abnormalities found in homozygous and heterozygous animals became less obvious in later generations. It is well known that genetic background can influence observed phenotypes significantly, in particular behavioral phenotypes (Crawley, 1996; Gerlai, 1996; Lathe, 1996). For the generation of the CLIP-115 knockout mice, we used E14 ES cells derived from 129/Ola inbred mice. Chimeras were subsequently backcrossed into C57/Bl6. This results in a different genetic background surrounding the targeted allele than that surrounding the

wild type allele. To compensate for this difference we not only used wild type littermates as controls, but also mice that contained the targeted allele but were not subjected to Cre-recombinase. These latter mice, called CLIP-T, still express the gene encoding CLIP-115 but the genomic region surrounding the gene is 129/Ola-derived instead of C57/Bl6-derived. In neither of the tests we found significant differences between wild type littermates and CLIP-T mice, suggesting that the phenotypic abnormalities observed in homozygous and heterozygous mice as compared to wild type animals could be contributed directly to the deficiency in CLIP-115 and not to differences in genetic background. However, when we repeated the experiments with later generations, the phenotype became less obvious. Apart from genetic background another important determinant in behavioral testing is the laboratory environment (Crabbe et al., 1999), including the experimental set-up, the social status of the mice and the housing environment. Changes in these parameters have possibly changed the outcome of the repeated behavioral assays.

The CLIP-170 knockout line was generated using a different strategy than was used for the CLIP-115 knockout line. Instead of removing the majority of the coding sequences, we introduced a neomycin resistance marker in front of the ATG, thereby interrupting the gene. This, however, resulted in a leaky allele, leaving residual CLIP-170 protein in adult lung and in the embryo (Akhmanova et al., 2005). CLIP-170 protein was absent in all other tissues tested, as well as in fibroblasts derived from homozygous CLIP-170 knockout mice. Despite the leaky allele, it was shown that CLIP-170 is involved in the formation and/or maintenance of the spermatid manchette. Generation and analysis of the complete CLIP-170 knockout mouse strain, in which all coding sequences have been removed, is necessary to determine the influence of the residual CLIP-170 protein, especially during embryogenesis.

Although both CLIP-115 knockout mice and CLIP-170 knockout mice display particular abnormalities, the phenotypes are surprisingly mild. At the cellular level, no abnormalities could be observed other than an increased level of CLIP-170 and dynactin at the microtubule plus-ends. This mild phenotype might be explained by an important degree of redundancy, since the two proteins are highly similar. To prove this redundancy and to determine the effect of the absence of both CLIPs, we crossed CLIP-115 knockout mice with CLIP-170 knockout mice to generate double CLIP-115 and CLIP-170 knockout mice. The deficiency for both CLIPs caused obvious abnormalities, both in fibroblasts and in mice. In double knockout fibroblast cultures, the average surface area of cells was significantly larger and many cells displayed an altered distribution of microtubules, resulting in large areas without any microtubules but with aggregates that contained several proteins including cytoplasmic dynein and most components of the dynactin complex. Analysis of the parameters of microtubule dynamics revealed a decrease in the rescue frequency, leaving microtubules to shrink all the way back to the centrosome instead of fluctuating at the cell periphery. In addition, double CLIP-115 and CLIP-170 knockout mice turned out to have significantly enlarged ventricles, evolving into severe hydrocephalus in a number of cases. In the following sections the different aspects of the observed phenotypes and the putative function of the CLIPs in the altered processes will be addressed.

5.3 CLIPs and fibroblast spreading

In our experiments using embryonic and dermal fibroblasts, we found that the double CLIP-115 and CLIP-170 populations contained a significant number of cells with an increased surface area relative to wild type populations. The aberrant microtubule distribution and accompanying aggregation of components of the dynein-dynactin system was generally more severe in the

larger cells. Further analysis showed that wild type and double knockout cells had similar volumes when they were detached from the surface, indicating a difference in cell spreading rather than cell size. This aspect of the cellular phenotype of double knockout fibroblasts touches the fundamental process of restraining cellular spreading in an environment other than a three-dimensional tissue. Although fibroblasts seeded in low numbers in a culture dish do not face any extracellular restraint in terms of spreading, such as the presence of other cells, the surface area of these cells does not increase indefinitely. What mechanism does a cell have to prevent it from spreading too far?

Cell spreading depends on adhesion to the extracellular matrix via integrins, transmembrane receptors that mediate the interaction between the extracellular matrix and the cytoskeleton (Hynes, 2002). Binding of a ligand to the integrin receptors initiates a cascade of cytoplasmic events such as activation of Rho GTPases (del Pozo et al., 2000; Ren et al., 1999). These regulate the organization of the cytoskeleton (Nobes and Hall, 1995; Palazzo et al., 2004) and the recruitment of focal adhesion proteins. Since the formation of new focal adhesions is fundamental to both cell motility and cell spreading, it is assumed that these processes are, in part, analogous. In migrating cells, motility depends on the formation of new focal adhesions rather that the translocation of existing ones (Rottner et al., 1999; Smilenov et al., 1999), but disassembly of substrate contact-sites at the retracting side of the cell is necessary for the cell to advance. It was shown that turnover of focal adhesions takes place in spreading cells as well and might even be critical for the extension of the focal adhesions to the periphery of the cell (Partridge and Marcantonio, 2006).

The assembly and turnover of adhesion sites is regulated by an intricate signaling cascade leading to the phosphorylation of the focal adhesion scaffold protein paxillin (Brown and Turner, 2002; Turner, 2000a; Turner, 2000b; Zaidel-Bar et al., 2007). An extensive discussion of this cascade is beyond the scope of this thesis, but several studies have shown that changes in the phosphorylation status of paxillin or proteins involved in the upstream signaling cascade affect cell spreading, either leading to inhibition (Jacamo et al., 2007; Jamieson et al., 2005; Richardson et al., 1997) or acceleration of the spreading process (Brown et al., 2005). Recently it has been suggested that the spreading process after plating consists of two phases. First a rapid flattening of the cell through the approximately symmetrical projection of filopodia, followed by a more slowly asymmetrical spreading of the cell through the restructuring of nascent focal adhesions and the formation of actin stress fibers (Partridge and Marcantonio, 2006). Regulation of the extent to which a cell spreads might be regulated particularly during this second phase. For example, fibroblasts deficient for Src family kinase (SFKs), ubiquitously expressed non-receptor tyrosine kinases, have very low phosphotyrosine levels and are significantly delayed in the later phase of cell spreading (Klinghoffer et al., 1999; Partridge and Marcantonio, 2006).

Here we have shown that, although deletion of both CLIP-115 and CLIP-170 does not alter the amount of paxillin or phosphorylated focal adhesion kinase in focal adhesions, it does lead to an increase in the amount of phosphorylated tyrosines as shown by staining for PT66. This suggests a direct involvement of the microtubule network in the regulation of the phosphorylation status of focal adhesions. It has already been shown that targeting of microtubule plus-ends to focal adhesion sites promotes their detachment or disassembly (Kaverina et al., 1999; Kaverina et al., 1998) and Kinesin-I has been suggested to focally deliver components involved in the disassembly of the adhesion sites (Krylyshkina et al., 2002). Because of a decrease in microtubule dynamics in double CLIP-115 and CLIP-170 knockout fibroblasts, the frequency of microtubules targeting focal adhesion sites is likely to be lower, hampering the delivery of factors necessary for the disassembly of focal adhesions. These factors possibly include proteins

involved in phosphorylation or dephosphorylation, such as phosphatases, resulting in changes in the phosphorylation status of proteins such as paxillin. The alterations in cell-matrix contacts might have an effect on the extent to which a cell is able to spread.

Since cell migration and cell spreading are partly analogous, alterations in the maintenance of cell-matrix interactions are likely to affect cell migration as well. Wound healing experiments using CLIP-115 and CLIP-170 double knockout fibroblasts, however, did not show any changes in the parameters of migrations, such as protein translocations to the leading edge and migration speed (data not shown). Hence, the deficiency for both CLIPs does not hamper the cell in the polarization process and the accompanied organization of the leading edge. But what about the trailing edge? The experimental set-up of the wound-healing assay complicates a proper examining of this side of the migrating cell, since cells are grown to confluence. If, however, the absence of the CLIPs affects the disassembly of focal adhesions, it is likely that migrating CLIP-115 and CLIP-170 double knockout fibroblasts have a deficit in the retraction of their trailing edge. This would influence not only cell migration, but also cell spreading. It has become clear that the spread area of a cell is actively regulated and depends on the balance between the rate of protrusion and retraction, and that a causal relationship exists between these two processes (Dunn and Zicha, 1995). Interestingly, it appears that fluctuations in retraction lead to changes in protrusion, suggesting that retraction is always the cause and protrusion is the effect. Restriction of the spread area of the cell is thought to arise through the limitation of material needed for protrusion, e.g. focal adhesion components, which only become available after retraction of existing cell-matrix interactions. If this is the case, a decrease in the retraction rate in CLIP-115 and CLIP-170 double knockout cells because disassembly of focal adhesions is impaired, could only result in an increase of the surface area when the double knockout cells have a larger pool of available focal adhesion proteins. This remains to be determined.

In addition to a limitation in the proteins needed for cell-matrix interactions, cell spreading is also limited by mechanical factors such as membrane tension (Raucher and Sheetz, 2000). The increase of membrane area accompanying the spreading process cannot be facilitated by the stretching of the plasma membrane (Waugh, 1983). Thus, to increase the membrane surface area additional membrane must be synthesized or drawn from internal compartments of the cell. It has also been suggested that cells maintain a plasma membrane reservoir in the form of wrinkles that can accommodate acute changes in cell shape (Raucher and Sheetz, 1999). Cell spreading may be limited because of the finite nature of this reservoir. Further investigation is necessary to determine whether CLIP-115 and CLIP-170 double knockout cells synthesize more membrane, draw more membrane from internal compartments or have increased their plasma membrane reservoir.

5.4 CLIPs and microtubule distribution

Cellular analysis also demonstrated that a significant number of double CLIP deficient fibroblasts contain multiple, differently sized microtubule-free areas in which components of the dynactin complex are often found to aggregate with other proteins such as dynein intermediate chain and BICD2 (Figure 1). We find these aggregate-containing areas in wild type cells and in single CLIP deficient cells as well, although not in so many cells and often less severe. Interestingly, not all microtubule-free areas contein the dynactin containing aggregates.

The fact that the observed cellular phenotype is not exclusively found in double knockout fibroblasts, but rather has intensified relative to wild type, suggests that the formation of the aggregate-containing microtubule-free areas is a stochastic process with an increased chance in

CLIP deficient cells. Although is seems like microtubules constantly cover all areas of the cell, a consequence of their dynamic behavior will be that certain areas can be temporarily unoccupied. The same dynamic behavior normally ensures that new microtubules will immediately grow into these kind of microtubule-free areas. In CLIP-115 and CLIP-170 double knockout fibroblasts, however, microtubule dynamics is decreased as a result of a lower rescue frequency (see section 5.5), reducing the chance of new microtubules growing into the transiently unoccupied area. And since microtubules provide the cell with strength to maintain its form, areas that are devoid

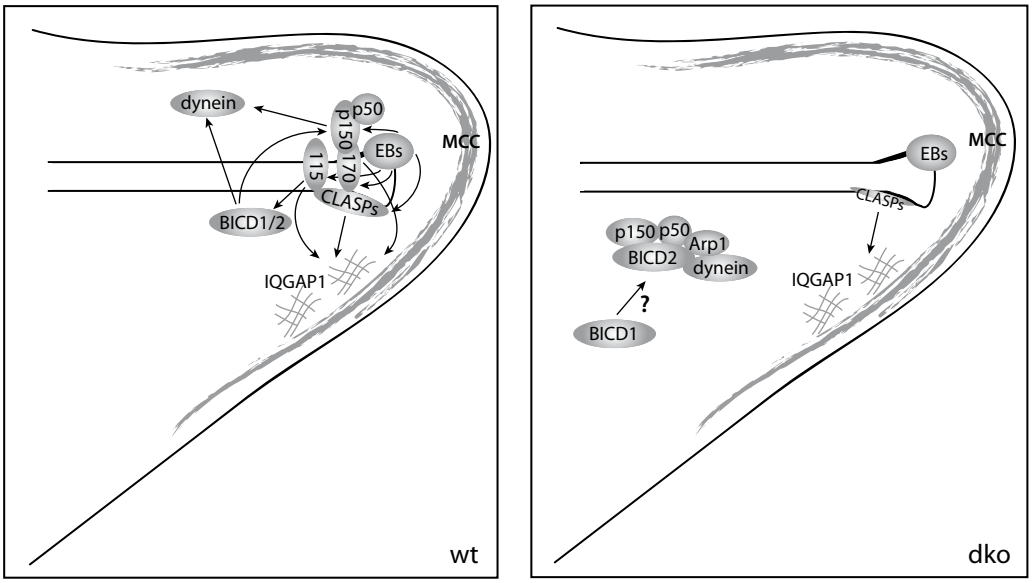

Figure 1. Effect of CLIP-115 and CLIP-170 double deficiency on microtubule plus-end-binding proteins.
Schematic representation of the protein interactions at the microtubule plus-end in wild type (left panel) and in CLIP-115 and CLIP-170 double knockout cells (right panel). Since the start of the project described in this thesis, the list of microtubule plus-end-binding proteins has extended steadily, and more insight has been gathered into the complexity of the interactions between these proteins. Thus, the schematic representation of the microtubule plus-end in wild type cells (left panel) includes additional information compared to the representation shown in figure 3 of chapter 1. To ensure the clarity of the figure, only a selection of proteins and interactions, which are discussed in this thesis, are shown. Notably, it has been shown that the EB proteins interact with virtually all +TIPs that have been shown to associate with the microtubule plus-end directly (Lansbergen and Akhmanova, 2006). Furthermore, several proteins have been identified as members of the microtubule-capture-complex (MCC), including the CLASPs, LL5β, ELKS and phosphatidylinositol-3,4,5-triphosphate (PIP3) (Lansbergen et al., 2006). This has led to the idea that the CLASPs are essential factors in the MCC, and that their accumulation at the cell cortex is not mediated by their association with the microtubule plus-end, but by membrane-interacting proteins.
Depletion of both CLIP-115 and CLIP-170 results in the relocalization of $p150^{Glued}$ from the plus-end to the cytoplasm, where it is found in cytoplasmic aggregates. In addition, these aggregates also contain p50 (dynamitin), Arp1, cytoplasmic dynein and BICD2. It is noteworthy to mention that both $p150^{Glued}$ and BICD2 are CLIP-interacting proteins. Surprisingly, although the absence of the CLIPs decreases the amount of CLASP associated with the plus-end, the accumulation of CLASP in the microtubule-capture-complex at the leading edge of the cells remains unchanged. Furthermore, the CLASPs are not found in the cytoplasmic aggregates. The accumulation of EBs at the plus-end is not affected by the removal of the CLIPs.

of microtubules for a longer period are prone to collapse. After a collapse, microtubule ingrowth has become more difficult or even impossible because of the physical obstruction of the limited space remaining. As a result, such an area will be permanently microtubule-free.

The altered microtubule dynamics might play a role in the formation of the described microtubule-free areas with dynactin aggregates, but it cannot be the only explanation. We have shown that overexpression of a GFP-fusion of the amino-terminal domain of CLIP-170,

which is able to bind microtubules but lacks the protein-interacting carboxy-terminal domain, restores microtubule dynamics to wild type levels but does not remove the aggregate-containing microtubule-free areas. In contrast, cells overexpressing full length CLIP-115 or CLIP-170 no longer show this phenotype. This means that the CLIPs have another function independent of their regulatory role in microtubule dynamics, and they are, at least in part, redundant for both functions.

Although the additional function of the CLIPs remains to be elucidated, the present data allow us to speculate on it. Given the diversity of protein interactions at the microtubule plus-ends, removal of the CLIPs is bound to have an effect on other plus-end binding proteins. The presence of dynactin in the observed aggregates might suggest that this protein is involved in the unknown additional function of the CLIPs. It has already been shown that CLIP-170 is required for the localization of $p150^{Glued}$ at growing microtubule ends, since dynactin is lost from the plus-ends when CLIP-170 is absent, while its accumulation increases when CLIP-170 is overexpressed (Goodson et al., 2003; Lansbergen et al., 2004; Valetti et al., 1999; Watson and Stephens, 2006). Even though dynactin localization to the plus-end is already affected in single CLIP-170 deficient cells, they do not show an increase in aggregate-containing microtubule-free areas relative to wild type cells. So the relocation of the microtubule-bound fraction of $p150^{Glued}$ is not sufficient to cause its aggregation. Besides, in wild type cells the major fraction of $p150^{Glued}$ is not bound to microtubules and this does not form aggregates. CLIP-170 has been shown to be able to bind dynactin independently of microtubule binding [Lansbergen, 2004], and might do so to prevent it from aggregation.

No direct interaction has been shown between CLIP-115 and dynactin, which fits with the fact that CLIP-115 lacks the $p150^{Glued}$-binding domain of CLIP-170. Any effect of CLIP-115 must therefore involve one or more other proteins. We provide evidence that CLIP-115 binds to BICD1 and BICD2, the mammalian homologues of the *Drosophila* Bicaudal D protein. The BICD proteins have been shown to recruit dynein to membranes positive for the small GTPase Rab6 through simultaneous binding to Rab6 and to dynein and dynactin complexes (Hoogenraad et al., 2001; Matanis et al., 2002; Short et al., 2002). The presence of BICD2 in the aggregates found in the CLIP-115 and CLIP-170 double knockout fibroblasts suggests that this protein might be the intermediate factor via which CLIP-115 prevents dynactin from aggregation in the absence of CLIP-170. This does, however, not rule out the possibility that other proteins mediate this interaction between CLIP-115 and dynactin.

5.5 CLIPs and microtubule dynamics

We further show that in CLIP-115 and CLIP-170 double knockout fibroblasts the frequency of microtubule rescue, the transition from depolymerization to polymerization, is five times lower relative to wild type fibroblasts. This suggests that the CLIPs promote microtubule rescue, either by themselves or by recruiting another rescuing factor. As mentioned above, the rescue frequency can be restored by overexpression of the amino-terminal domain of clip-170. Since interactions with other proteins depend largely on the carboxy-terminal domain (Lansbergen et al., 2004), it seems unlikely that the rescuing function of the CLIPs depends on the recruitment of another factor. When the CLIPs function as rescue factors themselves, however, this implies that they are able to bind to shrinking microtubules and thereby convert them to the growing phase, although this seems to contradict the characteristic feature of binding specifically to growing microtubule plus-ends.

The mechanism with which CLIP-170 associates with the microtubule plus-end, most likely

shared by CLIP-115, has been studied intensively since its first report as a plus-end-tracking protein (Perez et al., 1999). Research has focused on three possible mechanisms of plus-end tracking. First, motor-driven transport, in which CLIP-170 is physically moved toward the microtubule tip by motor proteins. This has been shown for the yeast homologues Bik1p and Tip1p (Busch and Brunner, 2004; Busch et al., 2004; Carvalho et al., 2004). Second, surfing, in which CLIP-170 moves on an energy wave created by a conformation or protein specific for the microtubule plus-end. The APC homologue in *Saccharomyces cerevisiae*, Kar9p, appears to use this mechanism via Bim1p (Liakopoulos et al., 2003). Third, end-loading or treadmilling, in which CLIP-170 specifically binds at the microtubule end and rapidly dissociates shortly after binding. Several studies indicate that this third mechanism is used by CLIP-170 to track microtubule plus-ends (Diamantopoulos et al., 1999; Folker et al., 2005; Perez et al., 1999). In addition to the mechanism of binding, it remains unclear what leads to the specific localization at the microtubule plus-end. CLIPs might recognize a specific structural conformation such as the tubulin sheets observed at the growing ends of microtubules, and the closure of these sheets might results in their dissociation from the tubule (Perez et al., 1999). Or the CLIPs might associate with unpolymerized tubulin dimers or polymers and subsequently copolymerize to target the growing ends of microtubules. Several studies seem to favor the second mechanism, since CLIPs have been shown to interact with unpolymerized tubulin, and no preferential binding to distinct microtubule conformations has been observed (Diamantopoulos et al., 1999; Folker et al., 2005).

The question remains, however, how the CLIPs as plus-end binding proteins are able to rescue shrinking microtubules. Recently, is has been shown that the microtubule binding-domain of CLIP-170, without the presence of any other factors, promotes the formation of curved and circular tubulin oligomers and increases the rescue frequency (Arnal et al., 2004). It has long been known that depolymerizing microtubules display outwardly curved protofilaments (Mandelkow et al., 1991; Muller-Reichert et al., 1998). Arnal *et al.* propose a model in which the curved CLIP-170-bound tubulin oligomers interact with the curled microtubule ends, and that subsequent straightening of the protofilaments would initiate a new round of polymerization. Since this mechanism requires the presence of the microtubule binding domain of CLIP-170, which is highly similar in CLIP-115, this would explain why the rescue frequency is not altered in single CLIP-115 or CLIP-170 knockout cells.

5.6 CLIPs and hydrocephalus

In the population of double knockout mice, we regularly found homozygous mice with obvious hydrocephalus. Since homozygous CLIP-115 knockout mice have an enlargement of all major ventricles, we carried out high resolution MRI analysis to determine the volumes of the ventricular system in wild type and homozygous double CLIP-115 and CLIP-170 knockout mice. In all homozygous double knockout mice tested, the lateral ventricles and the third ventricle were significantly enlarged, whereas the size of the fourth ventricle was similar to that in wild type mice.

Hydrocephalus has been reported in a number of different transgenic mouse models (Ibanez-Tallon et al., 2002; Kobayashi et al., 2002; Rolf et al., 2001; Sapiro et al., 2002; Taulman et al., 2001). Notably, in most of these mice the enlargement of the ventricles is restricted to the lateral and the third ventricles. This form of hydrocephalus is often described as non-communicating and is generally associated with a physical obstruction within the ventricular system. In the CLIP-115 and CLIP-170 double knockout mice, an obstruction of the aqueduct of Sylvius,

the long and narrow connection between the third and fourth ventricle, seems to result from the invasion of cerebellar neurons due to aberrant migration. Abnormal migration has been associated with hydrocephalus in other studies (Ma et al., 2006). Although in many cases of non-communicating hydrocephalus it is unclear whether stenosis of complete closure of the aqueduct is the primary cause or whether it is a secondary effect that results from the compression exerted by the expanding ventricles (Perez-Figares et al., 2001), in the CLIP double knockout mice it is likely to be the primary defect.

In addition to the physical obstruction of the aqueduct of Sylvius, we must also consider a possible defect in the formation or maintenance of motile cilia. These are present on the ependymal cells lining the ventricles and are involved in maintaining the flow of cerebrospinal fluid (CSF). This flow is essential for proper functioning of the ventricular system is the flow of cerebrospinal fluid. Although the bulk displacement of CSF results from changing blood pressures in the cerebral arterial tree (Bradley et al., 1986), an additional laminar flow near the ependymal surface results from the beating of the ependymal cilia. This latter flow is thought to be particularly important for the circulation of CSF at the narrow segments of the ventricular system (Shimizu and Koto, 1992). In mice lacking for instance axonemal dynein heavy chain 5 (*MDNAH5*), neural adhesion molecule L1, sperm-associated antigen 6 (*Spag6*), DNA polymerase λ, and in mice expressing mutated Polaris (Ibanez-Tallon et al., 2002; Kobayashi et al., 2002; Rolf et al., 2001; Sapiro et al., 2002; Taulman et al., 2001), the observed hydrocephalus is linked to the immotility of the ependymal cilia. In many, but not all, of these cases the hydrocephalus is accompanied by recurrent respiratory infections, a randomization of left-right symmetry and male infertility resulting from a dysfunction of all motile cilia (primary ciliary dyskinesia) (Zariwala et al., 2006). Although no *situs inversus* or respiratory problems were observed in the double CLIP-115 and CLIP-170 knockout mice, this does not rule out the possibility that immotile cilia underlie the ventricular enlargement. Cilia in the respiratory system and in the developing embryo might be unaffected because of the residual CLIP-170 protein in adult lung and in the embryo. Double knockout males already are subfertile due to the absence of CLIP-170 during spermiogenesis, which does not affect the motility of the spermatozoa but rather the morphology of the sperm head (Akhmanova et al., 2005). Future studies in CLIP-115 and CLIP-170 double knockout mice and analysis of the recently generated CLIP-115 and CLIP-170 double knockout mice in which all tissues are deficient for CLIP-170, will be necessary to determine whether the cilia in the reproductive system and the respiratory tract display normal motility.

Like most motile cilia, ependymal cilia consist of a highly ordered structure of nine peripheral microtubule doublets arranged around two central microtubules (9+2 axoneme) that are interconnected by a number of multiprotein complexes including projections of axonemal dynein. The ATPase activity of these dynein arms generates the sliding of microtubule doublets, resulting in a beating movement of the cilium. Immotility of the cilia is often associated with abnormal or absent axonemal dynein arms. In contrast to cytoplasmic dynein, axonemal dynein does not behave as a plus-end tracking protein and there is no evidence for an interaction with dynactin. Thus, the effect of the absence of CLIP-115 and CLIP-170 on dynactin and cytoplasmic dynein does not automatically suggest an effect on the presence or organization of the axonemal dynein arms. Electron microscopic analysis will be necessary to analyze the structural organization of the ependymal cilia in CLIP-115 and CLIP-170 double knockout mice.

Proper movement of CSF by the laminar flow can also be caused by ciliary problems other than the impairment of the dynein arms. There can be significantly fewer, or even no cilia lining the ventricular lumen, suggesting a defect in the formation or maintenance of cilia. The assembly and maintenance of cilia depends on intraflagellar transport (IFT), a bi-directional

microtubule-based transport system that ensures the delivery of flagellar precursors to the tip and the transport to return turnover products to the cell body (Qin et al., 2004). The anterograde transport requires the function of kinesin-II, whereas the retrograde transport is mediated by cytoplasmic dynein. Based on the effect of CLIP deficiency on the localization of dynactin and cytoplasmic dynein in fibroblasts, an effect of the absence of CLIP-115 and CLIP-170 on cytoplasmic dynein in ciliated epithelial cells cannot be ruled out. Furthermore, there might be a direct function of the CLIPs in the tip of the cilia. It has been shown that another plus-end tracking protein, EB1, localizes to the flagellar tip in *Chlamydomonas reinhardtii* and that its depletion results in a dramatic accumulation of IFT particles at the distal end of the flagella (Pedersen et al., 2003). It is suggested that EB1 might have an effect on IFT by affecting motor activity, but it is not ruled out that it is also involved in flagellar assembly and turnover through its function in regulating microtubule dynamics. It is not unlikely that, in addition to EB1, other plus-end binding proteins such as the CLIPs influence the formation and maintenance of cilia by regulating microtubule dynamics.

Finally, enlargement of the brain ventricles could result from neuronal loss. It has been shown that mice expressing high levels of Cre recombinase in neuronal progenitors suffer from severe hydrocephalus due to loss of neurons (Forni et al., 2006). Cre recombinase was used to remove CLIP-115 encoding sequences in ES-cells during the generation of the CLIP-115 knockout mice (Hoogenraad et al., 2002b). Although we cannot rule out the possibility that such aspecific Cre activity has affected the results obtained with the CLIP-115 single knockout mice, it seems highly unlikely to underlie the hydrocephalus in the CLIP-115 and CLIP-170 double knockout mice. Both single CLIP deficient mouse lines, as well as the double CLIP deficient mice have been crossed back into the C57BL6 background for several generations. Moreover, no indication of severe neuronal loss has been found in the brains of the CLIP double knockout mice.

In summary, it is becoming more and more clear that CLIP-115 and CLIP-170 function in a variety of processes necessary to maintain cellular homeostasis. A high level of redundancy between the two proteins prevents major abnormalities when either of the CLIPs is absent, but deficiency for both CLIPs has a noticeable effect on the processes the proteins are involved in, including microtubule dynamics, cellular morphology and brain morphology. Although our experiments have increased our knowledge on CLIP function substantially, future research is essential to answer remaining questions, in particular the analysis of the recently generated CLIP-115 and CLIP-170 double knockout mice in which CLIP-170 is completely absent in all tissues. This analysis will show whether the remaining CLIP-170 in the adult lung and the embryo of the double CLIP deficient mice used in this study influences the severity of the phenotype.

5.6. References

Akhmanova, A., A.L. Mausset-Bonnefont, W. van Cappellen, N. Keijzer, C.C. Hoogenraad, T. Stepanova, K. Drabek, J. van der Wees, M. Mommaas, J. Onderwater, H. van der Meulen, M.E. Tanenbaum, R.H. Medema, J. Hoogerbrugge, J. Vreeburg, E.J. Uringa, J.A. Grootegoed, F. Grosveld, and N. Galjart. 2005. The microtubule plus-end-tracking protein CLIP-170 associates with the spermatid manchette and is essential for spermatogenesis. *Genes Dev.* 19:2501-15.

Arnal, I., C. Heichette, G.S. Diamantopoulos, and D. Chretien. 2004. CLIP-170/tubulin-curved oligomers coassemble at microtubule ends and promote rescues. *Curr Biol.* 14:2086-95.

Bradley, W.G., Jr., K.E. Kortman, and B. Burgoyne. 1986. Flowing cerebrospinal fluid in normal and hydrocephalic states: appearance on MR images. *Radiology*. 159:611-6.

Brown, M.C., L.A. Cary, J.S. Jamieson, J.A. Cooper, and C.E. Turner. 2005. Src and FAK kinases cooperate to phosphorylate paxillin kinase linker, stimulate its focal adhesion localization, and regulate cell spreading and protrusiveness. *Mol Biol Cell*. 16:4316-28.

Brown, M.C., and C.E. Turner. 2002. Roles for the tubulin- and PTP-PEST-binding paxillin LIM domains in cell adhesion and motility. *Int J Biochem Cell Biol*. 34:855-63.

Busch, K.E., and D. Brunner. 2004. The microtubule plus end-tracking proteins mal3p and tip1p cooperate for cell-end targeting of interphase microtubules. *Curr Biol*. 14:548-59.

Busch, K.E., J. Hayles, P. Nurse, and D. Brunner. 2004. Tea2p kinesin is involved in spatial microtubule organization by transporting tip1p on microtubules. *Dev Cell*. 6:831-43.

Carvalho, P., M.L. Gupta, Jr., M.A. Hoyt, and D. Pellman. 2004. Cell cycle control of kinesin-mediated transport of Bik1 (CLIP-170) regulates microtubule stability and dynein activation. *Dev Cell*. 6:815-29.

Crabbe, J.C., D. Wahlsten, and B.C. Dudek. 1999. Genetics of mouse behavior: interactions with laboratory environment. *Science*. 284:1670-2.

Crawley, J.N. 1996. Unusual behavioral phenotypes of inbred mouse strains. *Trends Neurosci*. 19:181-2; discussion 188-9.

del Pozo, M.A., L.S. Price, N.B. Alderson, X.D. Ren, and M.A. Schwartz. 2000. Adhesion to the extracellular matrix regulates the coupling of the small GTPase Rac to its effector PAK. *Embo J*. 19:2008-14.

Diamantopoulos, G.S., F. Perez, H.V. Goodson, G. Batelier, R. Melki, T.E. Kreis, and J.E. Rickard. 1999. Dynamic localization of CLIP-170 to microtubule plus ends is coupled to microtubule assembly. *J Cell Biol*. 144:99-112.

Dunn, G.A., and D. Zicha. 1995. Dynamics of fibroblast spreading. *J Cell Sci*. 108 (Pt 3):1239-49.

Folker, E.S., B.M. Baker, and H.V. Goodson. 2005. Interactions between CLIP-170, tubulin, and microtubules: implications for the mechanism of Clip-170 plus-end tracking behavior. *Mol Biol Cell*. 16:5373-84.

Forni, P.E., C. Scuoppo, I. Imayoshi, R. Taulli, W. Dastru, V. Sala, U.A. Betz, P. Muzzi, D. Martinuzzi, A.E. Vercelli, R. Kageyama, and C. Ponzetto. 2006. High levels of Cre expression in neuronal progenitors cause defects in brain development leading to microencephaly and hydrocephaly. *J Neurosci*. 26:9593-602.

Gerlai, R. 1996. Gene-targeting studies of mammalian behavior: is it the mutation or the background genotype? *Trends Neurosci*. 19:177-81.

Goodson, H.V., S.B. Skube, R. Stalder, C. Valetti, T.E. Kreis, E.E. Morrison, and T.A. Schroer. 2003. CLIP-170 interacts with dynactin complex and the APC-binding protein EB1 by different mechanisms. *Cell Motil Cytoskeleton*. 55:156-73.

Hoogenraad, C.C., A. Akhmanova, S.A. Howell, B.R. Dortland, C.I. De Zeeuw, R. Willemsen, P. Visser, F. Grosveld, and N. Galjart. 2001. Mammalian Golgi-associated Bicaudal-D2 functions in the dynein-dynactin pathway by interacting with these complexes. *Embo J*. 20:4041-54.

Hoogenraad, C.C., B. Koekkoek, A. Akhmanova, H. Krugers, B. Dortland, M. Miedema, A. van Alphen, W.M. Kistler, M. Jaegle, M. Koutsourakis, N. Van Camp, M. Verhoye, A. van der Linden, I. Kaverina, F. Grosveld, C.I. De Zeeuw, and N. Galjart. 2002a. Targeted mutation of Cyln2 in the Williams syndrome critical region links CLIP-115 haploinsufficiency to neurodevelopmental abnormalities in mice. *Nat Genet*. 32:116-27.

Hoogenraad, C.C., B. Koekkoek, A. Akhmanova, H. Krugers, B. Dortland, M. Miedema, A. Van Alphen, W.M. Kistler, M. Jaegle, M. Koutsourakis, N. Van Camp, M. Verhoye, A. Van Der Linden, I. Kaverina, F. Grosveld, C.I. De Zeeuw, and N. Galjart. 2002b. Targeted mutation of Cyln2 in the Williams syndrome critical region links CLIP-115 haploinsufficiency to neurodevelopmental abnormalities in mice. *Nat Genet*. 32:116-27.

Hynes, R.O. 2002. Integrins: bidirectional, allosteric signaling machines. *Cell*. 110:673-87.

Ibanez-Tallon, I., S. Gorokhova, and N. Heintz. 2002. Loss of function of axonemal dynein Mdnah5 causes primary ciliary dyskinesia and hydrocephalus. *Hum Mol Genet*. 11:715-21.

Jacamo, R., X. Jiang, J.A. Lunn, and E. Rozengurt. 2007. FAK phosphorylation at Ser-843 inhibits Tyr-397 phosphorylation, cell spreading and migration. *J Cell Physiol*. 210:436-44.

Jamieson, J.S., D.A. Tumbarello, M. Halle, M.C. Brown, M.L. Tremblay, and C.E. Turner. 2005. Paxillin is essential for PTP-PEST-dependent regulation of cell spreading and motility: a role for paxillin kinase linker. *J Cell Sci*. 118:5835-47.

Kaverina, I., O. Krylyshkina, and J.V. Small. 1999. Microtubule targeting of substrate contacts promotes their relaxation and dissociation. *J Cell Biol*. 146:1033-44.

Kaverina, I., K. Rottner, and J.V. Small. 1998. Targeting, capture, and stabilization of microtubules at early focal adhesions. *J Cell Biol*. 142:181-90.

Klinghoffer, R.A., C. Sachsenmaier, J.A. Cooper, and P. Soriano. 1999. Src family kinases are required for integrin but not PDGFR signal transduction. *Embo J.* 18:2459-71.

Kobayashi, Y., M. Watanabe, Y. Okada, H. Sawa, H. Takai, M. Nakanishi, Y. Kawase, H. Suzuki, K. Nagashima, K. Ikeda, and N. Motoyama. 2002. Hydrocephalus, situs inversus, chronic sinusitis, and male infertility in DNA polymerase lambda-deficient mice: possible implication for the pathogenesis of immotile cilia syndrome. *Mol Cell Biol.* 22:2769-76.

Krylyshkina, O., I. Kaverina, W. Kranewitter, W. Steffen, M.C. Alonso, R.A. Cross, and J.V. Small. 2002. Modulation of substrate adhesion dynamics via microtubule targeting requires kinesin-1. *J Cell Biol.* 156:349-59.

Lansbergen, G., and A. Akhmanova. 2006. Microtubule plus end: a hub of cellular activities. *Traffic.* 7:499-507.

Lansbergen, G., I. Grigoriev, Y. Mimori-Kiyosue, T. Ohtsuka, S. Higa, I. Kitajima, J. Demmers, N. Galjart, A.B. Houtsmuller, F. Grosveld, and A. Akhmanova. 2006. CLASPs attach microtubule plus ends to the cell cortex through a complex with LL5beta. *Dev Cell.* 11:21-32.

Lansbergen, G., Y. Komarova, M. Modesti, C. Wyman, C.C. Hoogenraad, H.V. Goodson, R.P. Lemaitre, D.N. Drechsel, E. van Munster, T.W. Gadella, Jr., F. Grosveld, N. Galjart, G.G. Borisy, and A. Akhmanova. 2004. Conformational changes in CLIP-170 regulate its binding to microtubules and dynactin localization. *J Cell Biol.* 166:1003-14.

Lathe, R. 1996. Mice, gene targeting and behaviour: more than just genetic background. *Trends Neurosci.* 19:183-6; discussion 188-9.

Liakopoulos, D., J. Kusch, S. Grava, J. Vogel, and Y. Barral. 2003. Asymmetric loading of Kar9 onto spindle poles and microtubules ensures proper spindle alignment. *Cell.* 112:561-74.

Ma, X., S. Kawamoto, J. Uribe, and R.S. Adelstein. 2006. Function of the neuron-specific alternatively spliced isoforms of nonmuscle myosin II-B during mouse brain development. *Mol Biol Cell.* 17:2138-49.

Mandelkow, E.M., E. Mandelkow, and R.A. Milligan. 1991. Microtubule dynamics and microtubule caps: a time-resolved cryo-electron microscopy study. *J Cell Biol.* 114:977-91.

Matanis, T., A. Akhmanova, P. Wulf, E. Del Nery, T. Weide, T. Stepanova, N. Galjart, F. Grosveld, B. Goud, C.I. De Zeeuw, A. Barnekow, and C.C. Hoogenraad. 2002. Bicaudal-D regulates COPI-independent Golgi-ER transport by recruiting the dynein-dynactin motor complex. *Nat Cell Biol.* 4:986-92.

Muller-Reichert, T., D. Chretien, F. Severin, and A.A. Hyman. 1998. Structural changes at microtubule ends accompanying GTP hydrolysis: information from a slowly hydrolyzable analogue of GTP, guanylyl (alpha ,beta)methylenediphosphonate. *Proc Natl Acad Sci U S A.* 95:3661-6.

Nobes, C.D., and A. Hall. 1995. Rho, rac, and cdc42 GTPases regulate the assembly of multimolecular focal complexes associated with actin stress fibers, lamellipodia, and filopodia. *Cell.* 81:53-62.

Palazzo, A.F., C.H. Eng, D.D. Schlaepfer, E.E. Marcantonio, and G.G. Gundersen. 2004. Localized stabilization of microtubules by integrin- and FAK-facilitated Rho signaling. *Science.* 303:836-9.

Partridge, M.A., and E.E. Marcantonio. 2006. Initiation of attachment and generation of mature focal adhesions by integrin-containing filopodia in cell spreading. *Mol Biol Cell.* 17:4237-48.

Pedersen, L.B., S. Geimer, R.D. Sloboda, and J.L. Rosenbaum. 2003. The Microtubule plus end-tracking protein EB1 is localized to the flagellar tip and basal bodies in Chlamydomonas reinhardtii. *Curr Biol.* 13:1969-74.

Perez-Figares, J.M., A.J. Jimenez, and E.M. Rodriguez. 2001. Subcommissural organ, cerebrospinal fluid circulation, and hydrocephalus. *Microsc Res Tech.* 52:591-607.

Perez, F., G.S. Diamantopoulos, R. Stalder, and T.E. Kreis. 1999. CLIP-170 highlights growing microtubule ends in vivo. *Cell.* 96:517-27.

Qin, H., D.R. Diener, S. Geimer, D.G. Cole, and J.L. Rosenbaum. 2004. Intraflagellar transport (IFT) cargo: IFT transports flagellar precursors to the tip and turnover products to the cell body. *J Cell Biol.* 164:255-66.

Raucher, D., and M.P. Sheetz. 1999. Characteristics of a membrane reservoir buffering membrane tension. *Biophys J.* 77:1992-2002.

Raucher, D., and M.P. Sheetz. 2000. Cell spreading and lamellipodial extension rate is regulated by membrane tension. *J Cell Biol.* 148:127-36.

Ren, X.D., W.B. Kiosses, and M.A. Schwartz. 1999. Regulation of the small GTP-binding protein Rho by cell adhesion and the cytoskeleton. *Embo J.* 18:578-85.

Richardson, A., R.K. Malik, J.D. Hildebrand, and J.T. Parsons. 1997. Inhibition of cell spreading by expression of the C-terminal domain of focal adhesion kinase (FAK) is rescued by coexpression of Src or catalytically inactive FAK: a role for paxillin tyrosine phosphorylation. *Mol Cell Biol.* 17:6906-14.

Rolf, B., M. Kutsche, and U. Bartsch. 2001. Severe hydrocephalus in L1-deficient mice. *Brain Res.* 891:247-52.

Rottner, K., A. Hall, and J.V. Small. 1999. Interplay between Rac and Rho in the control of substrate contact dynamics. *Curr Biol.* 9:640-8.

Sapiro, R., I. Kostetskii, P. Olds-Clarke, G.L. Gerton, G.L. Radice, and I.J. Strauss. 2002. Male infertility, impaired sperm motility, and hydrocephalus in mice deficient in sperm-associated antigen 6. *Mol Cell Biol*. 22:6298-305.

Shimizu, A., and M. Koto. 1992. Ultrastructure and movement of the ependymal and tracheal cilia in congenitally hydrocephalic WIC-Hyd rats. *Childs Nerv Syst*. 8:25-32.

Short, B., C. Preisinger, J. Schaletzky, R. Kopajtich, and F.A. Barr. 2002. The Rab6 GTPase regulates recruitment of the dynactin complex to Golgi membranes. *Curr Biol*. 12:1792-5.

Smilenov, L.B., A. Mikhailov, R.J. Pelham, E.E. Marcantonio, and G.G. Gundersen. 1999. Focal adhesion motility revealed in stationary fibroblasts. *Science*. 286:1172-4.

Taulman, P.D., C.J. Haycraft, D.F. Balkovetz, and B.K. Yoder. 2001. Polaris, a protein involved in left-right axis patterning, localizes to basal bodies and cilia. *Mol Biol Cell*. 12:589-99.

Turner, C.E. 2000a. Paxillin and focal adhesion signalling. *Nat Cell Biol*. 2:E231-6.

Turner, C.E. 2000b. Paxillin interactions. *J Cell Sci*. 113 Pt 23:4139-40.

Valetti, C., D.M. Wetzel, M. Schrader, M.J. Hasbani, S.R. Gill, T.E. Kreis, and T.A. Schroer. 1999. Role of dynactin in endocytic traffic: effects of dynamitin overexpression and colocalization with CLIP-170. *Mol Biol Cell*. 10:4107-20.

Watson, P., and D.J. Stephens. 2006. Microtubule plus-end loading of p150(Glued) is mediated by EB1 and CLIP-170 but is not required for intracellular membrane traffic in mammalian cells. *J Cell Sci*. 119:2758-67.

Waugh, R.E. 1983. Effects of abnormal cytoskeletal structure on erythrocyte membrane mechanical properties. *Cell Motil*. 3:609-22.

Zaidel-Bar, R., R. Milo, Z. Kam, and B. Geiger. 2007. A paxillin tyrosine phosphorylation switch regulates the assembly and form of cell-matrix adhesions. *J Cell Sci*. 120:137-48.

Zariwala, M.A., M.R. Knowles, and H. Omran. 2006. Genetic Defects in Ciliary Structure and Function. *Annu Rev Physiol*.

Summary

Summary

An intracellular network of actin fibers, intermediate filaments and microtubules forms the cytoskeleton which provides the cell with structural support and is involved in intracellular transport, cell migration and cell division. This thesis focuses on the largest subunit of the cytoskeleton, the microtubules. Microtubules are hollow polar tubes with a fast-growing plus-end and a slower growing minus-end. In most cells, the minus-ends of microtubules are anchored near the centrosome, while the plus-ends radiate towards the cell periphery. There they frequently shift from a phase of growth to a phase of shrinkage (catastrophe) and the other way around (rescue). This behavior is called dynamic instability and is important for proper functioning of the microtubule cytoskeleton.

The dynamic behavior of the microtubule network is regulated by a large group of proteins that bind specifically to the microtubule plus-ends, the so-called plus-end-tracking proteins (+TIPs). Interactions between the different +TIPs result in an intricate network at the microtubule tip. The restricted binding behavior of the +TIPs suggests they have specific functions. For most of the proteins, however, these were largely unknown. This thesis focuses on the research into the functions of two members of the family of +TIPs, the cytoplasmic linker proteins CLIP-115 and CLIP-170.

The generation of a mouse line deficient for CLIP-115 is described in chapter 2. In humans, this protein is located in a chromosomal region that has been shown to be commonly deleted in patients suffering from Williams Syndrome, a rare neurodevelopmental disorder. The brain-specific expression of CLIP-115 makes it a likely candidate for involvement in the neurological features of the disease. And indeed, mice deficient for CLIP-115 show several features reminiscent of the symptoms of Williams Syndrome, such as a mild growth deficiency, brain abnormalities, hippocampal dysfunction and particular deficits in motor coordination. These results subscribe the suggestion that the absence of CLIP-115 might underlie the neurodevelopmental symptoms in individuals with Williams Syndrome. Surprisingly, analysis of fibroblasts derived from CLIP-115 knockout mice did not show any major differences.

Recently, our group also generated mice deficient for CLIP-170, which are not extensively described in this thesis. Although male CLIP-170 knockout mice are subfertile as a result of sperm malformations, knockout fibroblasts only displayed minor abnormalities as well. Since CLIP-115 and CLIP-170 are highly similar in structure they are suspected to have redundant functions, which might explain the surprisingly mild cellular phenotypes. To test this hypothesis of redundancy, CLIP-115 and CLIP-170 double knockout mice were generated by crossing the single knockout mice. Chapter 3 describes the analysis of fibroblasts derived from these CLIP double knockout mice. In contrast to the single knockout fibroblasts, double knockout cells show several abnormalities. First, microtubule dynamics in the double knockout fibroblasts is profoundly altered because the frequency of microtubule rescue is decreased five-fold. Second, the microtubule network is disturbed resulting in large microtubule-free areas, which are shown to be extremely flat. In these microtubule-free areas several proteins are found to form aggregates, including the CLIP-interacting proteins $p150^{Glued}$ and BICD2 and the motor protein cytoplasmic dynein. The aggregates cannot be removed by restoration of microtubule dynamics alone, suggesting a function for the CLIPs independent of their role in regulating microtubule dynamics. Third, the surface size of CLIP double knockout fibroblasts is two-fold larger relative to wild type cells, as a result of increased spreading.

The results of the characterization of the CLIP-115 and CLIP-170 double knockout mice is described in chapter 4. A significant number of homozygous double knockout mice developed severe hydrocephalus. MRI analysis showed that in fact all homozygous double knockout mice

had enlarged ventricles relative to wild type mice, also the mice without visible features of hydrocephalus. Further investigation of the brains revealed the presence of cerebellar neurons in cortical brain areas, sometimes obstructing the aqueduct of Sylvius, the narrow connection between the third and the fourth ventricle. In addition to the brain abnormalities, behavioral tests showed a surprising age-related increase in motor coordination performance, but a decrease in performance at older age. Further investigation has to point out whether the behavioral abnormalities are a result of the enlargement of the ventricles or whether there is another problem in the neuromuscular system.

Taken together, the results discussed in this thesis confirm the suspected redundancy between CLIP-115 and CLIP-170. Furthermore they show that the CLIPs are not only involved in regulating microtubule dynamics but also play a role in maintaining cellular homeostasis and morphology. In mice, abolishment of the functions of CLIP-115 and CLIP-170 results in abnormal neuronal migration and hydrocephalus in different levels of severity. Future studies will be necessary to answer remaining questions and to further elucidate the exact functions of CLIP-115 and CLIP-170.

Samenvatting

Samenvatting

De cel vormt de bouwsteen van alle levende wezens. Grote groepen cellen werken samen en vormen zo de organen van mens en dier en de bloemen en bladeren van planten. Er zijn talloze soorten cellen met elk een specifieke functie, bijvoorbeeld spiercellen, bloedcellen en hersencellen. Ondanks hun verschillende uiterlijk en functies hebben deze cellen veel gemeen. Ze bevatten allemaal het erfelijke materiaal in de vorm van een lange streng DNA waarop een groot aantal genen ligt. Niet al deze genen zijn in alle cellen in gebruik, sommige staan 'aan' en andere staan 'uit'. De verschillen tussen de cellen ontstaan doordat in elk type cel andere genen 'aan' en 'uit' staan. De mens heeft ongeveer 25.000 genen die de blauwdruk zijn voor de productie van naar schatting 250.000 eiwitten. Deze eiwitten doen in de cel het werk en fungeren als bouwstenen van de verschillende onderdelen van de cel.

Een van de onderdelen van de cel is het cytoskelet (cyto=cel). Dit cellulaire skelet vervult een aantal belangrijke functies in de cel. Ten eerste zorgt het, net als het menselijk skelet, voor stevigheid en vormbehoud en is het betrokken bij voortbeweging. Daarnaast heeft het ook een belangrijke functie bij het transport van stoffen binnen de cel, waarbij het cytoskelet als een soort spoorbaan fungeert waarover de eigenlijke transporteurs, de motoreiwitten, zich kunnen verplaatsen. Tenslotte speelt het cytoskelet een essentiële rol tijdens de deling van cellen. Voordat een cel zich deelt wordt het DNA verdubbeld, zodat beide dochtercellen elk een kopie van het genetisch materiaal krijgen. Het cytoskelet zorgt voor de scheiding van de twee DNA-strengen door ze uit elkaar te trekken.

Het cytoskelet bestaat uit drie typen vezels, te weten actine-vezels, intermediaire filamenten en microtubuli. Dit proefschrift concentreert zich op het derde type vezel, de microtubuli. Dit zijn holle buisvormige vezels met een diameter van 25 nm (0,000000025 m) die een netwerk vormen. Dit netwerk beslaat de gehele oppervlakte van de cel. De microtubuli zijn opgebouwd uit lange ketens van twee soorten eiwitten, α- en β-tubuline, die elkaar in de ketens afwisselen. Microtubuli zijn, anders dan de botten in het menselijk skelet, niet stijf en statisch. Ze worden continu opgebouwd en afgebroken, als een toren van LEGO waar steeds het bovenste stukje van wordt afgebroken om vervolgens weer te worden opgebouwd. Deze dynamiek zorgt dat het netwerk van microtubuli zich snel kan aanpassen als veranderingen in de omgeving van de cel dit vragen. Wanneer een cel zich bijvoorbeeld in een bepaalde richting moet verplaatsen, worden meer microtubuli gevormd in de richting van de verplaatsing dan aan de achterzijde van de cel.

Voor het opbouwen van een microtubulus worden paren van een α- en een β-tubuline-eiwit aan een bestaande keten toegevoegd. Dit kan aan beide uiteinden van de keten, maar aan de ene kant (het plus-einde) gaat dit sneller dan aan de andere kant (het min-einde). Bovendien zit in de meeste cellen het min-einde vast in het zogenaamde microtubulus-organiserend-centrum (MTOC), waardoor aan deze kant geen opbouw kan plaatsvinden. Om de opbouw en de afbraak van de microtubuli in goede banen te leiden bestaat er een grote groep eiwitten die kan binden aan de plus-einden, de zogenaamde plus-eind-bindende-eiwitten. Opvallend genoeg binden deze eiwitten alleen aan het plus-einde van de microtubulus als deze wordt opgebouwd en vallen ze eraf wanneer de microtubulus wordt afgebroken. Deze bijzondere eigenschap suggereert dat de plus-eind-bindende-eiwitten heel specifiek werk verrichten wanneer ze aan de microtubulus zijn gebonden. Behalve aan de microtubulus kunnen de verschillende plus-eind-bindende-eiwitten ook aan elkaar binden en op die manier invloed uitoefenen op elkaars werkzaamheden.

In het onderzoek dat is beschreven in dit proefschrift is geprobeerd de functie te bepalen van twee plus-eind-bindende-eiwitten, de cytoplasmatische linker eiwitten CLIP-115 en CLIP-170. Om de functie van een bepaald eiwit te achterhalen wordt vaak gebruik gemaakt van

diermodellen, in het bijzonder muizen. Door in muizen een specifiek eiwit uit te schakelen en onderzoek te doen naar de gevolgen hiervan, kan veel informatie worden verkregen over de functie van het eiwit. Ook wij hebben van deze techniek gebruik gemaakt.

In hoofdstuk 2 van dit proefschrift is beschreven op welke wijze het eiwit CLIP-115 is uitgeschakeld in muizen en wat de gevolgen zijn van deze uitschakeling. Er is bijzondere belangstelling voor de functie van CLIP-115 omdat is aangetoond dat dit eiwit, samen met een aantal andere eiwitten, afwezig is bij patiënten met Williams Syndroom (WS). Patiënten met deze zeldzame ziekte hebben afwijkingen aan de bloedvaten, maar hebben ook een scala aan hersengerelateerde symptomen. Aangezien het gen dat de blauwdruk vormt voor het eiwit CLIP-115 voornamelijk 'aan'-staat in de cellen van de hersenen, zou de afwezigheid van CLIP-115 een van de oorzaken kunnen zijn van de hersengerelateerde symptomen van WS-patiënten. Het onderzoek aan de muizen zonder CLIP-115 (CLIP-115 knockout muizen) heeft zich dan ook geconcentreerd op de hersenen. De hersenen van de CLIP-115 knockout muizen blijken in bepaalde gebieden anders te zijn gevormd dan de hersenen van normale (wild type) muizen. Ook bij bepaalde gedragstesten presteren de knockout muizen minder goed. De gevonden afwijkingen van de muizen doen denken aan de symptomen van de WS-patiënten, wat het vermoeden versterkt dat CLIP-115 betrokken is bij het ontstaan van deze ziekte. Er zijn echter nog meer eiwitten afwezig in WS-patiënten die de symptomen (mede) kunnen veroorzaken. Verder onderzoek is dan ook nodig om meer informatie te krijgen.

Naast CLIP-115 is door ons ook het eiwit CLIP-170 uitgeschakeld in muizen. Deze muizen worden niet uitgebreid beschreven in dit proefschrift, maar onderzoek heeft uitgewezen dat mannelijke CLIP-170 knockout muizen onvruchtbaar zijn doordat de spermacellen niet goed worden gevormd. In de zoektocht naar de functie van CLIP-115 en CLIP-170 wordt niet alleen gekeken naar afwijkingen in de hele muis (het organisme), maar vooral ook naar veranderingen in de bouwstenen van de muis, de cellen. Hiervoor worden verschillende soorten cellen gebruikt, onder andere huidcellen, die kunnen groeien door zich vast te hechten aan de bodem van een plastic schaaltje. Tegen de verwachting in vertoonden de huidcellen van de knockout muizen weinig afwijkingen. Aangezien CLIP-115 en CLIP-170 heel erg op elkaar lijken wordt vermoed dat CLIP-115, door iets harder te werken, de functie van CLIP-170 kan overnemen wanneer deze laatste is uitgeschakeld en vice versa. Hierdoor kunnen de cellen alles blijven doen wat ze normaal ook doen en vertonen de knockout cellen weinig afwijkingen.

Om te onderzoeken of dit vermoeden juist is hebben we de CLIP-115 knockout muizen gekruist met de CLIP-170 knockout muizen om zo nageslacht te krijgen waarin zowel CLIP-115 als CLIP-170 zijn uitgeschakeld, de zogenaamde CLIP dubbel knockout muizen. Omdat in deze muizen de functies van de uitgeschakelde eiwitten niet meer kunnen worden overgenomen verwachtten we grotere afwijkingen. En inderdaad, zowel de huidcellen als de muis zelf hebben grotere problemen. Hoofdstuk 3 van dit proefschrift beschrijft de afwijkingen die zijn gevonden in de huidcellen van de CLIP dubbel knockout muizen. Door de afwezigheid van beide CLIP-eiwitten beslaat het microtubuli-netwerk niet meer de hele oppervlakte van de cel, maar ontstaan er gaten in het netwerk. Daarnaast kunnen door de afwezigheid van de CLIP-eiwitten andere plus-eind-bindende eiwitten minder goed of zelfs helemaal niet aan de microtubuli binden. Een aantal van deze eiwitten blijkt op de plaatsen van de gaten in het microtubuli-netwerk samen te klonteren waardoor ze hun werk niet meer kunnen doen. Als gevolg van de verstoring van het microtubuli-netwerk kan het cytoskelet de vorm van de cellen niet goed ondersteunen. CLIP dubbel knockout cellen blijken veel groter te worden als ze zich vasthechten aan de bodem van het plastic schaaltje. Bovendien blijken de cellen op de plaatsen van de gaten in het netwerk veel platter te zijn dan op plaatsen waar het microtubuli-netwerk goed is gevormd. Hieruit

concluderen wij dat de CLIP-eiwitten een belangrijke functie hebben bij de vorming van het microtubuli-netwerk.

Het onderzoek waarbij is gekeken naar de CLIP dubbel knockout muizen is beschreven in hoofdstuk 4. Een gedeelte van de muizen waarin beide CLIP-eiwitten zijn uitgeschakeld krijgt in de loop van de tijd een waterhoofd. In de ernstige gevallen is dit duidelijk zichtbaar omdat de schedel van de muis boller wordt. Een waterhoofd ontstaat door een ophoping van het vocht dat aanwezig is in de hersenen. Het grootste gedeelte van dit hersenvocht bevindt zich in vier holle ruimtes, de ventrikels. Nieuw hersenvocht wordt doorlopend aangemaakt en tegelijkertijd wordt het oudere vocht afgevoerd via het ruggenmerg. Als het oudere vocht de hersenen niet meer uit kan, bijvoorbeeld door een verstopping van de afvoer, ontstaat een ophoping van hersenvocht in de ventrikels. Hierdoor loopt de druk in de hersenen op en kan in ernstige gevallen de schedel opbollen. In het geval van de CLIP dubbel knockout muizen ontwikkelde slechts een gedeelte van de muizen een duidelijk zichtbaar waterhoofd. Om de ventrikels van de andere muizen te onderzoeken hebben de muizen een MRI scan ondergaan. Met een dergelijke scan kan in levende (verdoofde) muizen naar de verschillende gebieden van de hersenen worden gekeken. Uit deze scans bleek dat alle CLIP dubbel knockout muizen grotere ventrikels hadden dan normale muizen. Bij verdere inspectie van de hersenen van deze muizen werden bepaalde cellen gevonden in hersengebieden waarin ze normaliter niet voorkomen. In sommige gevallen resulteerde dit in een gedeeltelijke of algehele blokkade van de afvoer van het hersenvocht.

Hoe komen hersencellen terecht in het verkeerde gebied van de hersenen? Tijdens de vorming van de hersenen voor de geboorte verplaatsen (migreren) hersencellen zich van het ene gebied naar het andere. Deze migratie moet strak zijn geregeld, zodat alle cellen uiteindelijk terechtkomen op de plaats waar ze horen. Het lijkt erop dat de migratie van hersencellen in de CLIP dubbel knockout muizen minder goed is geregeld. Dit suggereert dat CLIP-115 en CLIP-170 een rol spelen bij de regulatie van de migratie van hersencellen. Wat hun precieze rol is in dit proces moet nog verder worden onderzocht.

In hoofdstuk 5 passeren alle gevonden afwijkingen van de CLIP knockout muizen en cellen nog een keer de revue en wordt geprobeerd die afwijkingen te verklaren. Op basis van onze resultaten en wat bekend is uit andere onderzoeken wordt gespeculeerd over de mogelijke functies van CLIP-115 en CLIP-170.

Curriculum Vitae

Name: Marja Miedema
Born: 22 March 1976, Wageningen, The Netherlands

Sept. 1988 – June 1994	Atheneum, Hendrik Pierson College, Zetten	
Sept. 1994 – June 1998	Bachelor, Medical Microbiology, Noordelijke Hogeschool Leeuwarden	
	Graduation project:	Daniël den Hoed Kliniek, Rotterdam
	Subject:	Testicular germ cell tumors and the short arm of chromosome 12
	Supervision:	Prof.dr. J.W. Oosterhuis Dr. L.H.J. Looijenga
Aug. 1998 – Aug. 1999	Research technician, Genetics, Erasmus University Rotterdam	
	Supervision:	Prof.dr. J.H.J. Hoeijmakers Dr. G.T.J. van der Horst
Sept. 1999 – Sept. 2001	Master of Science, Biology, Leiden University	
	Graduation project:	Yeast Genetics, Institute for Molecular Plant Sciences, Leiden University
	Subject:	Analysis of the interaction between *Saccharomyces cerevisiae* 14-3-3 proteins and Gcr2p
	Supervision:	Prof.dr. H.Y. Steensma Dr. G.P.H. van Heusden
Sept. 2001 – Dec. 2006	PhD-student, Department of Cell Biology and Genetics, Erasmus Medical Center, Rotterdam	
	Promotor:	Prof.dr. F.G. Grosveld
	Co-promotor:	Dr.ir. N.J. Galjart
April 2007 – present	Advisor Scientific Communication, Erasmus Medical Center, Rotterdam	

Dankwoord

Op de laatste pagina's van mijn proefschrift mag ik terugkijken op een aantal intensieve, maar geweldige jaren waarin ik heb kunnen proeven van de geneugten en frustraties die horen bij wetenschappelijk onderzoek. Ik ben blij dat ik hier de gelegenheid krijg alle mensen te bedanken die mij gedurende ruim vijf jaar hebben geholpen en gesteund en die op verschillende manieren hebben bijgedragen aan de totstandkoming van dit boekje.

Allereerst wil ik mijn copromotor Niels Galjart bedanken. Niels, ik ben erg blij dat ik de kans heb gekregen de afgelopen jaren onder jouw begeleiding onderzoek te doen. Ik heb veel geleerd van je nimmer aflatende enthousiasme en je geloof in de goede afloop. Ondanks dat ik geen doorsnee AIO was, eerst parttime werken en later ook nog zwanger, heb jij altijd in me geloofd en me gesteund. Dit heeft mij steeds weer overtuigd van mijn mogelijkheden, vooral op de momenten dat ik het eventjes niet zag zitten. Je hulp tijdens de eindsprint naar de promotie was geweldig. Bedankt voor de les!

Mijn dank gaat ook uit naar mijn promotor Frank Grosveld. Frank, ondanks de wisselende frequentie van onze werkbesprekingen heb ik de discussies met jou altijd als zeer inspirerend ervaren. Bedankt dat ik op jouw afdeling mijn promotieonderzoek mocht doen en we komen elkaar in de toekomst zeker weer tegen!

Alle leden van mijn promotiecommissie, Bert van der Horst, Chris de Zeeuw, Dies Meijer, Annemie van der Linden, Rene Medema en Anna Akhmanova, heel erg bedankt dat jullie met mij van gedachten willen wisselen over de resultaten van mijn proefschrift. Bert, wie had gedacht toen ik in augustus 1998 als analist voor je kwam werken, dat je nu secretaris van mijn kleine commissie zou zijn? Bedankt voor je nuttige en uitgebreide commentaar. Chris (leuke suggestie van die twee extra figuren) en Dies, ook bedankt voor de tijd die jullie hebben geïnvesteerd als leden van de kleine commissie. Annemie, bedankt dat je uit Antwerpen wilt komen voor mijn promotie. Rene, gelukkig trekken wij ons niks aan van de rivaliteit tussen onze Friese en Groningse voorvaderen. Anna, bedankt voor je praktische hulp en je adviezen tijdens de eerste jaren van mijn promotieonderzoek.

In dit proefschrift zijn meerdere resultaten opgenomen van andere mensen zonder wiens inspanningen dit boekje niet tot stand had kunnen komen. Yulia Komarova, thank you for your experiments on microtubule dynamics. Marvin Tanenbaum, bedankt voor je onderzoek naar mitotische afwijkingen van mijn dubbel knockout cellen. Catherine Robin, thank you for your help with the FACS-analyses. Nadja van Camp, bedankt voor je MRI-analyse van mijn dubbel knockout muizen. Casper, dankzij jouw werkzaamheden aan CLIP-115 kon ik op een rijdende trein stappen. Elize, Mandy en Erika, heel erg bedankt voor jullie coupes en kleuringen en voor de gezelligheid tijdens mijn werkzaamheden op jullie lab. Mandy en Elize, jullie zijn een fenomenaal perfusie-team!

Mijn bijzondere waardering gaat uit naar mijn paranimfen, Gideon Lansbergen en Marco van Ham. Gideon, hoewel we vrijwel tegelijk zijn begonnen ben jij alweer ruim een jaar doctor. Ik kijk met ontzettend veel plezier terug op onze gezamenlijke congressen in Gosau (die fietstocht was vreselijk!) en Nice (met twee mannen op één kamer was een bijzondere ervaring). Ook met Marieke en Adriaan (in de tussentijd onze echtgenoten geworden) erbij hebben we veel lol gehad. Bedankt (?) dat je me hebt laten kennis maken met de muziek van Huub Hangop en Arrow FM. Ik weet nu in ieder geval wat ik niet op moet zetten! Leuk dat je mijn paranimf wilt zijn!

Marco, ik vond de jaren dat ik aan jouw rechterkant zat grandioos! Het is verdraaid stil op het lab sinds jij bent vertrokken. Natuurlijk vergeet ik nooit onze rosé-avond op het strand aan de Maas, en al helemaal niet de volgende ochtend. Ook ons congres in Nice met nachtzwemmen

en koude pizza op het strand blijft in de boeken. Rosé lijkt wel de rode draad te zijn in onze gezamenlijke uitstapjes… Bedankt dat je mijn paranimf wilt zijn!

Ik ben ervan overtuigd dat dit onderzoek heel anders was gelopen zonder de geweldige sfeer op lab 710 en later 1030 (beter of slechter laat ik aan ieders eigen beoordeling over). Daarom wil ik iedereen die tijdens enige periode van mijn onderzoek deel uitmaakte van deze groep hartelijk bedanken. In willekeurige volgorde: Nanda, bedankt voor de gezellige momenten in het muizenhuis. Vooral je acrobatische toeren tijdens de catwalk-experimenten zijn legendarisch. Jeffrey, nog bedankt voor de lift na afloop van de rosé-avond op het strand aan de Maas en de gezelligheid op de camping in Tiel. Frank, bedankt voor je enthousiasme op het lab, de geweldige kerstvideo's, je verfrissende muzieksmaak en onze discussies in de kroeg. Succes met je 'To do before I'm … -lijstjes. Laura, thank you for the Spanish lessons and lots of happiness for you and Juan in Madrid. Suzanne, succes met de laatste loodjes van je promotie en met je nieuwe taak als 'moeder'. Daniel, ook jij succes met de afronding en laat Boren niet te lang wachten! Dank je wel Michael, Katha, Ksenija, Helen, Anne-Laure (lots of happiness in Montpellier, and we will try to visit you whenever our holidays take us to the south of France), Filipe, Dorota en Zjak. Bedankt Rick, Phebe en Bjorn, hopelijk mag ik mee blijven lunchen als ik straks adviseur wetenschapscommunicatie ben.

Veel dank ben ik verschuldigd aan de dames van 'het muizenhuis'. Agnes, bedankt voor je spoedcursus 'mouse-handling', je gezelschap tijdens de langdurige open-field experimenten en onze koffie-afspraken in het DE-café. Yvette, Sandra en Jenny en de dames van A19-ivc, mede namens mijn muizen bedankt voor jullie goede zorgen. Heren van de computers, dames van de spoelkeukens, Marike en Jasperina, dames van de bestellingen, bedankt voor jullie ondersteuning. En laat ik vooral de vormgever Tom de Vries Lentsch niet vergeten. Tom, zonder jou was dit boekje niet half zo mooi geweest. Bedankt voor alle tijd en moeite die je erin hebt gestoken. Ondanks dat de kwaliteit van sommige figuren in eerste instantie bedroevend slecht was, is het eindresultaat prachtig!

Natuurlijk wil ik ook mijn familie en schoonfamilie bedanken. Pap en mam, bedankt dat jullie mij de mogelijkheid hebben gegeven om te gaan studeren en daarna nog een keer te gaan studeren. Pap, ik ben er trots op dat ik 20 jaar na jouw promotie in de voetsporen van mijn vader zal treden! Kees en Hannie, bedankt voor jullie interesse en warme belangstelling tijdens mijn studies en mijn promotie-traject. Ik vind het geweldig dat jullie al 14 jaar alle belangrijke gebeurtenissen meebeleven. Ingrid, Jan-Pieter, ooms en tantes, vrienden, ik hoop dat jullie na het lezen van de Nederlandse samenvatting iets beter zullen begrijpen waar ik de afgelopen jaren mee bezig ben geweest.

Maar mijn allergrootste dank gaat uit naar Adriaan. Al vanaf mijn laatste jaar op de middelbare school ben jij mijn maatje en mijn grootste fan. Jouw liefde en je onvoorwaardelijke vertrouwen in mijn kunnen waren regelmatig een duwtje in mijn rug om door te gaan. Ik kan me geen betere echtgenoot wensen. Ik verheug me op de toekomst met jou en met onze kleine vent!

Marja